NUREG/CR-5736
ORNL/TM-13748

Evaluation of WF-70 Weld Metal From the Midland Unit 1 Reactor Vessel

Oak Ridge National Laboratory

U.S. Nuclear Regulatory Commission
Office of Nuclear Regulatory Research
Washington, DC 20555-0001

AVAILABILITY OF REFERENCE MATERIALS IN NRC PUBLICATIONS

NRC Reference Material

As of November 1999, you may electronically access NUREG-series publications and other NRC records at NRC's Public Electronic Reading Room at www.nrc.gov/NRC/ADAMS/index.html. Publicly released records include, to name a few, NUREG-series publications; *Federal Register* notices; applicant, licensee, and vendor documents and correspondence; NRC correspondence and internal memoranda; bulletins and information notices; inspection and investigative reports; licensee event reports; and Commission papers and their attachments.

NRC publications in the NUREG series, NRC regulations, and *Title 10, Energy*, in the Code of *Federal Regulations* may also be purchased from one of these two sources.

1. The Superintendent of Documents
   U.S. Government Printing Office
   P. O. Box 37082
   Washington, DC 20402–9328
   www.access.gpo.gov/su_docs
   202–512–1800
2. The National Technical Information Service
   Springfield, VA 22161–0002
   www.ntis.gov
   1–800–533–6847 or, locally, 703–805–6000

A single copy of each NRC draft report for comment is available free, to the extent of supply, upon written request as follows:

Address: Office of the Chief Information Officer,
Reproduction and Distribution
Services Section
U.S. Nuclear Regulatory Commission
Washington, DC 20555-0001
E-mail: DISTRIBUTION@nrc.gov
Facsimile: 301–415–2289

Some publications in the NUREG series that are posted at NRC's Web site address www.nrc.gov/NRC/NUREGS/indexnum.html are updated periodically and may differ from the last printed version. Although references to material found on a Web site bear the date the material was accessed, the material available on the date cited may subsequently be removed from the site.

Non-NRC Reference Material

Documents available from public and special technical libraries include all open literature items, such as books, journal articles, and transactions, *Federal Register* notices, Federal and State legislation, and congressional reports. Such documents as theses, dissertations, foreign reports and translations, and non-NRC conference proceedings may be purchased from their sponsoring organization.

Copies of industry codes and standards used in a substantive manner in the NRC regulatory process are maintained at—

The NRC Technical Library
Two White Flint North
11545 Rockville Pike
Rockville, MD 20852–2738

These standards are available in the library for reference use by the public. Codes and standards are usually copyrighted and may be purchased from the originating organization or, if they are American National Standards, from—

American National Standards Institute
11 West 42nd Street
New York, NY 10036–8002
www.ansi.crg
212–642–4900

The NUREG series comprises (1) technical and administrative reports and books prepared by the staff (NUREG–XXXX) or agency contractors (NUREG/CR–XXXX), (2) proceedings of conferences (NUREG/CP–XXXX), (3) reports resulting from international agreements (NUREG/IA–XXXX), (4) brochures (NUREG/BR–XXXX), and (5) compilations of legal decisions and orders of the Commission and Atomic and Safety Licensing Boards and of Directors' decisions under Section 2.206 of NRC's regulations (NUREG–0750).

NUREG/CR-5736
ORNL/TM-13748

Evaluation of WF-70 Weld Metal From the Midland Unit 1 Reactor Vessel

Manuscript Completed: February 1998
Date Published: November 2000

Prepared by
D. E. McCabe, R. K. Nanstad, S. K. Iskander,
D. W. Heatherly, R. L. Swain

Oak Ridge National Laboratory
Managed by Lockheed Martin Energy Research Corporation

Oak Ridge National Laboratory
Oak Ridge, TN 37831-6151

C. J. Fairbanks, NRC Project Manager

Prepared for
Division of Engineering Technology
Office of Nuclear Regulatory Research
U.S. Nuclear Regulatory Commission
Washington, DC 20555-0001
NRC Job Code W6953

NUREG/CR-5736 has been reproduced from the best available copy.

ABSTRACT

Low upper-shelf (LUS) weld metal was sampled from the Midland Unit 1 reactor vessel. The weld metal was designated to be WF-70 by Babcock and Wilcox Company code. The sampling was taken from both the nozzle course and beltline girth welds. The as-received materials characterization using Charpy curves, drop-weight nil-ductility transition, tensile tests, and chemical analysis surveys indicated that the materials from the two locations were essentially the same except for the copper content. The expected nominal copper contents were 0.40 and 0.26 wt % for the nozzle course and beltline welds, respectively. Because the experiment involved detailed evaluations of both unirradiated and irradiated (1×10^{19} n/cm^2) conditions, the two weld metals were evaluated separately.

Fracture mechanics data were obtained for both the unirradiated and irradiated conditions; two methods of evaluating the transition temperatures were (1) the American Society of Mechanical Engineers (ASME) *Boiler and Pressure Vessel Code*, augmented with the American Society for Testing and Materials (ASTM) Method E 185, and (2) the relatively new master curve method. The ASME method uses a reference temperature determination (RT_{NDT}) from nonfracture mechanics test practices; the master curve method uses a transition temperature, T_o, obtained from fracture mechanics-based data. The deficiencies of the ASME method as applied to LUS materials were evident. The master curve method, supplemented with fracture mechanics–based R-curve data, proved to have sufficient sensitivity to show differences between the nozzle course and beltline materials. The ASME-recommended methods failed to detect differences, thereby revealing the lower sensitivity of the empirical methods associated with RT_{NDT}.

CONTENTS

FIGURES

TABLES

ACRONYMS

AISI	American Iron and Steel Institute
ASME	American Society of Mechanical Engineers
ASTM	American Society for Testing and Materials
CVN	Charpy V-notch
HAZ	heat-affected zone
HSSI	heavy-section steel irradiation
LUS	low upper shelf
MEA	Materials Engineering Associates
NDT	nil-ductility temperature
NRC	U.S. Nuclear Regulatory Commission
ORNL	Oak Ridge National Laboratory
PCVN	precracked Charpy V-notch
PVRC	Pressure Vessel Research Council
USE	upper-shelf energy

ACKNOWLEDGMENTS

This research was sponsored by the Office of Nuclear Regulatory Research, U.S. Nuclear Regulatory Commission, under Interagency Agreement DOE 1886-N695-3W with the U.S. Department of Energy under Contract No. DE-AC05-96OR22464 with Lockheed Martin Energy Research Corporation. I. I. Siman-Tov provided capsule design analyses, C. A. Baldwin managed the dosimetry work, and I. Remec computed the neutron exposures for Capsules 10.05 and 10.06. Their contributions to this project were invaluable. The authors would also like to acknowledge the contributions of Julia L. Bishop for preparation of the manuscript and Dave Cottrell for the graphics work. Also, the authors are indebted to M. A. Sokolov and R. E. Stoller for review and comments.

FOREWORD

The work reported here was performed at the Oak Ridge National Laboratory (ORNL) under the Heavy-Section Steel Irradiation (HSSI) Program, T. M. Rosseel, Program Manager. The program is sponsored by the Office of Nuclear Regulatory Research of the U.S. Nuclear Regulatory Commission (NRC). The technical monitor for the NRC is C. J. Fairbanks.

This report is designated HSSI Report 20. Reports in this series are listed below:

1. F. M. Haggag, W. R. Corwin, and R. K. Nanstad, Martin Marietta Energy Systems, Inc., Oak Ridge Natl. Lab., Oak Ridge, Tenn., *Irradiation Effects on Strength and Toughness of Three-Wire Series-Arc Stainless Steel Weld Overlay Cladding*, USNRC Report NUREG/CR-5511 (ORNL/TM-11439), February 1990.

2. L. F. Miller, C. A. Baldwin, F. W. Stallman, and F. B. K. Kam, Martin Marietta Energy Systems, Inc., Oak Ridge Natl. Lab., Oak Ridge, Tenn., *Neutron Exposure Parameters for the Metallurgical Test Specimens in the Sixth Heavy-Section Steel Irradiation Series*, USNRC Report NUREG/CR-5409 (ORNL/TM-11267), March 1990.

3. S. K. Iskander, W. R. Corwin, and R. K. Nanstad, Martin Marietta Energy Systems, Inc., Oak Ridge Natl. Lab., Oak Ridge, Tenn., *Results of Crack-Arrest Tests on Two Irradiated High-Copper Welds*, USNRC Report NUREG/CR-5584 (ORNL/TM-11575), December 1990.

4. R. K. Nanstad and R. G. Berggren, Martin Marietta Energy Systems, Inc., Oak Ridge Natl. Lab., Oak Ridge, Tenn., *Irradiation Effects on Charpy Impact and Tensile Properties of Low Upper-Shelf Welds*, HSSI Series 2 and 3, USNRC Report NUREG/CR-5696 (ORNL/TM-11804), August 1991.

5. R. E. Stoller, Martin Marietta Energy Systems, Inc., Oak Ridge Natl. Lab., Oak Ridge, Tenn., *Modeling the Influence of Irradiation Temperature and Displacement Rate on Radiation-Induced Hardening in Ferritic Steels*, USNRC Report NUREG/CR5859 (ORNL/TM-12073), August 1992.

6. R. K. Nanstad, D. E. McCabe, and R. L. Swain, Martin Marietta Energy Systems, Inc., Oak Ridge Natl. Lab., Oak Ridge, Tenn., *Chemical Composition RTNDT Determinations for Midland Weld WF-70*, USNRC Report NUREG/CR-5914 (ORNL-6740), December 1992.

7. R. K. Nanstad, F. M. Haggag, D. E. McCabe, S. K. Iskander, K. O. Bowman, and B. H. Menke, Martin Marietta Energy Systems, Inc., Oak Ridge Natl. Lab., Oak Ridge, Tenn., *Irradiation Effects on Fracture Toughness of Two High-Copper Submerged-Arc Welds*, USNRC Report NUREG/CR-5913 (ORNL/TM-12156/V1), October 1992.

8. S. K. Iskander, W. R. Corwin, and R. K. Nanstad, Martin Marietta Energy Systems, Inc., Oak Ridge Natl. Lab., Oak Ridge, Tenn., *Crack-Arrest Tests on Two Irradiated High-Copper Welds*, USNRC Report NUREG/CR-6139 (ORNL/TM-12513), March 1994.

9. R. E. Stoller, Martin Marietta Energy Systems, Inc., Oak Ridge Natl. Lab., Oak Ridge, Tenn., *A Comparison of the Relative Importance of Copper Precipitates and Point Defects in Reactor Pressure Vessel Embrittlement*, USNRC Report NUREG/CR-6231 (ORNL/TM-6811), December 1994.

10. D. E. McCabe, R. K. Nanstad, S. K. Iskander, and R. L. Swain, Martin Marietta Energy Systems, Inc., Oak Ridge Natl. Lab., Oak Ridge, Tenn., *Unirradiated Material Properties of Midland Weld WF-70*, USNRC Report NUREG/CR-6249 (ORNL/TM-12777), October 1994.

11. P. M. Rice and R. E. Stoller, Lockheed Martin Energy Systems, Oak Ridge Natl. Lab., Oak Ridge, Tenn., *Microstructural Characterization of Selected AEA/UCSB Model FeCuMn Alloys*, USNRC Report NUREG/CR-6332 (ORNL/TM-12980), June 1996.

12. J. H. Giovanola and J. E. Crocker, SRI International, *Fracture Toughness Testing with Cracked Round Bars: Feasibility Study*, USNRC Report NUREG/CR-6342 (ORNL/SUB/94-DHK60), to be published.

13. F. M. Haggag and R. K. Nanstad, Lockheed Martin Energy Systems, Oak Ridge Natl. Lab., Oak Ridge, Tenn., *Effects of Thermal Aging and Neutron Irradiation on the Mechanical Properties of Three-Wire Stainless Steel Weld Overlay Cladding*, USNRC Report NUREG/CR-6363 (ORNL/TM-13047), May 1997.

14. M. A. Sokolov and D. J. Alexander, Lockheed Martin Energy Systems, Oak Ridge Natl. Lab., Oak Ridge, Tenn., *An Improved Correlation Procedure for Subsize and Full-Size Charpy Impact Specimen Data*, USNRC Report NUREG/CR-6379 (ORNL/TM-13088), March 1997.

15. S. K. Iskander and R. E. Stoller, Lockheed Martin Energy Research Corporation, Oak Ridge Natl. Lab., Oak Ridge, Tenn., *Results of Charpy V-Notch Impact Testing of Structural Steel Specimens Irradiated at ~30°C to 1 $\times 10^{6}$ neutrons/cm^{2} in a Commercial Reactor Cavity*, USNRC Report NUREG/CR-6399 (ORNL-6886), April 1997.

16. S. K. Iskander, P. P. Milella, and A. Pini, Lockheed Martin Energy Research Corporation, Oak Ridge Natl. Lab., Oak Ridge, Tenn., *Results of Crack-Arrest Tests on Irradiated A 503 Class 3 Steel*, USNRC Report NUREG/CR-6447 (ORNL-6894), February 1998.

17. P. Pareige, K. F. Russell, R. E. Stoller, and M. K. Miller, Lockheed Martin Energy Research Corporation, Oak Ridge Natl. Lab., Oak Ridge, Tenn., *Influence of Long-Term Thermal Aging on the Microstructural Evolution of Nuclear Reactor Pressure Vessel Materials: An Atom Probe Study*, USNRC Report NUREG/CR-6537(ORNL-13406), March 1998.

18. I. Remec, C. A. Baldwin, and K. B. K. Kam, Lockheed Martin Energy Research Corporation, Oak Ridge Natl. Lab., Oak Ridge, Tenn., *Neutron Exposure Parameters for Capsule 10.05 in the Heavy-Section Steel Irradiation Program Tenth Irradiation Series*, USNRC Report NUREG/CR-6600 (ORNL/TM-13548), October 1998.

19. I. Remes, C. A. Baldwin, and F. B. K. Kam, Lockheed Martin Energy Research Corporation, Oak Ridge Natl. Lab., Oak Ridge, Tenn., *Neutron Exposure Parameters for the Dosimetry Capsule in the Heavy-Section Steel Irradiation Program Tenth Irradiation Series*, USNRC Report NUREG/CR-6601 (ORNL/TM-13549), October 1998.

20. This report.

The HSSI Program includes both follow-on and the direct continuation of work that was performed under the Heavy-Section Steel Technology (HSST) Program. Previous HSST reports related to irradiation effects in pressure vessel materials and those containing unirradiated properties of materials used in HSSI and HSST irradiation programs are tabulated below as a convenience to the reader.

C. E. Childress, Union Carbide Corp. Nuclear Div., Oak Ridge Natl. Lab., Oak Ridge, Tenn., *Fabrication History of the First Two 12-in.-Thick A-533 Grade B, Class 1 Steel Plates of the Heavy-Section Steel Technology Program*, ORNL-4313, February 1969.

T. R. Mager and F. O. Thomas, Westinghouse Electric Corporation, PWR Systems Division, Pittsburgh, Pa., *Evaluation by Linear Elastic Fracture Mechanics of Radiation Damage to Pressure Vessel Steels*, WCAP-7328 (Rev.), October 1969.

P. N. Randall, TRW Systems Group, Redondo Beach, Calif., *Gross Strain Measure of Fracture Toughness of Steels*, HSSTP-TR-3, Nov. 1, 1969.

L. W. Loechel, Martin Marietta Corporation, Denver, Colo., *The Effect of Testing Variables on the Transition Temperature in Steel*, MCR-69-189, Nov. 20, 1969.

W. O. Shabbits, W. H. Pryle, and E. T. Wessel, Westinghouse Electric Corporation, PWR Systems Division, Pittsburgh, Pa., *Heavy-Section Fracture Toughness Properties of A533 Grade B Class 1 Steel Plate and Submerged Arc Weldment*, WCAP-7414, December 1969.

C. E. Childress, Union Carbide Corp. Nuclear Div., Oak Ridge Natl. Lab., Oak Ridge, Tenn., *Fabrication History of the Third and Fourth ASTM A-533 Steel Plates of the Heavy-Section Steel Technology Program*, ORNL-4313-2, February 1970.

P. B. Crosley and E. J. Ripling, Materials Research Laboratory, Inc., Glenwood, Ill., *Crack Arrest Fracture Toughness of A533 Grade B Class 1 Pressure Vessel Steel*, HSSTP-TR-8, March 1970.

F. J. Loss, Naval Research Laboratory, Washington, D.C., *Dynamic Tear Test Investigations of the Fracture Toughness of Thick-Section Steel*, NRL-7056, May 14, 1970.

T. R. Mager, Westinghouse Electric Corporation, PWR Systems Division, Pittsburgh, Pa., *Post-Irradiation Testing of 2T Compact Tension Specimens*, WCAP-7561, August 1970.

F. J. Witt and R. G. Berggren, Union Carbide Corp. Nuclear Div., Oak Ridge Natl. Lab., Oak Ridge, Tenn., *Size Effects and Energy Disposition in Impact Specimen Testing of ASTM A533 Grade B Steel*, ORNL/TM-3030, August 1970.

D. A. Canonico, Union Carbide Corp. Nuclear Div., Oak Ridge Natl. Lab., Oak Ridge, Tenn., *Transition Temperature Considerations for Thick-Wall Nuclear Pressure Vessels*, ORNL/TM-3114, October 1970.

T. R. Mager, Westinghouse Electric Corporation, PWR Systems Division, Pittsburgh, Pa., *Fracture Toughness Characterization Study of A533, Grade B, Class 1 Steel*, WCAP-7578, October 1970.

W. O. Shabbits, Westinghouse Electric Corporation, PWR Systems Division, Pittsburgh, Pa., *Dynamic Fracture Toughness Properties of Heavy-Section A533 Grade B Class 1 Steel Plate*, WCAP-7623, December 1970.

C. E. Childress, Union Carbide Corp. Nuclear Div., Oak Ridge Natl. Lab., Oak Ridge, Tenn., *Fabrication Procedures and Acceptance Data for ASTM A-533 Welds and a 10-in.-Thick ASTM A-543 Plate of the Heavy Section Steel Technology Program*, ORNL-TM-4313-3, January 1971.

D. A. Canonico and R. G. Berggren, Union Carbide Corp. Nuclear Div., Oak Ridge Natl. Lab., Oak Ridge, Tenn., *Tensile and Impact Properties of Thick-Section Plate and Weldments*, ORNL/TM-3211, January 1971.

C. W. Hunter and J. A. Williams, Hanford Eng. Dev. Lab., Richland, Wash., *Fracture and Tensile Behavior of Neutron-Irradiated A533-B Pressure Vessel Steel, HEDL-TME-71-76*, Feb. 6, 1971.

C. E. Childress, Union Carbide Corp. Nuclear Div., Oak Ridge Natl. Lab., Oak Ridge, Tenn., *Manual for ASTM A533 Grade B Class 1 Steel (HSST Plate 03) Provided to the International Atomic Energy Agency*, ORNL/TM-3193, March 1971.

P. N. Randall, TRW Systems Group, Redondo Beach, Calif., *Gross Strain Crack Tolerance of A533-B Steel*, HSSTP-TR-14, May 1, 1971.

C. L. Segaser, Union Carbide Corp. Nuclear Div., Oak Ridge Natl. Lab., Oak Ridge, Tenn., *Feasibility Study, Irradiation of Heavy-Section Steel Specimens in the South Test Facility of the Oak Ridge Research Reactor*, ORNL/TM-3234, May 1971.

H. T. Corten and R. H. Sailors, University of Illinois, Urbana, Ill., *Relationship Between Material Fracture Toughness Using Fracture Mechanics and Transition Temperature Tests*, T&AM Report 346, Aug. 1, 1971.

L. A. James and J. A. Williams, Hanford Eng. Dev. Lab., Richland, Wash., *Heavy Section Steel Technology Program Technical Report No. 21, The Effect of Temperature and Neutron Irradiation Upon the Fatigue-Crack Propagation Behavior of ASTM A533 Grade B, Class 1 Steel*, HEDL-TME 72-132, September 1972.

P. B. Crosley and E. J. Ripling, Materials Research Laboratory, Inc., Glenwood, Ill., *Crack Arrest in an Increasing K-Field*, HSSTP-TR-27, January 1973.

W. J. Stelzman and R. G. Berggren, Union Carbide Corp. Nuclear Div., Oak Ridge Natl. Lab., Oak Ridge, Tenn., *Radiation Strengthening and Embrittlement in Heavy-Section Steel Plates and Welds*, ORNL-4871, June 1973.

J. M. Steichen and J. A. Williams, Hanford Eng. Dev. Lab., Richland, Wash., *High Strain Rate Tensile Properties of Irradiated ASTM A533 Grade B Class 1 Pressure Vessel Steel*, HEDL-TME 73-74, July 1973.

J. A. Williams, Hanford Eng. Dev. Lab., Richland, Wash., *The Irradiation and Temperature Dependence of Tensile and Fracture Properties of ASTM A533, Grade B, Class 1 Steel Plate and Weldment*, HEDL-TME 73-75, August 1973.

J. A. Williams, Hanford Eng. Dev. Lab., Richland, Wash., *Some Comments Related to the Effect of Rate on the Fracture Toughness of Irradiated ASTM A553-B Steel Based on Yield Strength Behavior*, HEDL-SA 797, December 1974.

J. A. Williams, Hanford Eng. Dev. Lab., Richland, Wash., *The Irradiated Fracture Toughness of ASTM A533, Grade B, Class 1 Steel Measured with a Four-Inch-Thick Compact Tension Specimen*, HEDL-TME 75-10, January 1975.

J. G. Merkle, G. D. Whitman, and R. H. Bryan, Union Carbide Corp. Nuclear Div., Oak Ridge Natl. Lab., Oak Ridge, Tenn., *An Evaluation of the HSST Program Intermediate Pressure Vessel Tests in Terms of Light-Water-Reactor Pressure Vessel Safety*, ORNL/TM-5090, November 1975.

J. A. Davidson, L. J. Ceschini, R. P. Shogan, and G. V. Rao, Westinghouse Electric Corporation, Pittsburgh, Pa., *The Irradiated Dynamic Fracture Toughness of ASTM A533, Grade B, Class 1 Steel Plate and Submerged Arc Weldment*, WCAP-8775, October 1976.

J. A. Williams, Hanford Eng. Dev. Lab., Richland, Wash., *Tensile Properties of Irradiated and Unirradiated Welds of A533 Steel Plate and A508 Forgings*, NUREG/CR-1158 (ORNL/SUB-79/50917/2), July 1979.

J. A. Williams, Hanford Eng. Dev. Lab., Richland, Wash., *The Ductile Fracture Toughness of Heavy-Section Steel Plate*, NUREG/CR-0859, September 1979.

K. W. Carlson and J. A. Williams, Hanford Eng. Dev. Lab., Richland, Wash., *The Effect of Crack Length and Side Grooves on the Ductile Fracture Toughness Properties of ASTM A533 Steel*, NUREG/CR-1171 (ORNL/SUB-79/50917/3), October 1979.

G. A. Clarke, Westinghouse Electric Corp., Pittsburgh, Pa., *An Evaluation of the Unloading Compliance Procedure for J-Integral Testing in the Hot Cell, Final Report*, NUREG/CR-1070 (ORNL/SUB-7394/1), October 1979.

P. B. Crosley and E. J. Ripling, Materials Research Laboratory, Inc., Glenwood, Ill., *Development of a Standard Test for Measuring KIa with a Modified Compact Specimen*, NUREG/CR-2294 (ORNL/SUB-81/7755/1), August 1981.

H. A. Domian, Babcock and Wilcox Company, Alliance, Ohio, *Vessel V-8 Repair and Preparation of Low Upper-Shelf Weldment*, NUREG/CR-2676 (ORNL/SUB/81-85813/1), June 1982.

R. D. Cheverton, S. K. Iskander, and D. G. Ball, Union Carbide Corp. Nuclear Div., Oak Ridge Natl. Lab., Oak Ridge, Tenn., *PWR Pressure Vessel Integrity During Overcooling Accidents: A Parametric Analysis*, NUREG/CR-2895 (ORNL/TM-7931), February 1983.

J. G. Merkle, Union Carbide Corp. Nuclear Div., Oak Ridge Natl. Lab., Oak Ridge, Tenn., *An Examination of the Size Effects and Data Scatter Observed in Small Specimen Cleavage Fracture Toughness Testing*, NUREG/CR-3672 (ORNL/TM-9088), April 1984.

W. R. Corwin, Martin Marietta Energy Systems, Inc., Oak Ridge Natl. Lab., Oak Ridge, Tenn., *Assessment of Radiation Effects Relating to Reactor Pressure Vessel Cladding*, NUREG/CR-3671 (ORNL-6047), July 1984.

W. R. Corwin, R. G. Berggren, and R. K. Nanstad, Martin Marietta Energy Systems, Inc., Oak Ridge Natl. Lab., Oak Ridge, Tenn., *Charpy Toughness and Tensile Properties of a Neutron Irradiated Stainless Steel Submerged-Arc Weld Cladding Overlay*, NUREG/CR-3927 (ORNL/TM-9709), September 1984.

J. J. McGowan, Martin Marietta Energy Systems, Inc., Oak Ridge Natl. Lab., Oak Ridge, Tenn., *Tensile Properties of Irradiated Nuclear Grade Pressure Vessel Plate and Welds for the Fourth HSST Irradiation Series*, NUREG/CR-3978 (ORNL/TM-9516), January 1985.

J. J. McGowan, Martin Marietta Energy Systems, Inc., Oak Ridge Natl. Lab., Oak Ridge, Tenn., *Tensile Properties of Irradiated Nuclear Grade Pressure Vessel Welds for the Third HSST Irradiation Series*, NUREG/CR-4086 (ORNL/TM-9477), March 1985.

W. R. Corwin, G. C. Robinson, R. K. Nanstad, J. G. Merkle, R. G. Berggren, G. M. Goodwin, R. L. Swain, and T. D. Owings, Martin Marietta Energy Systems, Inc., Oak Ridge Natl. Lab., Oak Ridge, Tenn., *Effects of Stainless Steel Weld Overlay Cladding on the Structural Integrity of Flawed Steel Plates in Bending, Series 1*, NUREG/CR-4015 (ORNL/TM-9390), April 1985.

W. J. Stelzman, R. G. Berggren, and T. N. Jones, Martin Marietta Energy Systems, Inc., Oak Ridge Natl. Lab., Oak Ridge, Tenn., *ORNL Characterization of Heavy-Section Steel Technology Program Plates 01, 02, and 03*, NUREG/CR-4092 (ORNL/TM-9491), April 1985.

G. D. Whitman, Martin Marietta Energy Systems, Inc., Oak Ridge Natl. Lab., Oak Ridge, Tenn., *Historical Summary of the Heavy-Section Steel Technology Program and Some Related Activities in Light-Water Reactor Pressure Vessel Safety Research*, NUREG/CR-4489 (ORNL-6259), March 1986.

R. H. Bryan, B. R. Bass, S. E. Bolt, J. W. Bryson, J. G. Merkle, R. K. Nanstad, and G. C. Robinson, Martin Marietta Energy Systems, Inc., Oak Ridge Natl. Lab., Oak Ridge, Tenn., *Test of 6-in.-Thick Pressure Vessels. Series 3: Intermediate Test Vessel V-8A - Tearing Behavior of Low Upper-Shelf Material*, NUREG-CR-4760 (ORNL-6187), May 1987.

D. B. Barker, R. Chona, W. L. Fourney, and G. R. Irwin, University of Maryland, College Park, Md., *A Report on the Round Robin Program Conducted to Evaluate the Proposed ASTM Standard Test Method for Determining the Plane Strain Crack Arrest Fracture Toughness, K_{Ia}, of Ferritic Materials*, NUREG/CR-4966 (ORNL/SUB/79-7778/4), January 1988.

L. F. Miller, C. A. Baldwin, F. W. Stallman, and F. B. K. Kam, Martin Marietta Energy Systems, Inc., Oak Ridge Natl. Lab., Oak Ridge, Tenn., *Neutron Exposure Parameters for the Metallurgical Test Specimens in the Fifth Heavy-Section Steel Technology Irradiation Series Capsules*, NUREG/CR-5019 (ORNL/TM-10582), March 1988.

J. J. McGowan, R. K. Nanstad, and K. R. Thoms, Martin Marietta Energy Systems, Inc., Oak Ridge Natl. Lab., Oak Ridge, Tenn., *Characterization of Irradiated Current-Practice Welds and A533 Grade B Class 1 Plate for Nuclear Pressure Vessel Service*, NUREG/CR-4880 (ORNL-6484/V1 and V2), July 1988.

R. D. Cheverton, W. E. Pennell, G. C. Robinson, and R. K. Nanstad, Martin Marietta Energy Systems, Inc., Oak Ridge Natl. Lab., Oak Ridge, Tenn., *Impact of Radiation Embrittlement on Integrity of Pressure Vessel Supports for Two PWR Plants*, NUREG/CR-5320 (ORNL/TM-10966), February 1989.

J. G. Merkle, Martin Marietta Energy Systems, Inc., Oak Ridge Natl. Lab., Oak Ridge, Tenn., *An Overview of the Low-Upper-Shelf Toughness Safety Margin Issue*, NUREG/CR-5552 (ORNL/TM-11314), August 1990.

R. D. Cheverton, T. L. Dickson, J. G. Merkle, and R. K. Nanstad, Martin Marietta Energy Systems, Inc., Oak Ridge Natl. Lab., Oak Ridge, Tenn., *Review of Reactor Pressure Vessel Evaluation Report for Yankee Rowe Nuclear Power Station (YAEC No. 1735)*, NUREG/CR-5799 (ORNL/TM-11982), March 1992.

1. INTRODUCTION

The purpose of the present Heavy-Section Steel Irradiation (HSSI) Tenth Irradiation Series was to characterize the mechanical properties and chemical variability in a commercially produced low upper-shelf (LUS) weld metal identified as WF-70 in the unirradiated and irradiated conditions. The plan also included irradiation embrittlement evaluation by various known ductile-brittle evaluation methods.

The WF-70 weld metal was obtained from the Midland nuclear reactor facility owned by Consumers Power Company, Midland, Michigan. The Unit 1 reactor pressure vessel became available for research when the utility decided to abandon plans to operate the plant. A consortium representing utilities, vendors, and the U.S. Nuclear Regulatory Commission (NRC) was formed on October 5, 1989, to plan research studies that could be of value. Subsequently, the entire beltline circumferential weld and portions of the nozzle shell course circumferential weld were removed in segments of about 1.17 m (46 in.) long and 0.76 m (30 in.) wide spanning the weld line[1] (see Figure 1). The vessel wall was about 0.2 m (8.75 in.) thick at the beltline course, and the nozzle course wall was 0.305 m (12 in.) thick.

ORNL 98-8320/rra

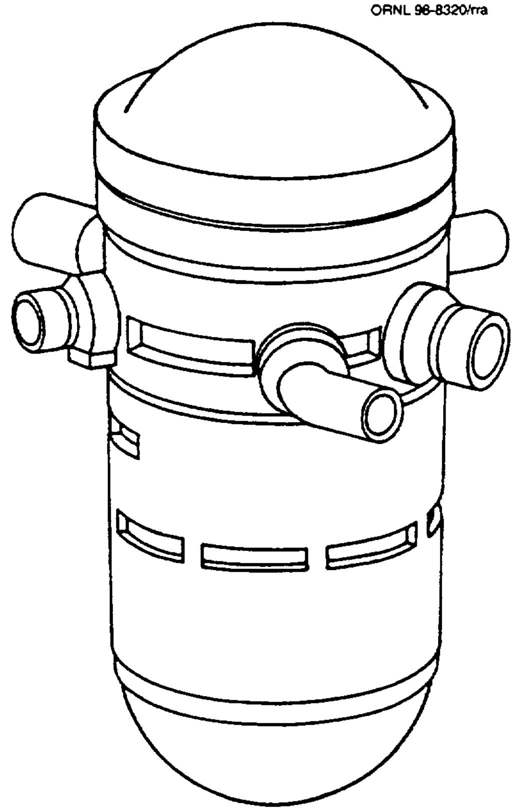

Figure 1. Sampling locations in the Midland Unit 1 reactor pressure vessel.

The WF-70 designation is a Babcock and Wilcox Company code that identifies the specific heat of weld wire (Heat 72105) and the specific welding flux lot (Linde 80, lot 8669) used. WF -70 is known as an LUS weld metal because it displays a relatively low upper-shelf energy and because of its Charpy behavior when evaluated according to a procedure set forth in Article 2300, Section III, of the American Society of Mechanical Engineers (ASME) Boiler and Pressure Vessel Code.[2] LUS steels often display less than 68 J (50 ft-lb) Charpy V-notch (CVN) energy at a temperature 33°C (60°F) above the drop-weight nil-ductility transition (NDT) temperature, in which case the reference temperature, RT_{NDT}, is determined by the Charpy impact properties, which will be higher than the drop-weight NDT temperature.

The salient features of the HSSI Tenth Irradiation Series experimental plan are presented in Table 1. The three phases are (1) development of baseline material properties using conventional test methods, (2) development of fracture mechanics–related properties for the unirradiated condition, and (3) evaluation of the transition temperature shift from irradiation damage using both the conventional ASME evaluation method and a relatively new fracture mechanics–based "master curve" method.

Table 1. HSSI Tenth Irradiation Series experimental plan for Midland weld WF-70

Phase 1—Material characterization
Charpy V-notch transition curves Drop-weight NDT Chemical composition
Phase 2—Unirradiated fracture mechanics development
K_{Jc} transition curves J-R curves K_{Ia} crack-arrest transition Tensile properties
Phase 3—Irradiation effects
Scoping Capsules 10.01 and 10.02 (0.5×10^{19} n/cm^2) Two large fracture mechanics Capsules 10.05 and 10.06 (1×10^{19} n/cm^2) Compact specimens, 1/2T, 1T J-R curve specimens, 1T Standard Charpy specimens Tensile specimens

2. MATERIALS

Figure 1 shows the sampling locations in the Midland Unit 1 RPV. Seven of the eight 1.17-m-long coupon cutouts from the beltline weld were provided to the HSSI program. Only two of the six nozzle course coupons were provided to this program. Figure 2 shows the identification codes assigned to the coupon cutouts. Only the digits after the dash in the beltline code were carried over into the test specimen identification plan. Both of the nozzle course coupon identification numbers were carried over into that specimen identification plan.

A 13-mm-thick (0.5-in.) through-thickness slice was taken of both welds to view the cross-section shape and dimensions of the welds (Figures 3 and 4). The beltline weld was a double-V, containing all WF-70 filler weld. The forging thickness is about 0.2 m (8.75 in.). A later discovery revealed that there had been repair welding in several locations. Coupon 1-13 had about 0.15 m (6 in.) of repair weld, and Coupons 1-12 and 1-14 each had about 0.25 m (10 in.) of repair. Additional details can be found in NUREG/CR- 5914.[3] The nozzle course weld, shown in Figure 4, at first created some confusion until it was realized that the broad weld band that intersects the interior half of the double-V was part of a nozzle insert weld. No weld metal of interest was lost because the inside weld was WF-67, not intended for this study. The overall thickness of the nozzle course ring is 0.30 m (12 in.). Postweld heat treatments were 22.5 h for the beltline and 25.5 h for the nozzle course, both at 607°C (1125°F). The

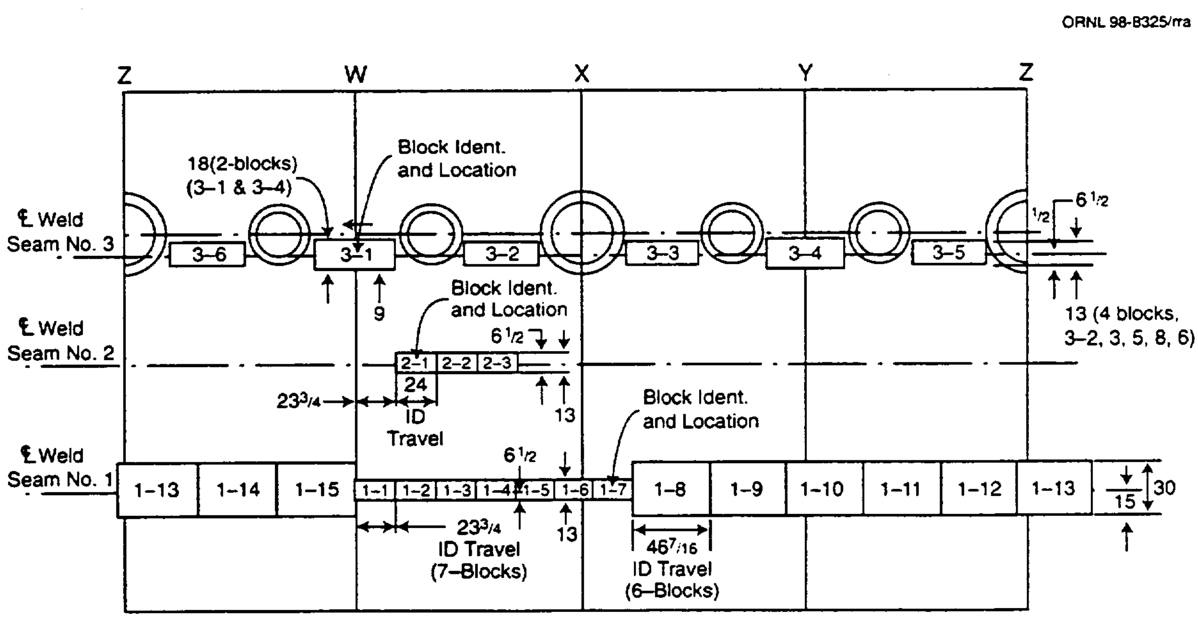

Figure 2. **Sampling layout for Midland beltline Sections 1-8 through 1-15 and nozzle course Sections 3-1 through 3-6.**

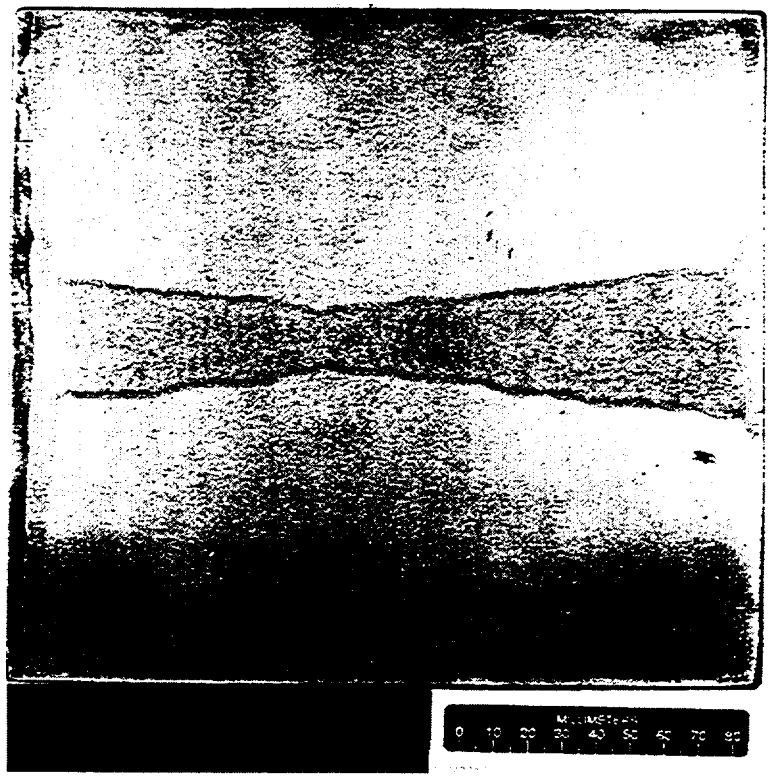

Figure 3. Beltline weld, showing double-V weld of submerged-arc layered WF-70 weld metal on both sides.

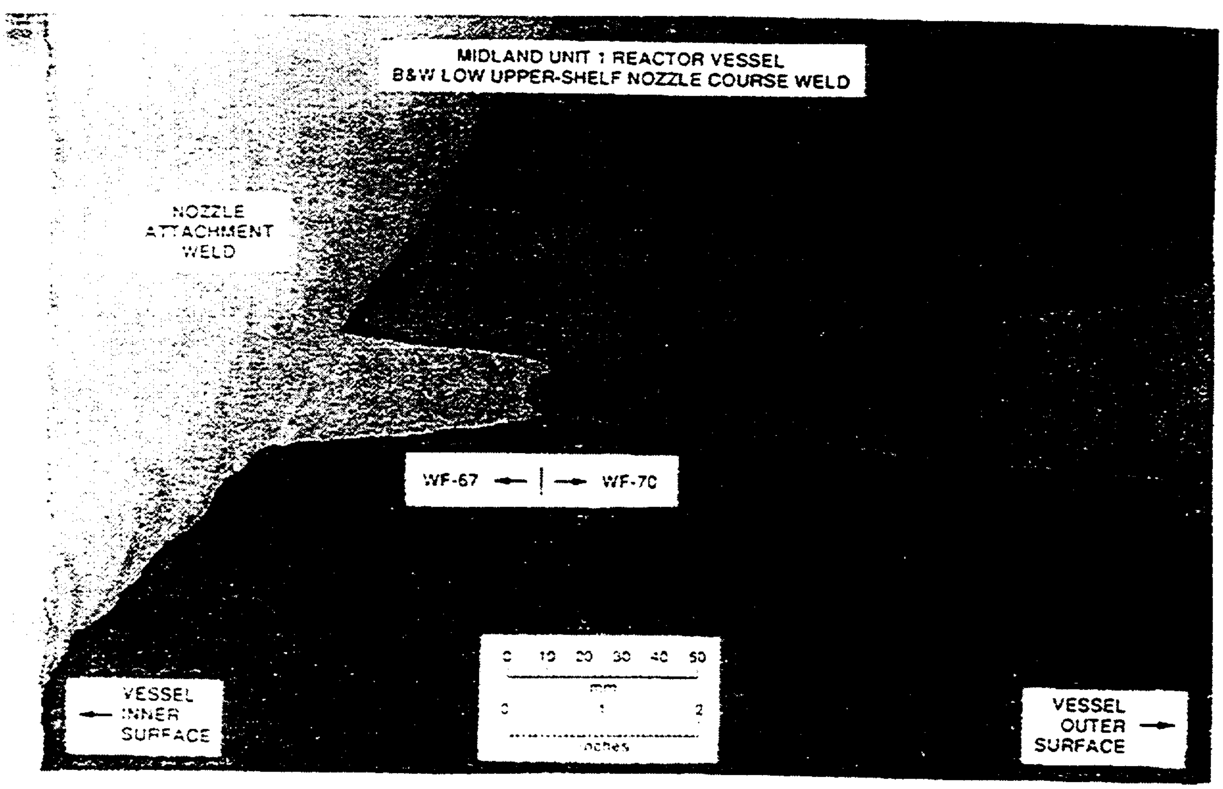

Figure 4. Nozzle course double-V weld showing WF-67 and WF-70 weld halves.

base metal was American Society for Testing and Materials (ASTM) A 508 class 2, as modified according to Code Case 1332-4 and the 1968 Edition of the ASME Code, Section III.

The specimen sampling plan was to slice each 1.17-m-long coupon at varied intervals to suit the various specimen sizes needed. An alphabetic code sequence was applied to these slices. A second alphabetic sequence was applied for sampling of specimen blanks traversing in the through-thickness direction. The wide variety of specimen types and sizes is too complex for further detailing here. Records are being maintained on the specimen locations for future reference, if needed. A general policy applied was to position fracture-mechanics type specimens as much as possible about the 1/4t and 3/4t through-thickness locations.

Crack propagation direction in all fracture toughness type specimens, except for drop-weight NDT specimens was in the weld path direction with the normals to the crack plane projecting into the base metal (T-L). The crack propagation direction for NDT was in the through-thickness direction of the weld.

3. UNIRRADIATED MATERIAL PROPERTIES

The baseline material property characterizations presented in this section are CVN transition curves, drop-weight NDT temperatures, yield and tensile strengths, and the specific chemical elements that are known to sensitize steels to irradiation damage. For this part of the study, four of the beltline weld coupons and both nozzle course weld coupons were used. The beltline weld was sampled from the coupons spaced at 90° intervals around the girth. The two nozzle course weld coupons were spaced about 180° apart. The beltline weld was tested for chemistry and CVN at five through-thickness locations; the nozzle course was tested at three positions in the WF-70 half of that weld.

Table 2 summarizes the results of the multiple through-thickness chemical element distributions. The five elements displayed are the important ones to consider for sensitivity to irradiation damage. All elements in the beltline and nozzle course welds are essentially the same except for copper. In the WF-70 beltline weld, the copper content was considerably less than the 0.40 wt % generic value reported by Babcock and Wilcox for WF-70.[4] The WF-70 nozzle course weld had a copper content almost the same as the reported generic value. The copper content in the WF-70 welds is not expected to be uniform because the copper comes principally from the protective copper coating applied to the filler wire. The coating thickness apparently is not always rigorously controlled. In fact, the lower values

Table 2. Summary of major radiation-sensitive elements for Midland Unit 1 reactor vessel welds

Section number	n[a]	Element (wt % ± 1σ)				
		Cu[b]	Ni	P	Mn	Si
Beltline weld						
1-9	8	0.26 ± 0.041 (0.22–0.34)	0.566 ± 0.031	0.016 ± 0.0013	1.629 ± 0.050	0.605 ± 0.031
1-11	8	0.258 ± 0.027 (0.23–0.31)	0.57 ± 0.007	0.016 ± 0.0014	1.615 ± 0.015	0.62 ± 0.029
1-13	5	0.248 ± 0.039 (0.21–0.32)	0.604 ± 0.016	0.018 ± 0.002	1.55 ± 0.067	0.62 ± 0.041
1-15	7	0.254 ± 0.026 (0.22–0.29)	0.567 ± 0.009	0.018 ± 0.0013	1.614 ± 0.014	0.644 ± 0.016
Average	28	0.256 ± 0.034 (0.21–0.34)	0.574 ± 0.023	0.017 ± 0.0019	1.607 ± 0.049	0.622 ± 0.033
Nozzle course weld						
3-1	4	0.398 ± 0.034 (0.37–0.46)	0.576 ± 0.021	0.015 ± 0.001	1.59 ± 0.045	0.548 ± 0.051
3-4	5	0.392 ± 0.016 (0.38–0.42)	0.567 ± 0.008	0.015 ± 0.002	1.61 ± 0.018	0.55 ± 0.043
Average	9	0.396 ± 0.028 (0.37–0.46)	0.572 ± 0.017	0.015 ± 0.002	1.59 ± 0.037	0.55 ± 0.048
Total average	18	0.290 ± 0.068 (0.21–0.46)	0.574 ± 0.022	0.016 ± 0.002	1.604 ± 0.046	0.605 ± 0.048

[a]Number of measurements.
[b]Range of copper shown in parentheses.

reported for the beltline weld only agree with the copper content of 0.27 wt % reported in the Midland weld qualification records. More detailed information on the chemistry determinations is given in NUREG/CR-5914.[3]

As a result of the difference in copper content between the beltline and nozzle course welds, the materials were considered as different materials for irradiation damage evaluations.

3.1 Drop-Weight NDT

Type P-3 drop-weight specimens were fabricated using single-pass brittle weld beads. The testing was performed according to ASTM Standard Method E 208-95a.[5] The specimens were aligned with the long dimension transverse to the weld path direction and the crack propagation direction through thickness. Table 3 lists the NDT temperatures for each sampled coupon. The average value of −50°C fairly represents WF-70 weld metal, and, as it was with the CVN results, no significant difference was found between WF-70 beltline and nozzle course welds. Because WF-70 is an LUS weld metal, these NDT results did not define RT_{NDT} and as such could not be used for the placement of ASME K_{Ic} or K_{Ia} lower-bound curves according to code practice.

3.2 Charpy Transition Temperature Results

CVN transition temperature is usually indexed to specific energy levels such as the temperatures at 41 or 68 J (30 or 50 ft-lb). The upper-shelf energies are reputed to correlate with the material's resistance to ductile tearing (R-curves). The standard practice to measure transition temperature shift

Table 3. Drop-weight test results for Midland welds

Through-thickness location	NDT temperature [°C (°F)]					
	1-9	1-11	1-13	1-15	3-1	3-4
1/4t	−60 (−76)	−60 (−76)	−60 (−76)	−45 (−49)	−45[a] (−49)	−55[a] (−67)
3/4t	−50 (−58)	−50 (−58)	−45 (−49)	−55 (−67)	−40 (−40)	−50 (−58)

[a]Nozzle welds 3-1 and 3-4 at 7/8t positions instead of 1/4t.

caused by irradiation is usually referenced from the 41-J energy level.[6] LUS materials generally result in RT_{NDT} reference temperatures based on the CVN 68-J temperature minus 33°C.[2] As has been previously noted, WF-70 is such a material.

CVN transition curves were determined at five through-thickness positions in three of the seven available beltline weld coupons. A fourth coupon, 1-13, had four through-thickness positions. These data are presented in Table 4. The box designated "RT_{NDT}" had determinations made exactly according to the wording used in the ASME Code, Section III, Article NB-2331. Note that the range of RT_{NDT} temperatures covers from –20 to 37°C; a 57°C spread. Table 5 is similarly constructed from the CVN data of the WF-70 nozzle course weld. In this case, there were only two coupons and three through-thickness positions sampled, for a total of six RT_{NDT} determinations.

The conclusion drawn from these CVN results was that the beltline and nozzle course unirradiated fracture toughness properties were essentially the same. Consequently, all CVN data (see Appendix A) were combined to make one CVN curve (Figure 5). Similar data scatter has been seen before in the HSSI Fifth Irradiation Series. However, in that case, the weld metal was specially fabricated using precisely controlled welding techniques for maximized uniformity of material properties.

3.3 Tensile Properties

Tensile specimens of the geometry shown in Figure 6 were aligned transverse to the longitudinal direction of the weld. This alignment was chosen so that tensile properties would be determined in the direction normal to the crack plane of fracture toughness specimens. Hence, the parallel section of tensile specimens was WF-70 weld metal, the radius section entering the shoulder was the heat-affected zone (HAZ), and the shoulders were all base metal. This orientation turned out to be an unfortunate choice in the case of the beltline welds because the HAZ material appeared to be of slightly lower strength, and all tensile specimens displayed the final separation at the fusion line. This did not develop with the nozzle course specimens, however. The results are given in Table 6, Part 1. The previous concern about the effect of a weakness in HAZ was checked by gathering tensile data from other sources (Table 6, Part 2). Consequently, a new set of tensile specimens for the beltline weld were made oriented in the longitudinal direction. These were 100% weld metal. Part 3 of Table 6 contains the final results. See also Appendix A for individual datum. These results were selected to

Table 4. Summary of unirradiated Charpy impact results for Midland Unit 1 reactor vessel beltline weld sections

Through-thickness position	Charpy V-notch tests												RT$_{M}$,[a] °C (°F), at weld section				RT$_{NDT}$,[b] °C (°F), at weld section			
	41-J temperature, °C (°F), at weld section				68-J temperature, °C (°F), at weld section				Upper-shelf energy, J (ft-lb), at weld section											
	1-13	1-9	1-11	1-15	1-13	1-9	1-11	1-15	1-13	1-9	1-11	1-15	1-13	1-9	1-11	1-15	1-13	1-9	1-11	1-15
1/4t	−11 (12)	−6 (21)	−13 (8)	4 (39)	21 (69)	37 (98)	25 (76)	50 (122)	101 (74)	77 (57)	91 (67)	82 (60)	−9 (15)	3 (37)	−9 (16)	16 (61)	−13 (9)	14 (57)	−9 (16)	16 (61)
1/2t	−16 (3)	−11 (13)	−4 (25)	−9 (15)	29 (84)	25 (77)	23 (74)	17 (63)	104 (77)	83 (61)	91 (67)	88 (65)	−5 (24)	−8 (17)	−10 (14)	−16 (3)	2 (36)	−8 (17)	−10 (14)	−15 (5)
5/8t	−22 (−7)	−18 (0)	−10 (13)	3 (37)	9 (48)	18 (64)	17 (63)	49 (121)	108 (80)	88 (65)	90 (66)	85 (62)	−25 (−12)	−16 (3)	−16 (3)	15 (60)	−20 (−3)	−16 (3)	−16 (3)	8 (47)
3/4t	−2 (27)	3 (38)	14 (57)	−6 (21)	37 (98)	53 (128)	58 (136)	28 (82)	90 (66)	81 (60)	84 (62)	89 (66)	3 (37)	20 (68)	24 (76)	−6 (21)	6 (43)	20 (68)	37 (99)	−6 (22)
7/8t		−3 (26)	−13 (8)	−8 (18)		46 (116)	30 (86)	22 (72)		78 (57)	79 (58)	83 (61)		13 (55)	−4 (25)	−12 (11)		13 (56)	18 (65)	−3 (26)

[a]Determined from T_{50}–60°F (T_{68}–33°C) using median curve fit, where T_{50} is the temperature corresponding to 50 ft-lb.
[b]Determined from T_{50}–60°F (T_{68}–33°C) using minimum curve fit, where T_{50} is the temperature corresponding to 50 ft-lb.

Table 5. Summary of Charpy impact results for Midland Unit 1 reactor vessel nozzle course weld sections

Through-thickness position	Charpy V-notch tests: 41-J temperature, °C (°F), at weld section		68-J temperature, °C (°F), at weld section		Upper-shelf energy, J (ft-lb), at weld section		RT_M,[a] °C (°F), at weld section		RT_{NDT},[b] °C (°F), at weld section	
	3-1	3-4	3-1	3-4	3-1	3-4	3-1	3-4	3-1	3-4
1/2t	5 (42)	–11 (13)	47 (117)	51 (125)	86 (63)	88 (65)	14 (57)	18 (65)	14 (57)	18 (65)
3/4t	2 (35)	–1 (30)	49 (120)	45 (112)	89 (65)	85 (63)	16 (61)	11 (52)	16 (61)	11 (52)
7/8t	-10 (15)	5 (42)	26 (78)	47 (116)	90 (66)	89 (66)	–8 (18)	14 (57)	–8 (18)	14 (57)

[a]Determined from T_{50} – 60°F (T_{68} – 33°C) using median curve fit.
[b]Determined from T_{50} – 60°F (T_{68} – 33°C) using minimum curve fit.

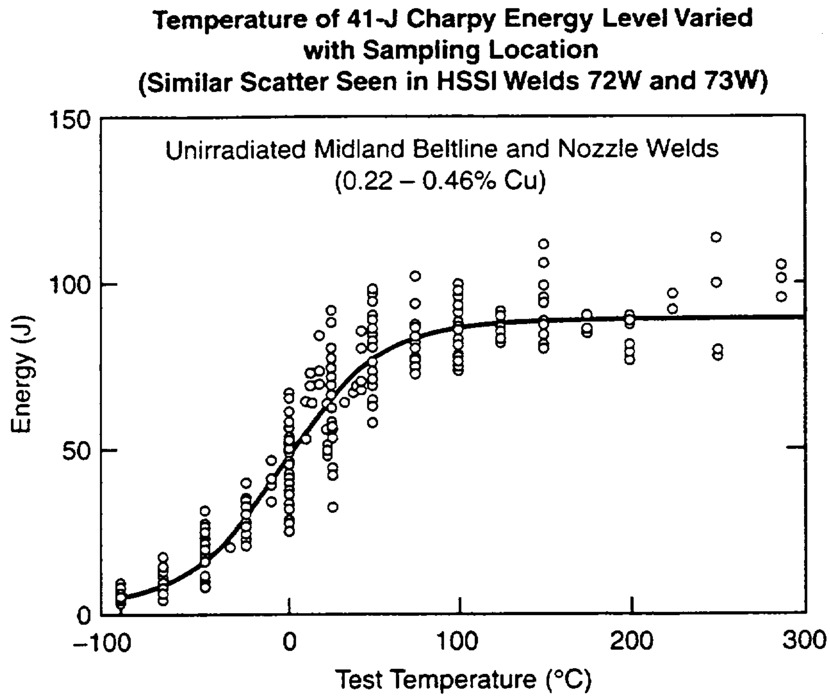

Figure 5. **Assembly of 19 beltline and 6 nozzle course Charpy V-notch data sets.**

ORNL 98-8327/rra

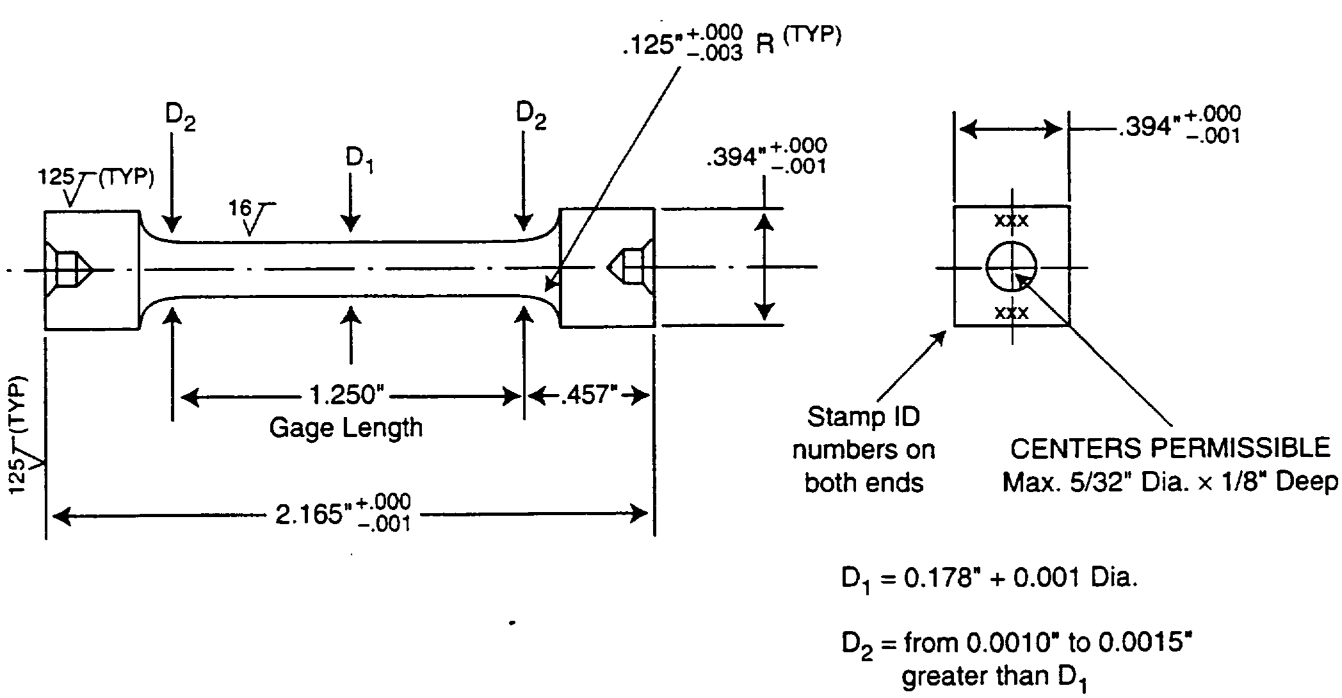

Figure 6. **Square-end tensile specimen used for unirradiated and irradiated tensile testing.**

Table 6. Unirradiated tensile strength data
(average from duplicate specimens)

Material	Test temperature (°C)	Yield strength		Ultimate tensile strength	
		(MPa)	(ksi)	(MPa)	(ksi)
Part 1—Initial tests made with transverse specimens					
Beltline[a]	23	407	59.2	586	85.7
Nozzle	23	545	79.3	655	94.9
Part 2—WF-70 tensile properties reported elsewhere					
PQD beltline[b] WF-70	23	500	72.5	603	87.5
NBD nozzle[c] WF-70	23	534	77.4	639	92.7
66W nozzle WF-70	23	527	76.5	632	91.7
Part 3—Longitudinal beltline and transverse nozzle - tensile properties					
Beltline	Room	512	74.3	613	88.9
	288	469	69.7	609	88.4
	150	478	69.0	585	84.8
	–25	556	80.7	671	97.3
	–50	569	82.6	694	100.7
	–100	625	90.7	764	110.8
Nozzle	Room	545	79.3	655	94.9
	288	484	70.3	587	85.2
	160	485	70.4	587	85.2
	–50	580	84.1	718	104.2
	–100	650	94.3	816	118.9

[a]All fractures at weld fusion line.
[b]PQD = weld process qualification data.
[c]NBD = nozzle belt dropout.

represent the true baseline tensile properties for the beltline weld metal in this project. Longitudinally oriented beltline weld tensile specimens were included with the transverse specimens slated for irradiation capsules.

The bottom line on these tensile property determinations is that the WF-70 nozzle course weld metal had slightly higher strength properties than the WF-70 beltline weld metal. This may have resulted from a thickness-caused difference in the effectiveness of the postweld stress relief anneal.

3.4 Fracture Mechanics Tests

Fracture mechanics–based data have been generated using compact specimens, C(T), and to a lesser extent, precracked Charpy V-notch (PCVN) specimens. The size of C(T) specimens varied from 1/2T to 4T, and the test data were generated principally within the transition temperature range. Data validity requirements for K_{Ic} by ASTM Standard Method E 399[7] were cast aside in favor of more liberal specimen size allowances based on both experimental evidence and by three-dimensional finite-element analyses. These more relaxed specimen size requirements are described in ASTM Test Method E1921-97. For transition range data, the initial remaining ligament, b_o, requirement for acceptable control of constraint is calculated from:

$$b_o \geq 30\ K_{Jc}^2 / \left(E\sigma_{ys}\right), \tag{1}$$

where K_{Jc} is an elastic-plastic stress intensity factor obtained by conversion from J-integral. J_c is calculated at the point of onset of cleavage instability. Here it is assumed that the specimen thickness dimension, B, is at least equal to or greater than b_o. Another validity criterion is that slow-stable crack growth prior to instability must be less than 5% of b_o.

The fracture mechanics data development plan also included some upper-shelf R-curve determinations, and, in a few cases, full R-curves resulted at test temperatures where cleavage fracture transition range data were expected. In such cases, the K_J value at cessation of loading is regarded as an invalid K_{Jc} datum. However, if this test result is used to plot an R-curve, the leading coefficient in Equation (1) can be relaxed to 20 for data validity, as suggested in ASTM Standard Method E 1820-96.[8]

The test matrices and the test data were developed prior to the development of the new ASTM Test Method E 1921-97,[9] which provides guidelines for fracture mechanics–based transition temperature definition. Nevertheless, the data analysis practices used in the following sections of this report comply with most of the recently developed recommended practices.

4. FRACTURE MECHANICS EVALUATION METHODS

4.1 Current Federal Code Method

Fracture toughness requirements for nuclear vessel fabrication and control of operating conditions are defined by "Title 10," *Code of Federal Regulations*, Part 50 (10 CFR 50), which references ASME Code Sections III and XI. The methodology currently in use was developed in 1971 by an ad hoc Pressure Vessel Research Council (PVRC) task group that had very little fracture mechanics data and relevant technology development on structural steels available at that time.[10] Fracture mechanics had been developed for use on aerospace materials and not necessarily for structural steels. The only usable data validity requirement was for K_{Ic} as defined by ASTM Standard Method E 399, and dynamically developed K_{Ic} was believed to develop the lower bound of material fracture toughness with variability of the order of ±10%. Instead, the collection of all known valid dynamic K_{Ic} data on reactor vessel welds and base metals, when plotted after normalization to NDT temperature, or RT_{NDT}, did not produce the expected compacted lower-bound data set. Instead, data scatter developed on the order of 3 to 1 between highest and lowest dynamic K_{Ic} values. This same approach was later applied to lower bound scattered semistatic data using at first a visually fitted curve shape. This curve was later mathematically fitted with the following equation:[11]

$$K_{Ic} = 36.5 + 23.15 \exp\left[0.036\left(T - RT_{NDT}\right)\right] \quad \mathrm{MPa}\cdot\sqrt{m} \ . \tag{2}$$

Equation (2) has been regarded as a universal curve to be used for all pressure vessel steels and their weldments. RT_{NDT} is the reference nil-ductility temperature. Because of the K_{Ic} validity requirements, huge specimen sizes were required for fracture toughness evaluations in the transition range, and the use of fracture mechanics test methods to establish K_{Ic} fracture toughness was generally prohibitive. Instead, the highly empirical drop-weight NDT test (ASTM E 208-95a) and Charpy transition curves are used to determine RT_{NDT}, and the relationship of these two empirical methods to fracture mechanics test conditions was postulated without adequate supporting proof.

For dynamic conditions, data from dynamic crack initiation toughness, K_{Id}, and crack-arrest K_{Ia} values are used.[11] The mathematical equivalent lower-bound equation for dynamic loading is as follows:

$$K_{Ia} = 29.4 + 13.72 \exp\left[0.0261\left(T - RT_{NDT}\right)\right] \quad \mathrm{MPa}\sqrt{m} \ . \tag{3}$$

The experimental data for the WF-70 beltline weld metal, and the K_{Ic} curves established according to ASME rules (referenced to RT_{NDT}), are compared in Figure 7. The two K_{Ic} curves shown as dashed lines represent the two extreme RT_{NDT} values obtained using the Charpy curve data reported in Table 4. Hence, there is a strong possibility that if the Midland plant had been made operational, their initial lower-bound fracture toughness curve might have been somewhere between these two bounding K_{Ic} curves. A similar plot for the WF-70 nozzle course weld is given in Figure 8.

4.2 Data Analysis by Master Curve

The master curve method of data analysis applies statistical modeling of data scatter encountered with fracture mechanics testing of structural steels.[9] Extreme data scatter among replicate tests is accepted as typical for tests conducted in the transition range. In the present case, the following three-parameter Weibull model is used to fit data scatter patterns:

$$P_f = 1 - \exp\left[- \left(\frac{K_{Jc} - K_{min}}{K_o - K_{min}} \right)^b \right] . \tag{4}$$

P_f is the probability that any single arbitrarily selected fracture toughness specimen selected from a population will show toughness equal to or less than the K_{Jc} value input into Equation (4). Extensive data from several experiments reported in the literature were compared in a sensitivity study, leading to the observation that K_{min} and Weibull slope, b, can be assigned to be deterministic parameters of the three-parameter Weibull model. Namely, when K_{min} is set to 20 MPa $\sqrt{m}$, the Weibull slope for all data populations will tend to be at or very near 4.[12] Hence, only the scale parameter, K_o, needs to be determined from a data sampling plan. Monte Carlo simulation methods have demonstrated that as few as six replicate tests can yield suitably accurate determinations of K_o. A limitation on this Weibull modeling is that all specimens must have reasonably similar crack tip constraint control to ensure that all data belong in the same data population. Data control by Equation (1) ensures sufficient conformity to crack tip constraint control and suitable definition of J-integral.

Aside from constraint control, there is a subtle underlying specimen size effect that is caused by microstructural imperfections that are present in all commercial steels. Carbides, metallic inclusion, or other imperfections are randomly distributed throughout the microstructure. Such particles, when of a critical size and when located in the highly stressed crack tip region, will trigger cleavage crack

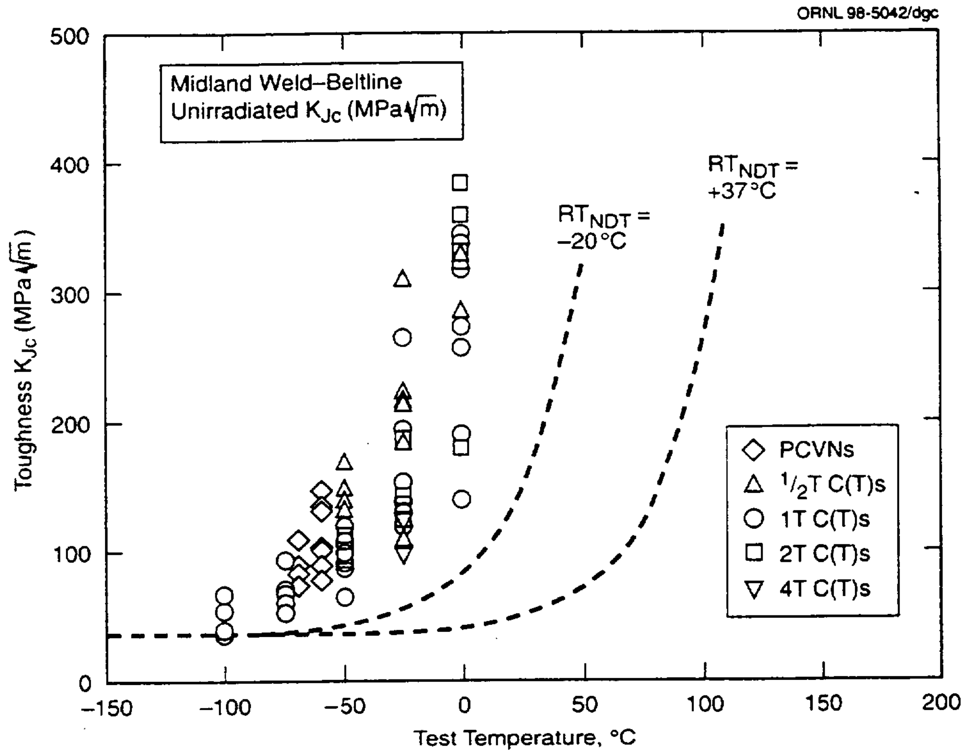

Figure 7. **Beltline weld K_{Jc} data and two ASME lower-bound K_{Ic} curves that represent the spread of RT_{NDT} temperatures determined from 19 Charpy V-notch transition curves.**

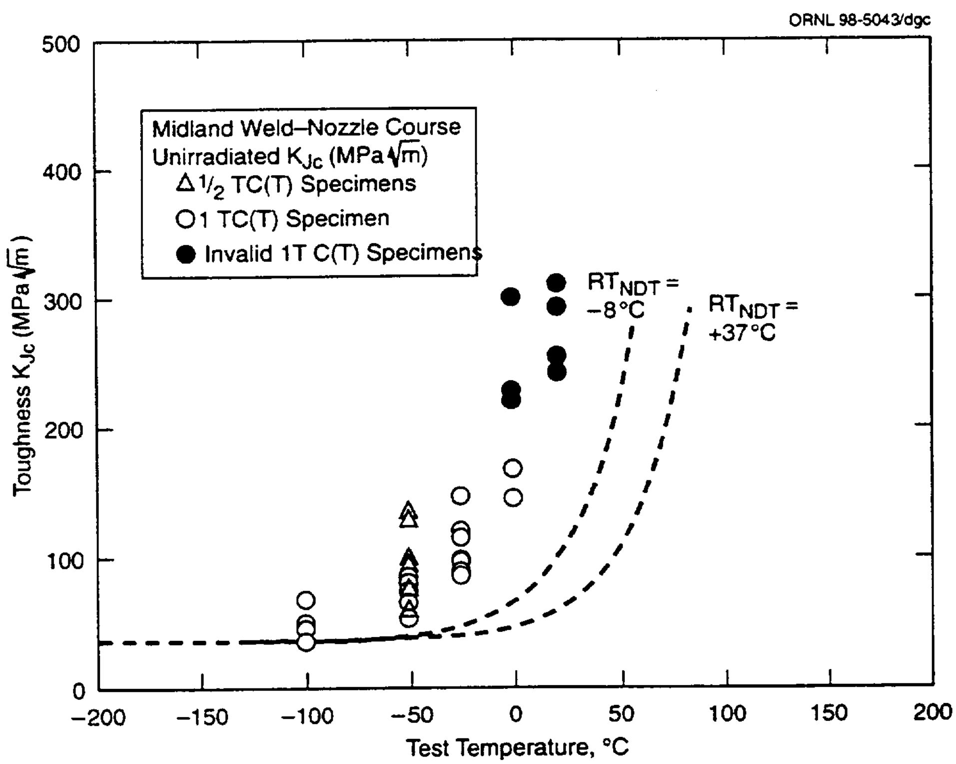

Figure 8. **Nozzle course weld K_{Jc} data and two ASME lower-bound K_{Ic} curves that represent the spread of RT_{NDT} temperatures determined from six Charpy V-notch transition curves.**

initiation. The result is a statistically based specimen size effect that is proportional to the volume of highly stressed material bordering the crack tip. A weakest-link statistical theory was used to develop the following mathematical representation of this size effect:

$$\left(K_{Jc(2)} - 20\right) = \left(K_{Jc(1)} - 20\right)\left[\frac{B_{(1)}}{B_{(2)}}\right]^{1/4} \quad \text{MPa}\sqrt{\text{m}} \; . \tag{5}$$

According to the theory, when specimens of size $B_{(1)}$ are tested, the resulting $K_{Jc(1)}$ can be converted to a fracture toughness value that would have been obtained with specimens of size $B_{(2)}$. Hence, it is possible to normalize data obtained from a variety of specimen sizes to data for one selected specimen size.

The determination of K_o by sampling from an infinite population allows an acceptably accurate determination of the median K_{Jc}, $K_{Jc(med)}$, and closed-form solutions can be formulated to set tolerance bounds on the spread of the data populations. A series of $K_{Jc(med)}$ solutions covering a range of test temperatures has led to the conclusion that there is one universal transition curve shape. When K_{Jc} data are converted to 1T specimen size equivalence and a variety of steels are similarly evaluated, the following universal transition range curve has emerged:

$$K_{Jc(med)} = 30 + 70 \exp\left[0.019\left(T - T_o\right)\right] \quad \text{MPa}\sqrt{\text{m}} \; . \tag{6}$$

Temperature, T_o, is the reference temperature and, if by chance the test temperature, T, happens to be selected at temperature, T_o, then the median K_{Jc} toughness would be 100 MPa $\sqrt{\text{m}}$.

Because the Weibull slope, b, is fixed at 4, the tolerance bounds on data scatter are defined by the following closed-form equation:

$$K_{Jc(0.xx)} = D1 + D2 \exp\left[0.019\left(T - T_o\right)\right] \quad \text{MPa}\sqrt{\text{m}} \; . \tag{7}$$

Coefficients D1 and D2 for each (0.xx) probability level can be computed and tabulated. As an example, 2% cumulative probability (0.02) has D1 = 24.3 and D2 = 30. Master curves and tolerance bound curves are then completely defined with the experimental determination of reference temperature, T_o. Hence, a material's entire fracture toughness transition characterization can be reasonably set up by replicate tests at one test temperature.

The K_{Jc} test data for beltline weld metal appear in Table 7 and in Table 8 for nozzle course weld metal. The T_o temperatures developed from these data are summarized in Table 9. The variability in T_o between individual data sets is normal for such tests. Accuracy tends to diminish at test temperatures that are substantially below T_o, and this appears to be most evident in the tests on WF-70 beltline weld metal. The evidence here indicates that there is a difference in fracture toughness transition temperature of about 20°C between the beltline and nozzle course weld metals. This difference could not be detected by drop-weight NDT nor by CVN transition temperature tests. On the other hand, tensile tests gave some hint of a difference between the two weldments.

Figures 9 and 10 show the data from Tables 7 and 8 plotted against the master curves developed using the grand total T_o values given in Table 9. All data shown have been converted to 1T equivalence using Equation (5). The tolerance bound is from Equation (7) at 2% cumulative probability. Note that the data at 0°C in Table 7 have not been used to calculate T_o temperatures. There is good reason for this, but this subject matter will be reserved for Section 6 discussions.

4.3 R-Curve Effects

Although the transition range fracture toughness evaluation of WF-70 weld metal was the subject of primary interest, some effort was given to R-curve development to bring upper-shelf properties into perspective. Upper-shelf ductile tearing properties can impact the high-temperature part of the transition range K_{Jc} data distributions. In particular, it can be shown that R-curves provide useful information if fracture mechanics K_{Jc}-based transition range curves should happen to indicate shape change as a consequence of irradiation. Table 10 shows the planned R-curve test matrix for this project. The complete package of R-curve information is detailed in NUREG/CR-6249.[13] Only R-curve properties of relevance to the subject of engineering significance were applied in the present report.

Occasionally, R-curves were obtained at test temperatures below the Table 10 range of test temperatures when a few transition range specimens failed to develop cleavage fracture.

The R-curve comparisons of interest here are beltline versus nozzle course weld, test temperature effects, specimen size effects, and side-grooving effects.

Table 7. Midland beltline weld unirradiated K_{Jc} values

Test temperature (°C)	1/2T Code	1/2T Side groove (%)	1/2T K_{Jc} (MPa $\sqrt{m}$)	1T Code	1T Side groove (%)	1T K_{Jc} (MPa $\sqrt{m}$)	2T Code	2T Side groove (%)	2T K_{Jc} (MPa $\sqrt{m}$)	b_o (in.)	Δa_p (in.)	Control K_{Jc} value[a]	Validity
21	MW11KEB	20	241.3							0.408	0.069	J_R curve	Invalid
	MW11MFA	20	266.9							0.417	0.083	J_R curve	Invalid
				MW11FC	20	300.0				0.816	0.096	J_R curve	Invalid
				MW15GB	20	255.1				0.807	0.091	J_R curve	Invalid
				MW11FB	0	337.0				0.815	0.101	J_R curve	Invalid
				MW15GA	0	318.5				0.796	0.108	J_R curve	Invalid
0	MW9KEA	0	328							0.433	0.082	J_R curve	Invalid
	MW9CEB	0	282							0.425	0.049	(192.4)	Invalid
				MW9CB	20	273.4				0.930	0.101	273.4	Invalid
				MW11IA	0	316.7				0.876	0.072	(276.2)	Invalid
				MW15FA	0	255.6				0.767	0.059	255.6	Invalid
				MW15GD	20	189				0.734	0.069	189	Invalid
				MW9IA	0	140.0				0.855	0.004	140.0	
				MW9FA	0	335.1				0.878	0.111	J_R curve	Invalid
				MW11GC	20	327.4				0.806	0.179	J_R curve	Invalid
				MW11JB	0	342.4				0.859	0.103	J_R curve	Invalid
				MW11GD	0	322.6				0.741	0.095	(258.1)	Invalid
							MW10C2	0	324.2	1.956	0.098	324.2	
							MW10D2	0	358.	1.9429	0.113	J_R curve	Invalid
							MW10G2	0	180.2	1.9503	0.013	180.2	
							MW10G1	0	381.6	1.918	0.123	J_R curve	Invalid
−25	MW14A[b]	0	98.4							3.136	0	98.4	
	MW14B	0	119.8							3.224	0	119.8	
				MW9FC	20	264.9				0.907	0.098	264.9	Invalid
				MW9FD	20	131.8				0.939	0.005	131.8	
				MW15FD	20	119.2				0.805	0.004	119.2	
				MS11FA	20	193.5				0.799	0.031	193.5	
				MW15FC	0	138.9				0.798	0.007	138.9	
				MW11GA	0	139.4				0.790	0.010	139.4	
				MW9FB	0	143.2				0.976	0.006	143.2	
				MW9CC	0	153.6				0.950	0.007	153.6	

Table 7 (continued)

Test temperature (°C)	1/2T Code	1/2T Side groove (%)	1/2T K_{Jc} (MPa $\sqrt{m}$)	1T Code	1T Side groove (%)	1T K_{Jc} (MPa $\sqrt{m}$)	2T Code	2T Side groove (%)	2T K_{Jc} (MPa $\sqrt{m}$)	b_o (in.)	Δa_p (in.)	Control K_{Jc} value[a]	Validity
−25	MW9HFB	0	220							0.426	0.010	220	
	MW11JEA	0	214.9							0.425	0.022	214.9	
	MW11MCB	0	212.6							0.429	0.023	212.6	
	MW10EIFB	0	183.2							0.436	0.016	183.2	
	MW11MDA	0	108.5							0.434	0.001	108.5	
	MW11LEA	0	307.6							0.412	0.084	(200.6)	Invalid
							MW10B1	0	120.0	1.945	0.018	120.0	
							MS12C1	0	184.2	1.920	0.010	184.2	
							MW10D1	0	124.7	1.935	0.004	124.7	
							MW15J1	0	141.0	1.931	0.005	141.0	
							MW10C1	0	144.4	1.943	0.006	144.4	
−50	MW10E2F	0	167.3							0.429	0.009	167.3	
	MW10E2E	0	91.6							0.421	0.001	91.6	
	MW9LFB	0	146.8							0.425	0.006	146.8	
	MW10EIFA	0	119.3							0.433	0.003	119.3	
	MW10EIEB	0	137.7							0.444	0.004	137.7	
	MW10EIEA	0	131.1							0.424	0.003	131.1	
				MW15FB	0	88.4				0.818	0.002	88.4	
				MW9CA	20	119.2				0.934	0.004	119.2	
				MW15GC	20	91.9				0.818	0.002	91.9	
				MW11FD	20	103.3				0.789	0.002	103.3	
				MW9CD	0	64.9				0.962	0	64.9	
				MW11GB	0	118.1				0.796	0.003	118.1	
							MW12C2	0	97.7	1.931	0.001	97.7	
							MW10H2	0	108.4	1.943	0.002	108.4	
							MW10B2	0	105.0	1.950	0.002	105.0	
							MW12D1	0	115.0	1.935	0.001	115.0	
							MW15J2	0	94.0	1.929	0.001	94.0	
−75				MW9JD	0	61.1				0.853	0	61.1	
				MW9ND	0	55.7				0.856	0	55.7	
				MW11LA	0	55.0				0.860	0	55.0	
				MW10EIC	0	72.2				0.875	0	72.2	
				MW10EIA	0	67.7				0.870	0	67.7	
				MW10EIB	0	93.8				0.861	0	93.8	

Table 7 (continued)

Test temperature (°C)	1/2T Code	1/2T Side groove (%)	1/2T K_{Jc} (MPa $\sqrt{m}$)	1T Code	1T Side groove (%)	1T K_{Jc} (MPa $\sqrt{m}$)	2T Code	2T Side groove (%)	2T K_{Jc} (MPa $\sqrt{m}$)	b_o (in.)	Δa_p (in.)	Control K_{Jc} value[a]	Validity
–100				MW11B	0	68.4				0.854	0	68.4	
				MW11KB	0	54.9				0.869	0	54.9	
				MW11KA	0	38.4				0.870	0	38.4	
				MW10EID	0	40.1				0.835	0	40.1	
				MW9IB	0	54.6				0.855	0	54.6	
				MW9KA	0	55.8						55.8	
	PCVNs												
–70	MW1108	0	74.3							0.183	0	74.3	
	MW15K3	0	75.8							0.190	0	75.8	
	MW11IB	0	84.6							0.190	0	84.6	
	MW112B	0	89.0							0.191	0	89.0	
	MW11AD	0	110.2							0.183	0	110.2	
–60	MW1106	20	102.5							0.190	0	102.5	
	MW1116	20	122.7							0.191	0	122.7	
	MW1126	20	144.9							0.179	0.006	(133.7)	Invalid
	MW1136	20	153.9							0.175	0.005	(132.3)	Invalid
	MW1146	20	109.3							0.193	0	109.3	Invalid
	MW11AD3	0	239.5							0.180	0.018	(134.1)	Invalid
	MW15AK4	0	222.8							0.169	0.015	(130.4)	
	MW11AK5	0	78.6							0.193	0	78.6	
	MW9BJ4	0	141.1							0.169	0	130.0	
	MW15AK2	0	104.3							0.199	0	104.3	
	MWIAB1	0	102.4							0.171	0	102.4	
	MWIAB3	0	90.0							0.171	0	90.0	
	MW9AA4	0	89.5							0.167	0	89.5	Invalid
	MW9AA5	0	262.1							0.215	0.028	(146.6)	

[a]Values in parentheses are calculated maximum $K_{Jc(limit)}$.
[b]4T specimens.

Table 8. Midland nozzle course weld unirradiated K_{Jc} values

Test temperature (°C)	1/2T Code	1/2T Side groove (%)	1/2T K_{Jc} (MPa $\sqrt{m}$)	1T Code	1T Side groove (%)	1T K_{Jc} (MPa $\sqrt{m}$)	PCVN Code	PCVN Side groove (%)	PCVN K_{Jc} (MP $\sqrt{m}$)	b_o (in.)	Δa_p (in.)	Control K_{Jc} value[a]	Validity
21				NC31DB	20	241.8				0.772	0.125		Non-test
				NC31DA	0	292.0				0.780	0.103	J_R curve	Invalid
				NC34FG	20	253.7				0.763	0.147		Non-test
				NC34IE	0	310.6				0.864	0.113	J_R curve	Invalid
0				NC34IA	0	144.6				0.755	0.011	144.6	
				NC34CA	0	167.3				0.784	0.018	167.3	
				NC31AC	0	299.5				0.757	0.126	299.5	Invalid
				NC31FA	20	220.1				0.771	0.095	220.1	Invalid
				NC34FA	20	228.4				0.771	0.098	228.4	Invalid
−25				NC31CB	20	146.8				0.740	0.005	146.8	
				NC34IE	0	120.6				0.870	0.001	120.6	
				NC31KD	0	113.7				0.867	0.001	113.7	
				NC34JE	0	120.9				0.889	0.008	120.9	
				NC31ID	0	97.4				0.875	0.002	97.4	
				NC31BC	0	95.9				0.769	0.002	95.9	
				NC31EB	20	87.3				0.782	0.003	87.3	
				NC34AC	0	84.5				0.768	0.002	84.5	
−50	B34M	0	133.7							0.416	0	133.7	
	A34M	0	125.7							0.428	0.002	125.7	
	G34M	0	98.1							0.433	0.004	98.1	
	F34M	0	93.2							0.439	0.001	93.2	
	J34M	0	77.9							0.429	0.001	77.9	
	E34M	0	74.5							0.424	0.001	74.5	
	D34M	0	58.0							0.426	0	58.0	
				NC34EA	0	81.1				0.786	0.001	81.1	
				NC31CA	0	84.6				0.776	0.001	84.6	
				NC34KE	0	63.9				0.882	0	63.9	
				NC34BC	20	63.8				0.774	0	63.8	
				NC34LD	0	75.4				0.860	0	75.4	
				NC31EB	20	54.8				0.784	0	54.8	

Table 8 (continued)

Test temperature (°C)	1/2T			1T			PCVN			b_o (in.)	Δa_p (in.)	Control K_{Jc} value[a]	Validity
	Code	Side groove (%)	K_{Jc} (MPa $\sqrt{m}$)	Code	Side groove (%)	K_{Jc} (MPa $\sqrt{m}$)	Code	Side groove (%)	K_{Jc} (MPa $\sqrt{m}$)				
150				NC34DA	20	203.5				0.764	0.086	J_R	Non-test
				NC34DB	20	199.6				0.763	0.074	J_R	Non-test
−100				NC31HB	0	35.6				0.884	0	35.6	
				NC31JB	0	36.8				0.873	0	36.8	
				NC31JD	0	49.1				0.793	0	49.1	
				NC31JE	0	67.9				0.864	0	67.9	
				NC31IB	0	50.2				0.863	0	50.2	
				NC34LC	0	47.1				0.872	0	47.1	
−60							NC34FI1	0	108.4	0.164	0	108.4	
							NC34AA2	0	103.8	0.147	0	103.8	
							NC34AF4	0	186.1	0.192	0	(139.7)	Invalid
							NC31BE2	0	177.9	0.172	0	(132.3)	Invalid
							NC34AEI	0	126.6	0.148	0	(122.7)	Invalid
							NC31BH2	0	139.4	0.168	0	(130.7)	Invalid
							NC34FI4	0	76.5	0.177	0	76.5	

[a]Values in parentheses are calculated maximum allowed $K_{Jc(limit)}$.

Table 9. Summary tabulation of T_o temperatures for unirradiated specimens

Material	Specimen size	Test temperature (°C)	T_o (°C)	Grand total, T_o
Beltline	2T	−25	−58	
	1T	−25	−61	
	1/2T	−25	−59	
	2T	−50	−58	
	1T	−50	−47	
	1/2T	−50	−58	
	1T	−75	−44	
	1T	−100	−41	
Grand total				−54
Nozzle course	1T	−25	−30	
	1T	−50	−19	
	1/2T	−50	−38	
	1T	−100	−35	
Grand total				−32

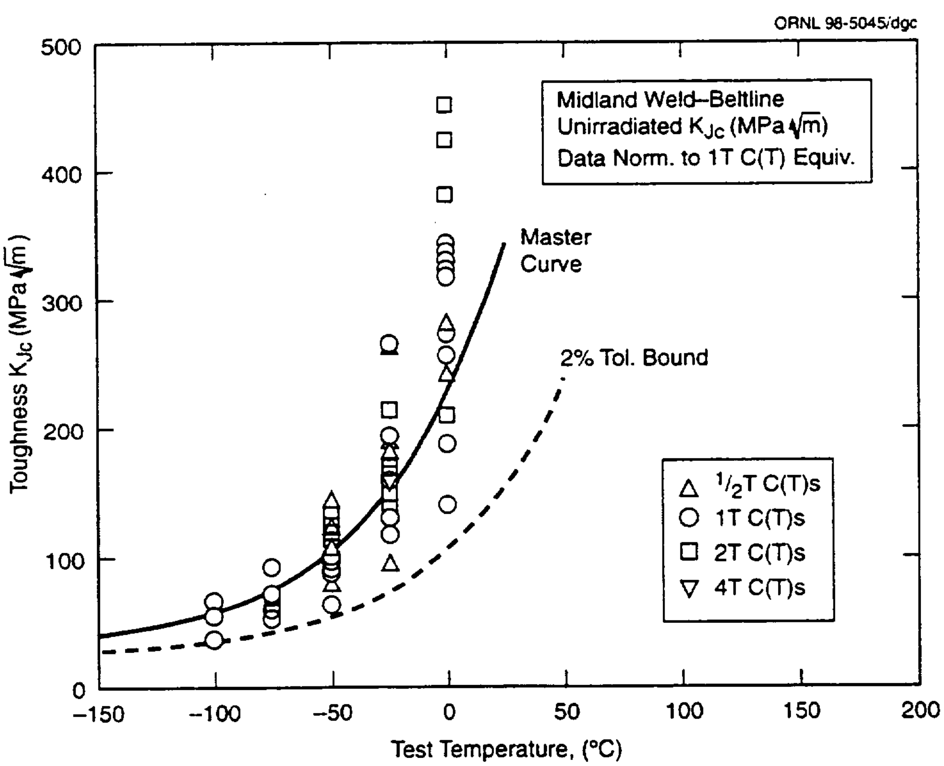

Figure 9. All beltline weld K_{Jc} values normalized to 1T equivalence with the master curve and 2% tolerance bound curve.

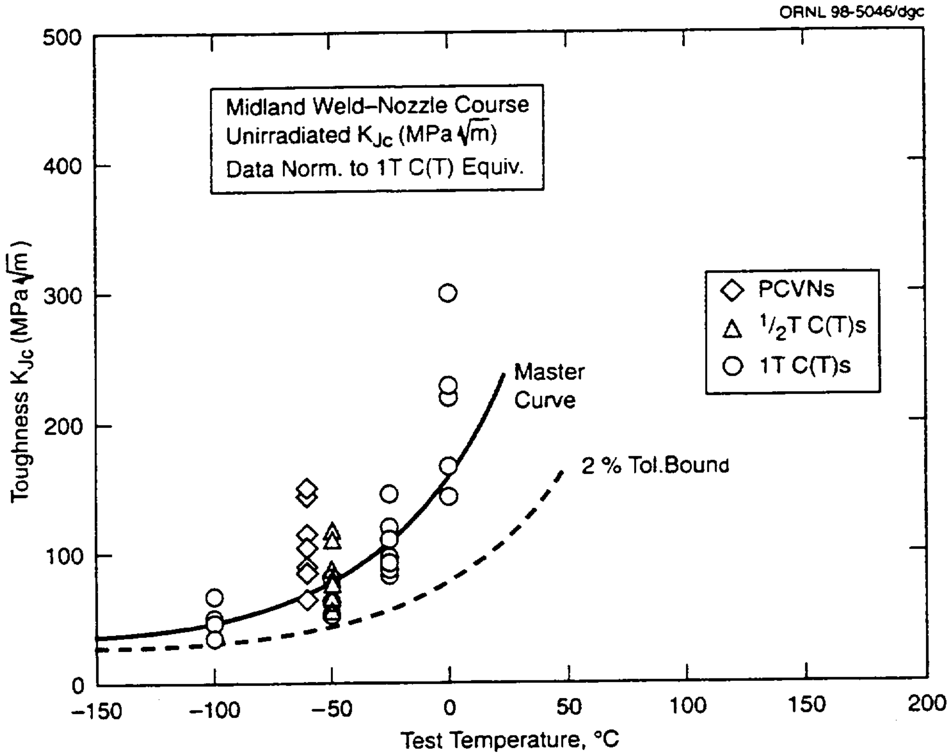

Figure 10. All nozzle course K_{Jc} values normalized to 1T equivalence with the master curve and 2% tolerance bound curve.

Table 10. R-curve test matrix

Specimen size	Number of specimens at various temperatures[a]		
	21°C (70°F)	150°C (302°F)	288°C (550°F)
Beltline			
1/2T 1T 4T	2 2 –	2 2 –	2 2 2
Nozzle course			
1/Tt 1T	– 4[b]	– 2	2 2

[a]All specimens 20% side grooved unless noted otherwise.
[b]Two specimens not side grooved.

In R-curve studies, crack-growth resistance can be expressed in terms of J-integral-equivalent stress intensity factors, K_J. Figure 11 shows that at a reactor vessel operating temperature of 288°C, the crack growth resistance development is severely reduced. However, the crack growth resistance rate peaks at room temperature and remains essentially unchanged entering the transition range. Figure 12 is representative of all R-curve comparisons made between beltline and nozzle course welds. Ductile tearing resistance of nozzle course weld was lower at all test temperatures. This was found despite no difference being indicated by Charpy upper-shelf energies. The magnitude of this difference was not sufficient to be detected by the Charpy impact method. There is not a significant specimen size effect in R-curve development, and Figure 13 shows that the low upper-shelf WF-70 weld metal behaves no differently than other steels in this regard. However, when deformation theory J is used, it is not unusual for small specimens such as 1/2T compacts to slightly underpredict R-curve fracture toughness, as seen in Figure 13. Modified J eliminates this slight difference, and Figure 14 shows the improved R-curve comparison.[14]

Side grooving of specimens has not been an issue in transition range tests because the preponderance of evidence collected has shown no effect on K_{Jc} values. However, when crack growth initiates prior to cleavage fracture, as with low upper-shelf materials, R-curve effects tend to exert some influence on fracture toughness characterization. An example of the side groove effect on WF-70

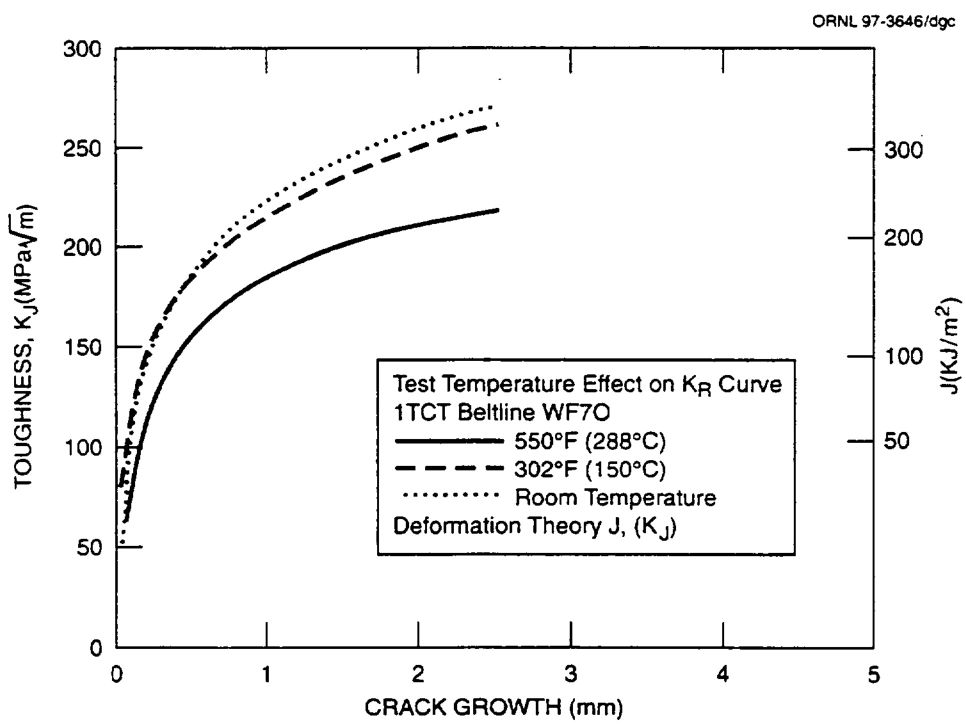

Figure 11. **K_R curves of beltline WF-70 weld metal showing a test temperature effect.**

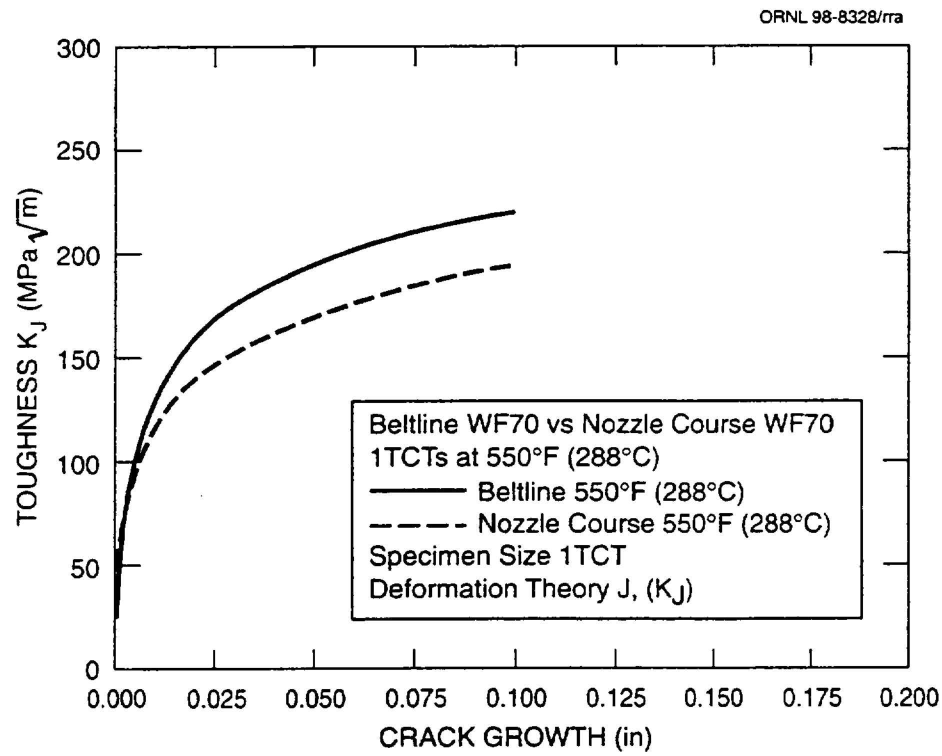

Figure 12. **K_R curve comparison between beltline and nozzle course WF-70 weld metal, showing a typical result for all test temperatures.**

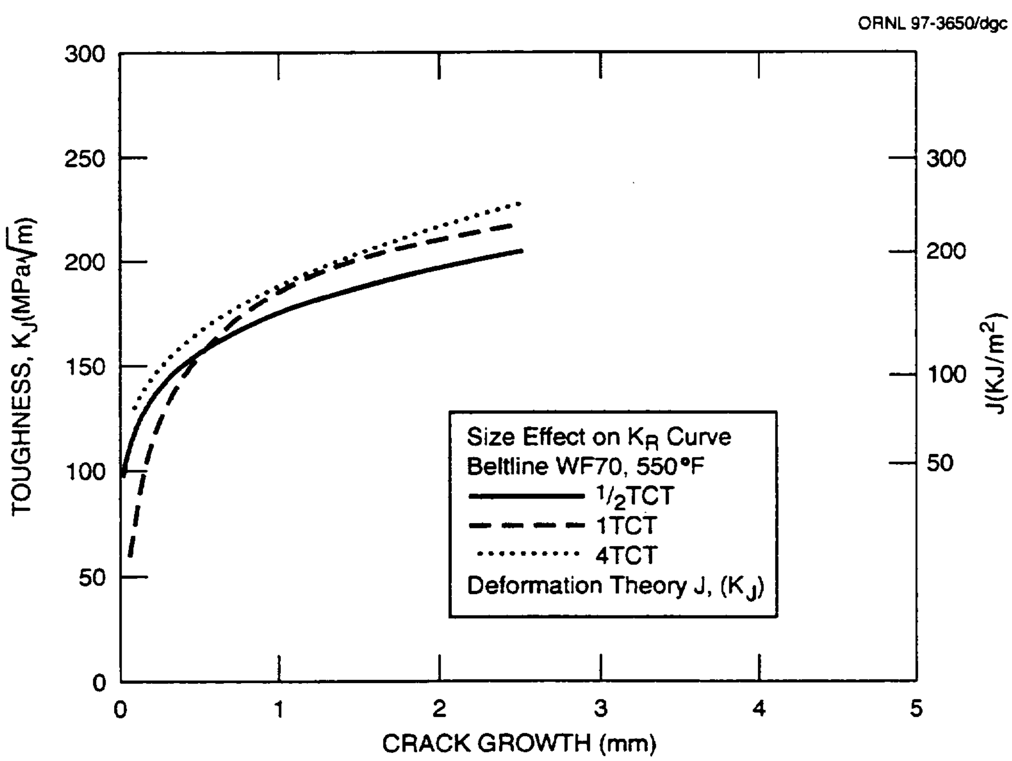

Figure 13. **Size effect study using three specimen sizes (deformation theory J converted to K_J).**

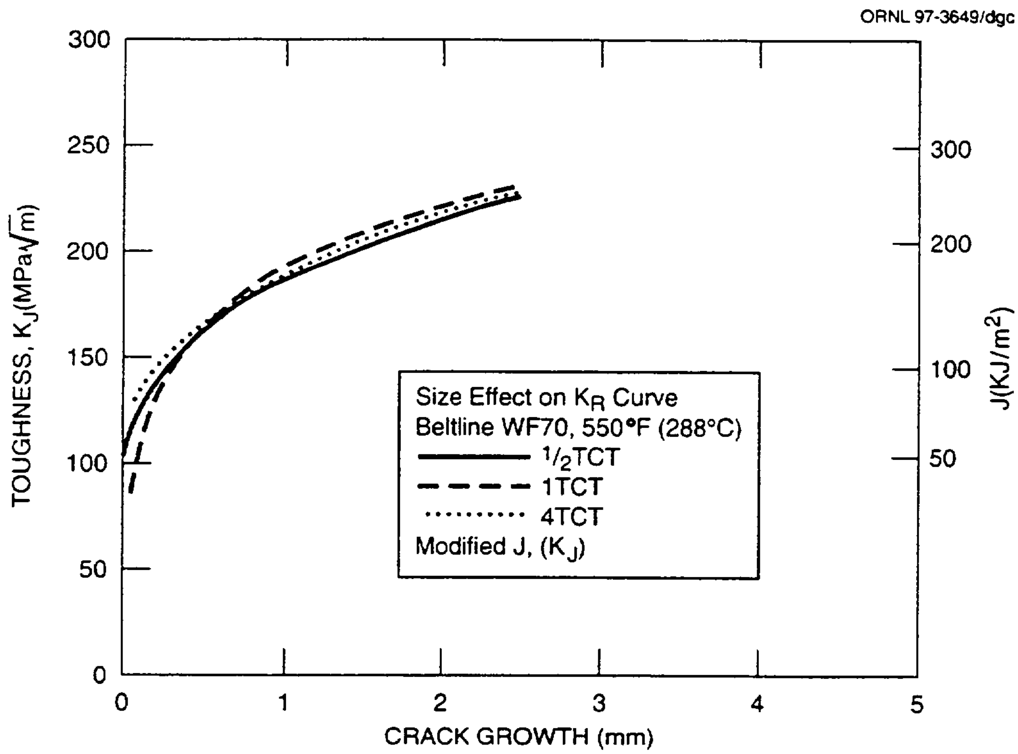

Figure 14. **Same K_R curve size effect study as Figure 13, except modified J was used prior to conversion to K_J.**

R-curves is given in Figure 15. ASTM E 1921-97[9] stipulates that K_{Jc} data are invalid if stable crack growth is more than 5% of b_o. For 1T compact specimens with a/W = 0.5, the allowed growth is 1.25 mm and the impact of side grooving on K_{Jc} is significant but not overly severe. If, on the other hand, the specimen size were 4T, the impact at 5 mm of crack growth and side grooving on K_{Jc} would be severe, and the shape of the data distribution and consequent impact on median K_{Jc} determinations becomes a matter for concern.

4.4 Crack Arrest Tests

Dynamic fracture toughness of the WF-70 beltline weld was determined by crack-arrest tests. The rules for this test method are established in ASTM Method E 1221-88,[15] "Determining Plane Strain Crack-Arrest Fracture Toughness, K_{Ia}, of Ferritic Steels." One specimen design used in this investigation is shown in Figure 16. This is the basic 2T compact specimen modified for crack-arrest testing. The specimen size was dictated by the available irradiation capsule space and specimen

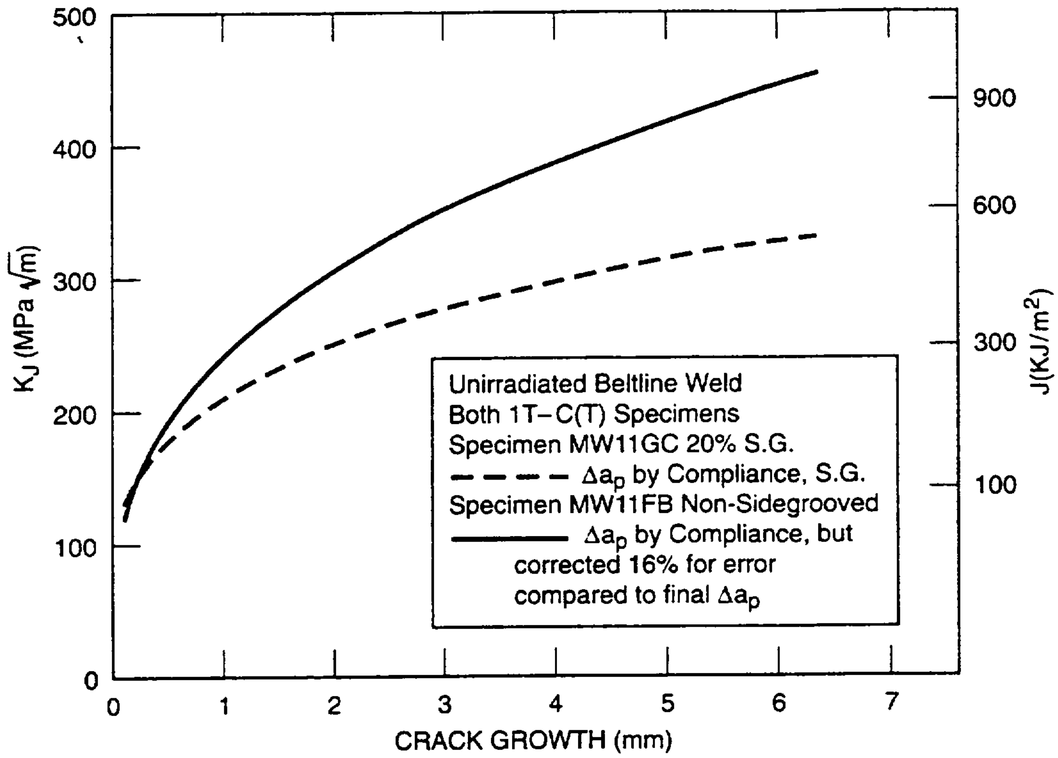

Figure 15. **Side-groove effect on K_R curve.**

ORNL 98-8324/rra

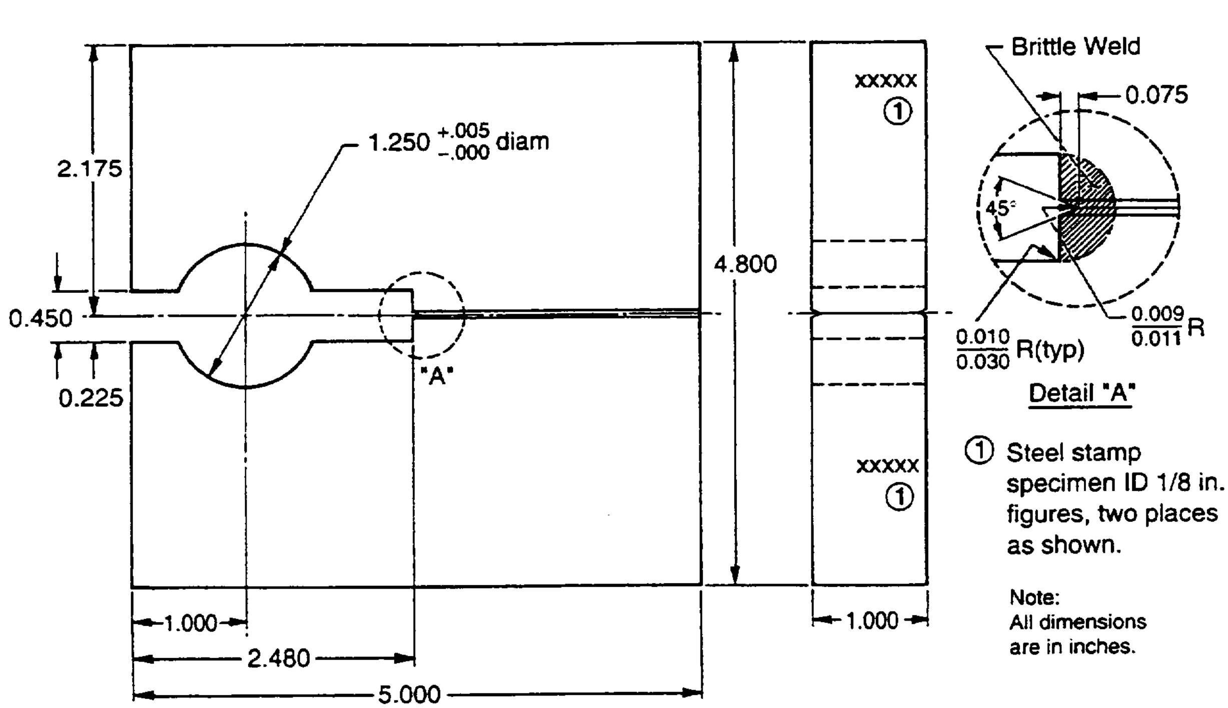

Figure 16. **Crack-arrest specimen of 2T planar proportionality.**

measuring capacity. About one-half of these specimens were to be irradiated. The specimen features a crack tip region consisting of a brittle weld bead that enables some control over crack initiation K levels. This particular test practice is highly technique-intensive because the crack initiation stress intensity amplitude must be controlled to ensure crack-arrest of the running cleavage crack well before the back edge of the specimen can be reached. The unbroken ligament (W-a) at arrest must be greater than 15% of the specimen width, W. In the present case, there was so much difficulty in meeting this particular requirement that an alternate specimen design (duplex specimen) was added to the program. Here a brittle steel such as ultrahigh-strength American Iron and Steel Institute (AISI) 4340 steel is electron-beam welded to the test material to act as a crack starter material. This brittle material replaces the entire front half of the specimen. The crack initiation tip that triggers a running crack is a drilled hole of a size suited to the desired crack initiation stress intensity factor. All results are reported in Table 11 and are plotted against the ASME lower-bound K_{Ia} curve in Figure 17. These data violate various parts of the ASTM E 1221-88 validity requirements, so they are to be regarded as provisional "K_a" data. If one assumes that the K_a values have only marginal violations, it again appears that the ASME curves do not accurately represent the lower bound of fracture toughness for this WF-70 weld metal. A detailed report of the crack-arrest toughness project for WF-70 will be published separately.

5. IRRADIATION EFFECTS

Two target irradiation dose levels were nominal fluences of 0.5 and 1.0 × 10^{19} n/cm^2 (>1 MeV). The irradiation temperature was nominally 288°C (550°F). An originally planned target fluence of 5 × 10^{19} n/cm^2 could not be accomplished.

The purpose of the varied fluence was principally to quantify the irradiation damage rate. Hence, only two small scoping capsules (0.5 × 10^{19} n/cm^2) were prepared, Capsules 10.01 and 10.02. Each contained 20 Charpy specimens, 8 tensile specimens, and 4 1/2T compact specimens. Capsule 10.01 contained predominantly beltline weld specimens, and Capsule 10.02 contained predominantly nozzle course weld specimens. Materials Engineering Associates (MEA) built these capsules and supervised the irradiation. They were irradiated at the Buffalo Materials Research Center at the State University of New York at Buffalo. Information submitted on these exposures is given in Appendix B.

Table 11. Crack-arrest toughness, K_a, of Midland WF-70 beltline submerged-arc weld metal specimens (specimens are oriented so that crack propagation is in the welding direction)

Specimen	Thickness (mm)	Test temperature (°C)	Arrested crack depth (a_a/W)	K_a (MPa $\sqrt{m}$)	If ≥ 1, respective criterion is met:[a]					Invalid according to criteria[a]
					A	B	C	D	E	
Weld-embrittled specimens (W = 104.2 mm)										
MW15IAB	33.0	–40.0	0.951	50.2	0.33	0.97	7.85	2.75	2.81	A,B
MW12A1B	25.4	–40.0	0.909	62.3	0.61,	1.17	3.92	2.54	1.93	A
MW12EBB	33.0	–40.0	0.926	79.9	0.49	0.58	3.10	2.63	1.35	A,B
MW12A1	33.1	–30.0	0.956	80.1	0.29	0.33	3.02	2.77	1.38	A,B
MW12D1A	33.0	–30.0	0.927	82.4	0.49	0.52	2.85	2.64	1.16	A,B
NW12HBB	33.0	–30.0	0.868	98.4	0.88	0.67	2.00	2.36	1.14	A,B
MW12EAB	33.0	–30.0	0.887	99.5	0.75	0.56	1.96	2.45	1.46	A,B
MW12GBB	33.0	–25.0	0.933	82.0	0.44	0.48	2.85	2.67	1.56	A,B
MW12GAB	33.0	–25.0	0.858	99.5	0.95	0.69	1.94	2.32	1.56	A,B
MW15HAA	25.4	–20.0	0.862	108.3	0.92	0.56	1.24	2.34	1.47	A,B
MW12FBB	33.0	–20.0	0.866	158.9	0.89	0.25	0.75	2.36	0.63	A,B,C,E
14DRW34	33.0	–10.0	0.891	114.8	0.73	0.39	1.41	2.47	1.23	A,B
MW12HBA	25.4	1.0	0.890	96.2	0.73	0.55	1.52	2.46	1.48	A,B
MW12HAA	25.4	10.0	0.860	147.6	0.93	0.29	0.64	2.32	1.08	A,B,C
Duplex specimens (W = 127 mm)										
MW15JC	29.1	–20.0	0.849	70.0	1.01	1.29	2.44	2.49		Valid
MW15JBr	33.0	–10.0	0.843	86.8	1.05	0.85	1.76	2.12		Valid
MW15JEr2	33.1	–10.0	0.883	101.3	0.78	0.47	1.30	2.38		A,B
MW15JEr1	33.1	0.0	0.620	106.7	2.54	1.34	1.15	1.02		Valid
MW15JF	33.0	10.0	0.647	131.6	2.36	0.80	0.74	1.08		Valid
MW15JD	33.0	10.0	0.525	171.3	3.16	0.64	0.44	0.51		B,C,D
MW15JE	33.1	22.0	0.448	174.7	3.68	0.70	0.41	0.13		B,C,D
MW15JB	33.0	24.0	0.475	186.5	3.50	0.58	0.36	0.24		B,C,D
MW15JA	33.0	25.6	0.550	171.3	3.00	0.59	0.43	0.60		B,C,D

[a]The letters correspond to those in Table 2 of ASTM E 1221-95 and are summarized as follows: A,B = remaining ligament too small; C = specimen too thin; D,E = insufficient crack jump length. The expression proposed for the upcoming revision of the standard was used. One or more letters for a specimen indicate that the test results did not meet one of the minimum lengths of the ASTM E 1221-88 validity criteria.

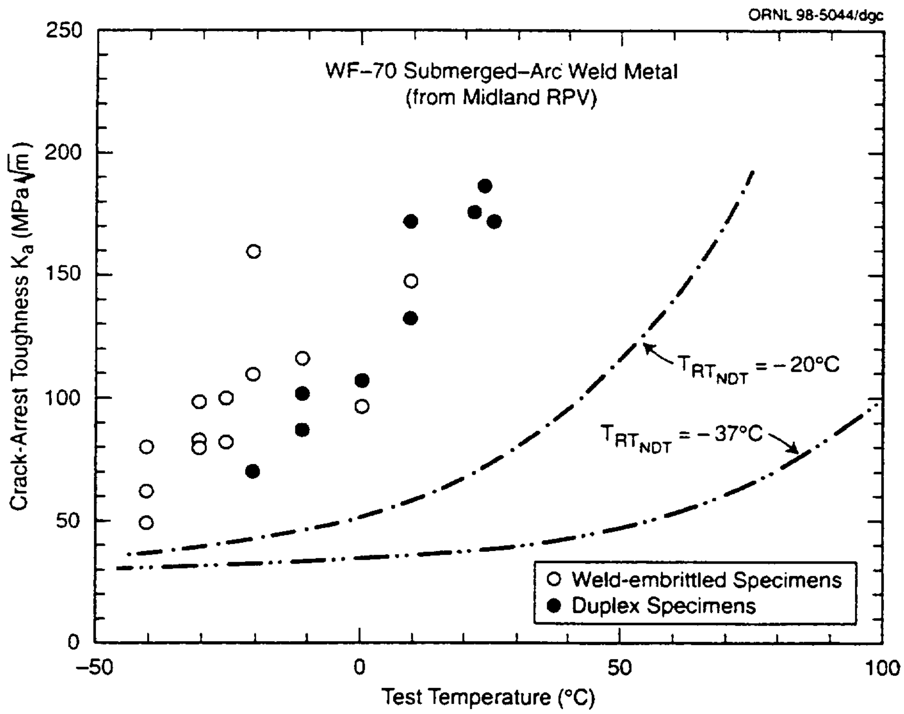

Figure 17. **K_a data on Midland beltline WF-70 weld metal and two ASME lower-bound K_{Ia} curves that cover the range of RT_{NDT} temperatures determined from 19 Charpy V-notch transition curves.**

Irradiation to a fluence of 1 × 10^{19} n/cm^2 represents the irradiation embrittlement focus of these studies. Two large capsules (10.05 and 10.06) were fabricated at Oak Ridge National Laboratory (ORNL) and the exposures were conducted cooperatively between the ORNL staff and the operators of the University of Michigan Ford Nuclear Reactor in Ann Arbor, Michigan. Records on these exposures are given in Appendices C and D.

5.1 Irradiated Tensile Properties

Table 12 summarizes the before-and-after irradiation strength measurements. The previously noted problem concerning the use of transversely oriented unirradiated beltline tensile specimens was avoided here. The seemingly low embrittlement indicated by tensile properties of the nozzle course weld at 0.5 × 10^{19} n/cm^2 compared with beltline weld is difficult to understand because the high copper content of nominally 0.4 wt % in nozzle course weld is greater than that of beltline weld. Both scoping capsules were simultaneously exposed in the core edge position of the Buffalo reactor in tandem, with Capsule 10.02 (above) and Capsule 10.01 (below). Both were ostensibly in a flat flux region at the reactor core edge.

Table 12. Before-and-after irradiation yield and tensile strengths

Test temperature (°C)	Unirradiated			Irradiated					
				0.5×10^{19} n/cm^2			1×10^{19} n/cm^2		
	Number of specimens	Strength (ksi)		Number of specimens	Strength (ksi)		Number of specimens	Strength (ksi)	
		Yield	Ultimate tensile		Yield	Ultimate tensile		Yield	Ultimate tensile
Beltline WF-70 weld metal									
288	2	69.7	88.4						
150	2	69.0	84.7	2	84.4	97.0	2	86.2	101.1
22	2	74.3	88.9	2	91.9	104.0	2	93.7	108.3
−50	2	82.6	100.6						
−100	2	90.7	110.8						
−150	1	106.9	123.4						
Nozzle course WF-70 weld metal									
288	2	70.2	85.2				2	91.1	103.9
150	2	70.4	85.1	2	74.8	94.0	2	92.0	104.5
22	2	79.0	94.9	2	86.4	102.9	1	101.7	114.8
−50	2	84.0	104.1						
−100	2	94.0	118.9						

The effect of copper on tensile properties determined after the 1×10^{19} n/cm^2 in the two ORNL capsules was more consistent with expectations. At 1×10^{19} n/cm^2 and for room temperature, both welds showed yield strength increases of about 25% (see also Appendix A).

5.2 Charpy Transition Curve Shifts

The before-and-after irradiation Charpy V-notch transition curves are shown in Figures 18 through 21. The raw data for the curves are presented in Appendix A. The two parameters most commonly used to indicate transition range shift are energy of fracture and back edge lateral expansion. Both parameters have ranked irradiation damage in order of fluence, except that the magnitude of damage appears to be inconsistent. Specifically, the damage is evidenced in terms of (1) transition curve shape change, (2) loss in upper-shelf energy (USE), (3) transition temperature shift at 41 J (ΔTT_{41J}), and (4) reduced lateral expansion (mils) as shown in Figures 18 and 19. See also Table 13. It is readily apparent that there is the usual curve shape change. Other consistent information is ΔTT_{41J} shift, and loss in upper-shelf lateral expansion. Note that there is no further USE loss between the fluences of 0.5 and 1.0×10^{19} n/cm^2. Here, the trend indicated by lateral expansion loss seems more logical. It is possible that the USE trend became enmeshed in sensitivity deficiencies inherent in the Charpy energy method. The trends in nozzle course parameters shown in Figures 20 and 21 appear to be closer to expectations. The rate of embrittlement up to the fluence of 0.5×10^{19} n/cm^2 is more accelerated, which is consistent with the higher copper content. Only the slow response of tensile properties, mentioned earlier, is difficult to rationalize.

In Table 13, the Charpy ΔTT_{41J} temperature shifts exceed the $\Delta TT_{50\%}$ values, but this is mainly a result of the USE loss and shape change of the energy transition curve. A similar observation had been made in the HSSI Fifth Irradiation Series.

5.3 Irradiation Damage Evaluation by Fracture Mechanics

Background information on the two fracture mechanics–based transition temperature evaluation methods has already been discussed in Section 4. The ASME method uses a universal lower-bound curve positioned by empirical parameters, namely, the RT_{NDT} defined using the drop-weight NDT temperature and/or Charpy V-notch curves. The universal curves used are Equations (2) and (3).

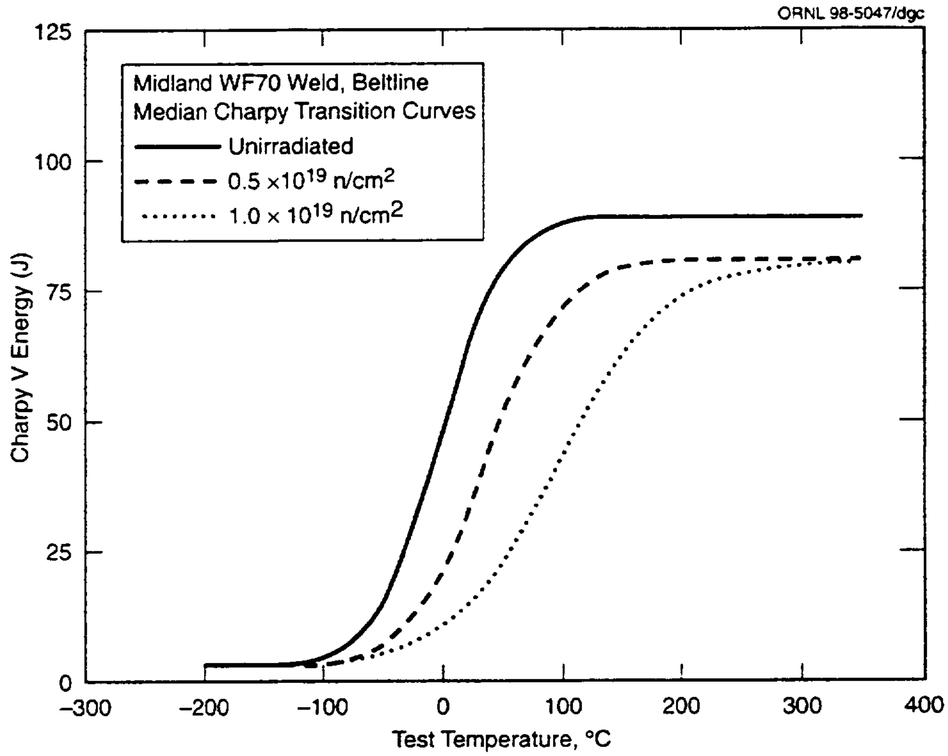

Figure 18. **Charpy V-notch transition energy curves before and after irradiation of beltline WF-70 weld.**

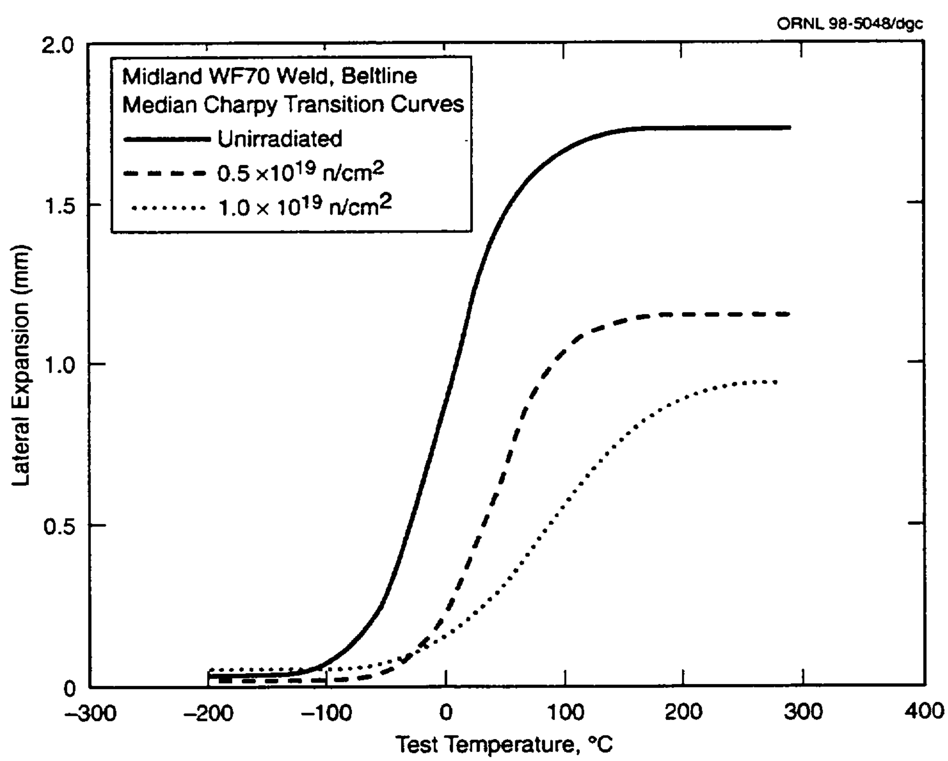

Figure 19. **Charpy V-notch lateral expansion of Charpy V-notch specimens before and after irradiation of WF-70 beltline weld.**

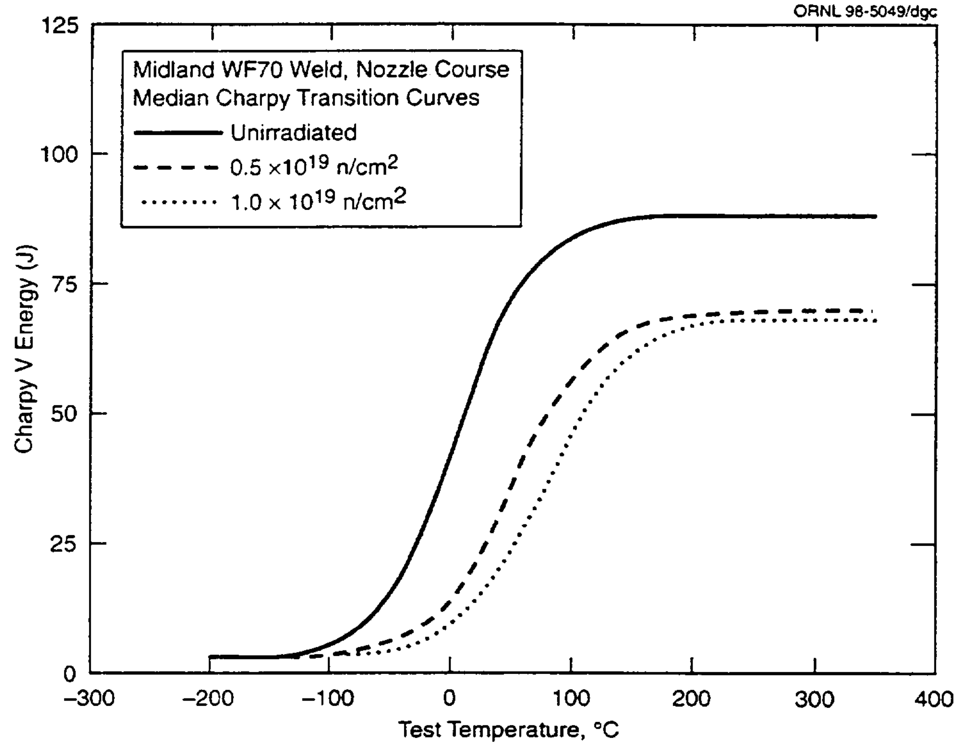

Figure 20. **Charpy V-notch transition energy curves before and after irradiation of WF-70 nozzle course weld.**

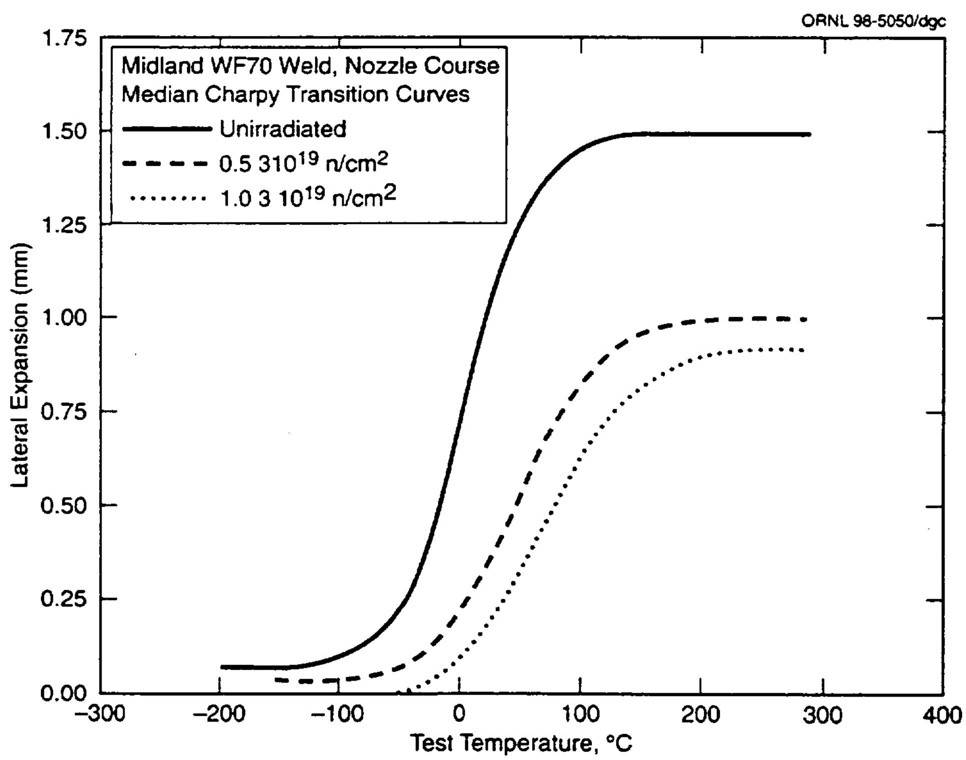

Figure 21. **Charpy V-notch lateral expansion of Charpy V-notch specimens before and after irradiation of WF-70 nozzle course weld.**

Table 13. Features of Charpy transition curve indices

Material	Energy criteria: 41-J temperature (°C)			Energy criteria: Charpy upper-shelf energy (USE) (J)		
	Unirradiated	Irradiated to 0.5×10^{19} n/cm^2	Irradiated to 1×10^{19} n/cm^2	Unirradiated	Irradiated to 0.5×10^{19} n/cm^2	Irradiated to 1×10^{19} n/cm^2
Beltline	–9	36	94	88.5	80.8	80.4
Nozzle course	–1	62	89	87.7	69.7	68.2

Material	Irradiated	Transition temperature change (°C)			Percent change in upper-shelf properties (%)	
		ΔTT_{41J}	$\Delta TT_{50\%}$[a]	ΔTT 50% lateral expansion[a]	Joules	Lateral expansion
Beltline	0.5×10^{19} n/cm^2	45	40	39	–10	–34
	1×10^{19} n/cm^2	103	100	85	–10	–46
Nozzle course	0.5×10^{19} n/cm^2	63	48	43	–20	–34
	1×10^{19} n/cm^2	90	72	65	–23	–40

[a]50% represents the midtransition curve by energy.

On the other hand, the master curve approach uses fracture mechanics–based data to position a median universal curve. The effectiveness of these two approaches as applied to WF-70 weld metal data will be presented and discussed in this section. The as-irradiated fracture mechanics K_{Jc} data are tabulated in Tables 14 and 15.

In addition to transition temperature evaluations, upper-shelf fracture toughness was evaluated by K_R-curves. The R-curve methodology measures resistance to slow-stable crack growth, and such properties are of relevance to the in-service performance of reactor pressure vessel steels only when the growth resistance is extremely low and ductile crack instability becomes a possibility. In the present experiment, the R-curve characteristics of low upper-shelf materials and the comparison between beltline versus nozzle course welds were two supplementary objectives.

5.3.1 Evaluation of Irradiation Damage by ASME Code

The shift of the ASME RT_{NDT} temperature caused by irradiation damage is referenced to the 41-J Charpy transition temperatures developed from specimens exposed in surveillance capsules. Federal Code 10 CFR 50 references ASTM E 185-82,[6] "Conducting Surveillance Tests for Light-Water-Cooled Nuclear Power Reactor Vessels." The Charpy specimens must be full size, as defined in ASTM E 23.[16] A minimum of 12 irradiated specimens is required; however, 14 irradiated specimens were used in the present experiment. The K_{Jc} data and lower-bound K_{Ic} curves shifted by ΔTT_{41J} are shown in Figures 22 and 23. The overly conservative placement of the K_{Ic} curves is the same, as had been seen before with unirradiated material. In the present case, however, the unirradiated material K_{Ic} curve offset is the same as the initial RT_{NDT} offset, suggesting that the ΔTT_{41J} shift is about equal to the shift of the fracture toughness data. To illustrate, an unrecommended alternate evaluation of this ASME methodology was made using NDT as the unirradiated RT_{NDT} temperature. The revised plots are given in Figures 24 and 25. Here the data are more accurately represented by the repositioned lower-bound K_{Ic} curve, but, in the case of the irradiated nozzle weld, some of the mid-transition data tended to slip slightly below the lower-bound K_{Ic} curve. This problem is partially due to the K_{Ic} curve shape. The current ASME methodology to define the K_{Ic} curve position for LUS materials was developed to be a conservative decision, again, made in the absence of supporting fracture toughness evidence. The conservative positioning of RT_{NDT} is not supported here as being a justifiably conservative decision to account for the fracture mechanics performance of steels. Propensity for easy slow-stable crack growth is the principal weakness in LUS steel that has been clearly identified. The application of a transition temperature margin does not provide protection from upper-shelf ductile ruptures.

Table 14. Midland irradiated beltline weld K_{Jc} values

Test temperature (°C)	1/2T			1T			PCVN			b_o (in.)	Δa_p (in.)	Control K_{Jc} value (MPa $\sqrt{m}$)	Validity
	Code	Side groove (%)	K_{Jc} (MPa $\sqrt{m}$)	Code	Side groove (%)	K_{Jc} (MPa $\sqrt{m}$)	Code	Side groove (%)	K_{Jc} (MPa $\sqrt{m}$)				
After irradiation to 1 × 10^{19} n/cm^2													
150				MW11HD	20	176.7				0.891	0.086	Non-test	Ductile instability
				MW9HB	20	264.1				0.928	0.278	J_R curve	
				MW11HB	0	389.8						J_R curve	
				MW9HD	0	300.7						J_R curve	
				MW14B22	20	242.6				0.904	0.152	J_R curve	
				MW14A22	20	221.5				0.922	0.185	J_R curve	
				MW14C23	20	212.0				0.917	0.154	J_R curve	
90				MW11LD	0	112.6				0.927	0	112.6	
				MW11JA	0	162.7				0.999	0.006	162.7	
				MW9ID	0	151.6				0.928	0	151.6	
				MW9LA	0	208.9				0.979	0.083	208.9	Invalid
				MW9MN	0	259.5				0.980	0.105	259.5	Invalid
				MW9IC	0	325.1				0.998	0.300	J_R curve	Invalid
				MW9JB	0	307.0				0.948	0.170	307.0	Invalid
75				MW9KD	0	110.3				0.945	0	110.3	
				MW11JD	0	115.2				0.943	0	115.2	
				MW11KD	0	134.9				0.955	0	134.9	
				MW9NA	0	183.6				0.947	0.022	183.6	
				MW11LB	0	211.9				0.942	0.029	211.9	
				MW9JC	0	240.0				0.950	0.025	240.0	
				MW11JC	0	345.1				0.908	0.312	J_R curve	Invalid
				MW9LB	0	260.7				0.937	0.080	260.7	Invalid
50	MW11LFB	0	107.1							0.486	0	107.1	
	MW11MCA	0	132.8							0.491	0	132.3	
	MW9LEB	0	133.8							0.485	0	133.8	
	MW11HEB	0	176.1							0.471	0	176.1	
	MW9HEA	0	217.3							0.488	0.059	217.3	Invalid

Table 14 (continued)

Test temperature (°C)	1/2T Code	1/2T Side groove (%)	1/2T K_{Jc} (MPa $\sqrt{m}$)	1T Code	1T Side groove (%)	1T K_{Jc} (MPa $\sqrt{m}$)	PCVN Code	PCVN Side groove (%)	PCVN K_{Jc} (MPa $\sqrt{m}$)	b_o (in.)	Δa_p (in.)	Control K_{Jc} value (MPa $\sqrt{m}$)	Validity
35				MW11ID	0	76.2				0.952	0	76.2	
				MW9LD	0	87.2				0.938	0	87.2	
				MW9JA	0	89.2				0.961	0	89.2	
				MW9KB	0	116.6				0.985	0	116.6	
				MW9LC	0	132.9				0.986	0	132.9	
				MW11IC	0	122.4				0.957	0	122.4	
20	MW9IFA	0	69.7							0.499	0	69.7	
	MW11JFA	0	68.5							0.485	0	68.5	
	MW9JFB	0	91.6							0.493	0	91.6	
	MW9OFA	0	118.7							0.485	0	118.7	
	MW11LEB	0	104.2							0.486	0	104.2	
	MW9IEA	0	140.3							0.497	0	140.3	
–50				MW9KC	0	71.7				0.952	0	71.7	
				MW11LC	0	41.1				0.965	0	41.1	
				MW11KC	0	47.3				0.959	0	47.3	
22							2DEO	0	61.4	0.180	0	61.4	
							2DE3	0	64.4	0.193	0	64.4	
							2DE1	0	92.3	0.191	0	92.3	
							2DE4	0	89.4	0.199	0	89.4	
							2DE7	0	95.8	0.195	0.007	95.8	
							2DE5	0	96.1	0.194	0.003	96.1	
							2DE2	0	116.4	0.192	0.005	116.4	
							2DE6	0	116.1	0.199	0.004	116.1	
							2DE8	0	174.2	0.193	0.008	(147.9)	Invalid
							2DE9	0	179.1	0.210	0.007	(154.3)	Invalid
0							MW9EE1		58.4	0.180	0	58.4	
							MW9EE3		54.4	0.177	0	54.4	
							MW15DE2		71.3	0.180	0	71.3	
							MW15DE1		57.1	0.182	0	57.1	
							MW15AE4		91.6	0.178	0	91.6	
							MW15AK3		72.4	0.179	0	72.4	
							MW15AE3		97.2	0.154	0	97.2	
							MW11CE2		78.2	0.178	0	78.2	

Table 14 (continued)

Test temperature (°C)	1/2T Code	1/2T Side groove (%)	1/2T K_{Jc} (MPa $\sqrt{m}$)	1T Code	1T Side groove (%)	1T K_{Jc} (MPa $\sqrt{m}$)	PCVN Code	PCVN Side groove (%)	PCVN K_{Jc} (MPa $\sqrt{m}$)	b_o (in.)	Δa_p (in.)	Control K_{Jc} value (MPa $\sqrt{m}$)	Validity
After irradiation to 0.5 × 10^{19} n/cm^2													
−12	MW9NEI	20	89.9							0.478	0	89.9	
	MW11MEB	20	55.1							0.472	0	55.1	
	MW9NE2	20	61.8							0.424	0	61.8	
	MW9IFA	20	77.3							0.499	0	77.3	
	MS11FB	20	77.8							0.439	0	77.8	
	MW9IEA	20	90.1							0.436	0	90.1	
−12							MW9ME4	0	140.6	0.153	0	(130.4)	Invalid
							MW9ME2	0	144.7	0.160	0	(133.5)	Invalid
							MW9ME3	0	110.5	0.163	0	110.5	
							MW9MEI	0	80.3	0.165	0	80.3	
							MW9ME5	0	71.4	0.166	0	71.4	
							MW9MF5	0	69.9	0.168	0	69.9	
							MW9BJ5	0	61.0	0.170	0	61.0	

Table 15. Midland irradiated nozzle course WF-70 weld material irradiated to 1 × 10^{19} n/cm^2

Test temperature (°C)	1/2T			1T			PCVN			b_o	Δ_a	Control K_{Jc} value (MPa $\sqrt{m}$)	Validity
	Code	Side groove (%)	K_{Jc} (MPa $\sqrt{m}$)	Code	Side groove (%)	K_{Jc} (MPa $\sqrt{m}$)	Code	Side groove (%)	K_{Jc} (MPa $\sqrt{m}$)				
150				31IA	20	187.5				0.847	0.081	Nontest	Ductile instability
				34KA	20	180.0				0.864	0.086	Nontest	Ductile instability
75				31HD	20	77.0				0.868	0	77.0	
				34LE	20	94.5				0.871	0	94.5	
				31JC	20	109.0				0.879	0	109.0	
				34IB	20	115.2				0.870	0	115.2	
				31KE	20	125.1				0.882	0	125.1	
				34KB	20	180.3				0.877	0	180.3	
65	E31L	0	102.3							0.434	0	102.3	
	F31L	0	121.9							0.426	0	121.9	
	G31L	0	109.1							0.419	0	109.1	
	H31L	0	121.2							0.418	0	121.2	
	I31L	0	126.8							0.429	0	126.8	
	J31L	0	121.7							0.407	0	121.7	
45				31IE	20	67.9				0.877	0	67.9	
				34JD	20	70.9				0.866	0	70.9	
				34JC	20	81.4				0.890	0	81.4	
				34LA	20	92.6				0.885	0	92.6	
				34LB	20	105.6				0.886	0	105.6	
				34KD	20	92.2				0.873	0	92.2	
				31HE	20	92.8				0.876	0	92.8	
25							NC31BH5	0	77.6	0.197	0.007	77.6	
							NC31BB1	0	114.9	0.229	0	114.9	
							NC31BH3	0	78.0	0.191	0.003	78.0	
							NC31BA4	0	110.4	0.194	0.001	110.4	
							NC34AA5	0	101.2	0.189	0.007	101.2	
							NC34BEI	0	97.4	0.188	0.001	97.4	
							NC34BH4	0	93.6	0.182	0.005	93.6	
							NC34F4	0	94.8	0.195	0.003	94.8	
							NC34AA1	0	99.9	0.181	0.002	99.9	

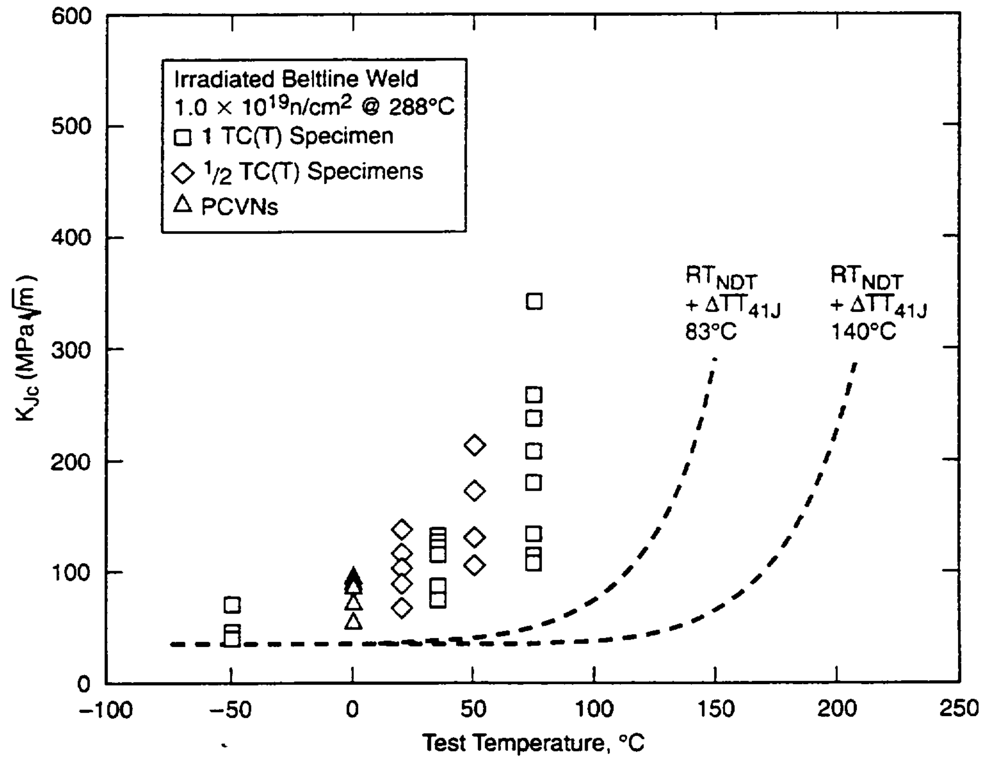

Figure 22. **Postirradiation beltline weld data and ΔTT_{41J} shifted lower-bound K_{Ic} curves.**

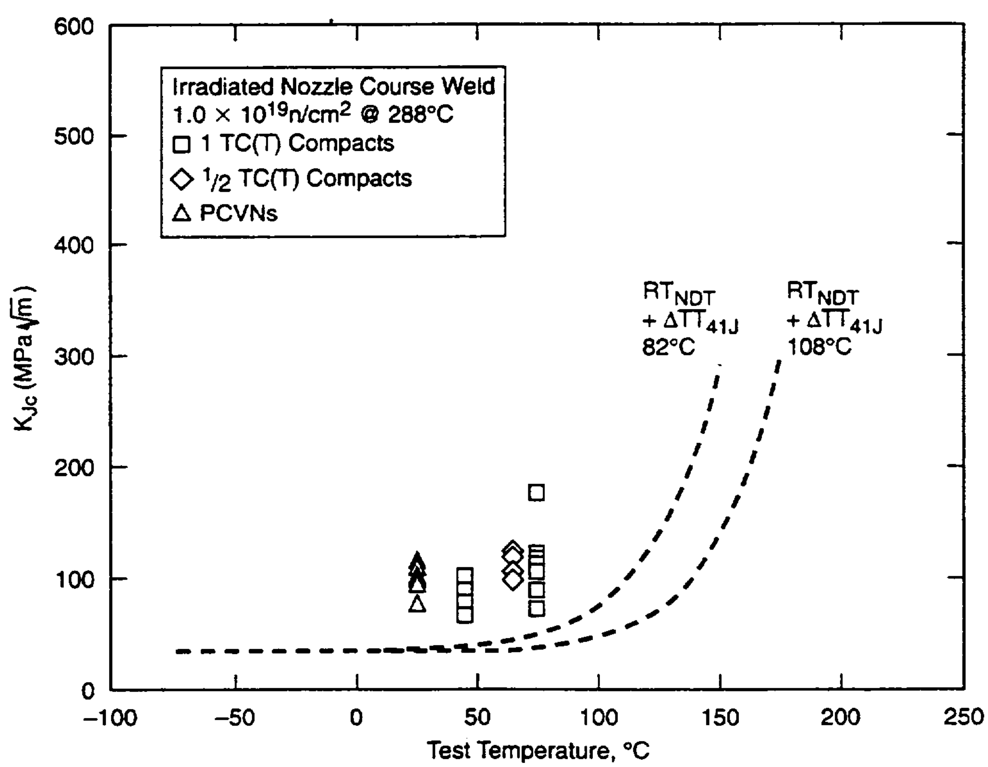

Figure 23. **Postirradiation nozzle course weld data and ΔTT_{41J} shifted lower-bound K_{Ic} curves.**

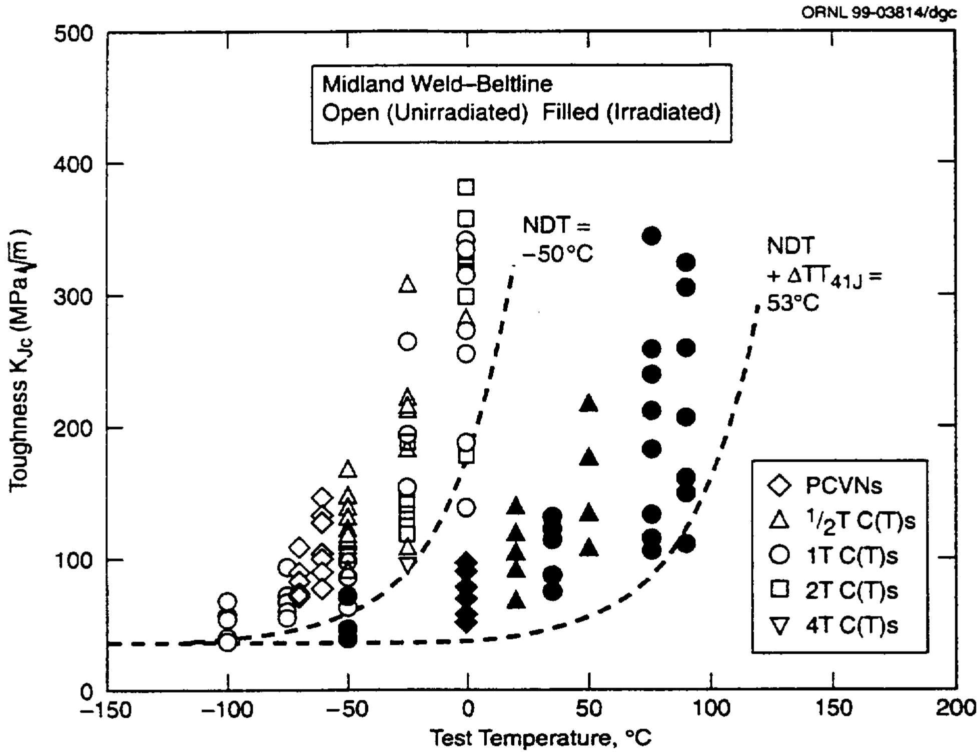

Figure 24. **Unirradiated and irradiated data for Midland beltline weld metal with the drop-weight NDT used as the reference temperature for lower-bound K_{Ic}.**

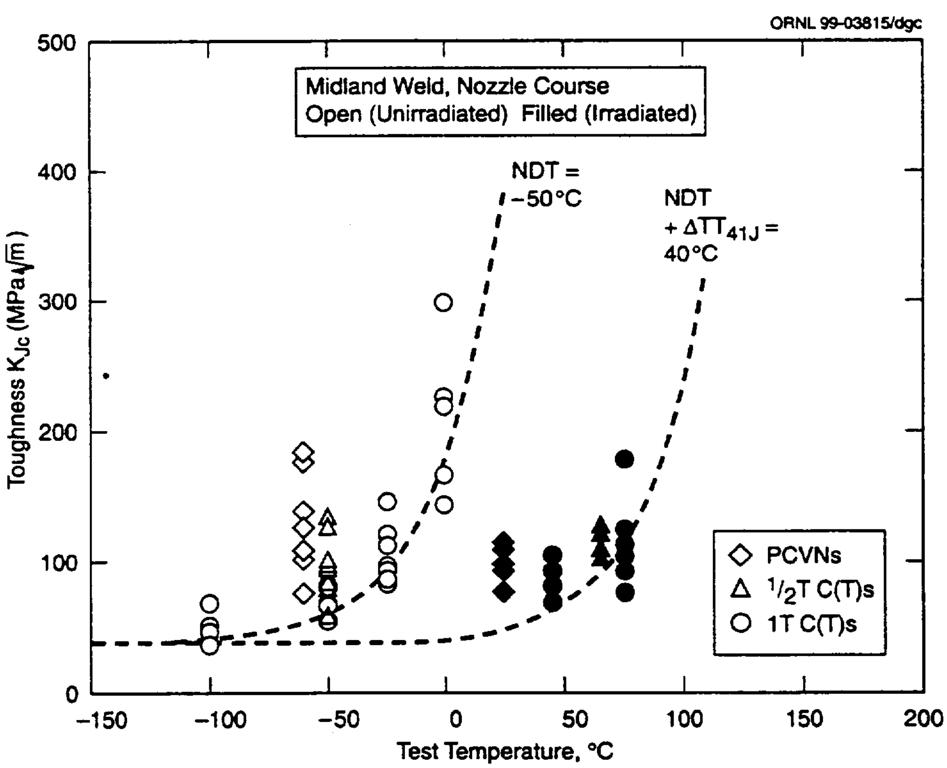

Figure 25. **Unirradiated and irradiated data for Midland nozzle course weld with the drop-weight NDT used as the reference temperature for lower-bound K_{Ic}.**

5.3.2 Master Curve Methodology

The master curve methodology uses information from fracture mechanics tests to establish a reference temperature, T_o. Temperature T_o corresponds to $K_{Jc(med)}$ = 100 MPa $\sqrt{m}$ for 1T compact specimens. Table 16 presents the various T_o temperatures based on the data groups listed in Tables 14 and 15. The grand total T_o value comes from combining all data into one calculation. The master curve tolerance bound results that are analogous to the ASME-based curves of Figures 24 and 25 are shown in Figures 26 and 27. The ASME lower-bound K_{Ic} curve has recently been statistically evaluated to be an approximate 2% confidence bound, covering the most important portion of the temperature range.[17] Hence, 2% tolerance bounds on master curve were chosen to be used in Figures 26 and 27. The curve shape in the master curve development has been established from multiple experimental and theoretical verifications. Because the master curve method is based on 1T specimen size, all data shown in Figures 26 and 27 are values at 1T equivalence. Table 16 summarizes T_o reference temperatures.

Table 17 summarizes transition temperature shifts as measured by four available methods: namely, the Charpy 41-J shift, ΔTT_{41J}, T_o temperature shift, ΔT_o, ΔTT by the NRC *Regulatory Guide 1.99*, chemistry factor, and ΔTT estimated from the change in tensile properties.[17] Figures 28 and 29 use *Regulatory Guide 1.99 (Rev. 2)* to lend some perspective to the data of Table 17. The true ΔTT shift is not always similarly defined by all four criteria. The 41-J Charpy shift of the beltline weld material at 0.5×10^{19} n/cm^2 was clearly different relative to estimation of the fracture toughness shift.

Table 16. Summary tabulation of T_o values for irradiated specimens

Material	Irradiation (n/cm^2)	Specimen size	Test temperature (°C)	T_o (°C)	Grand total T_o (°C)
Beltline	1×10^{19}	1T	75	22.5	
		1/2T	50	29.9	
		1T	35	33.0	
		1/2T	20	29.2	
					27.4
	0.5×10^{19}	1/2T	−12	23.9	23.9
Nozzle course	1×10^{19}	1T	75	60.4	
		1/2T	65	68.8	
		1T	45	59.5	
					62.2

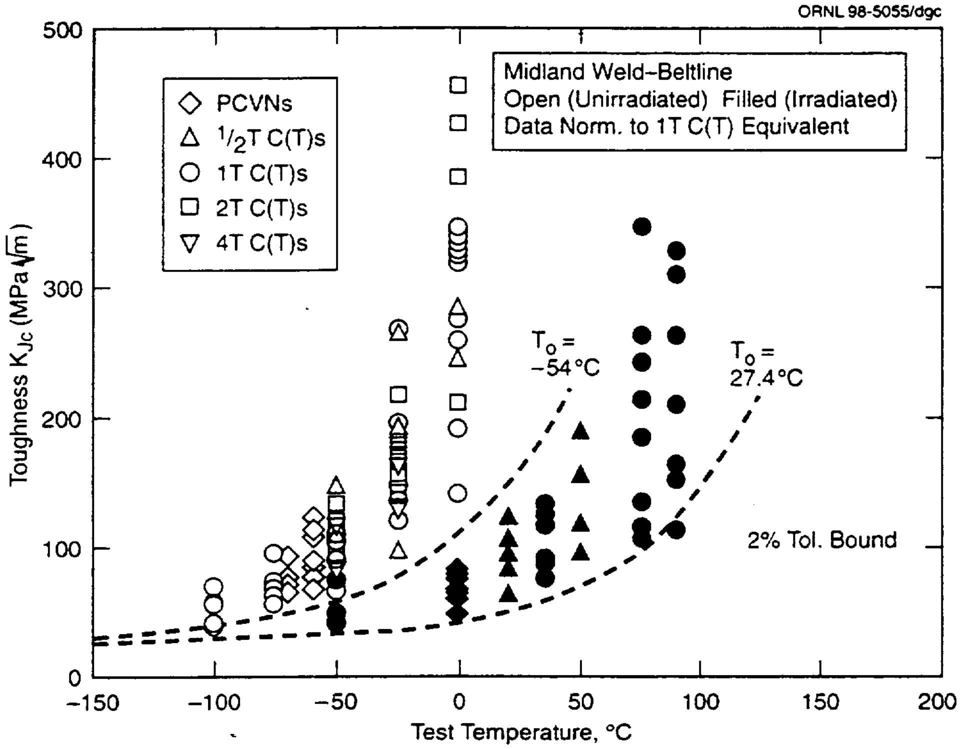

Figure 26. **Unirradiated and irradiated data for Midland beltline compared to the 2% tolerance bounds from the master curves.**

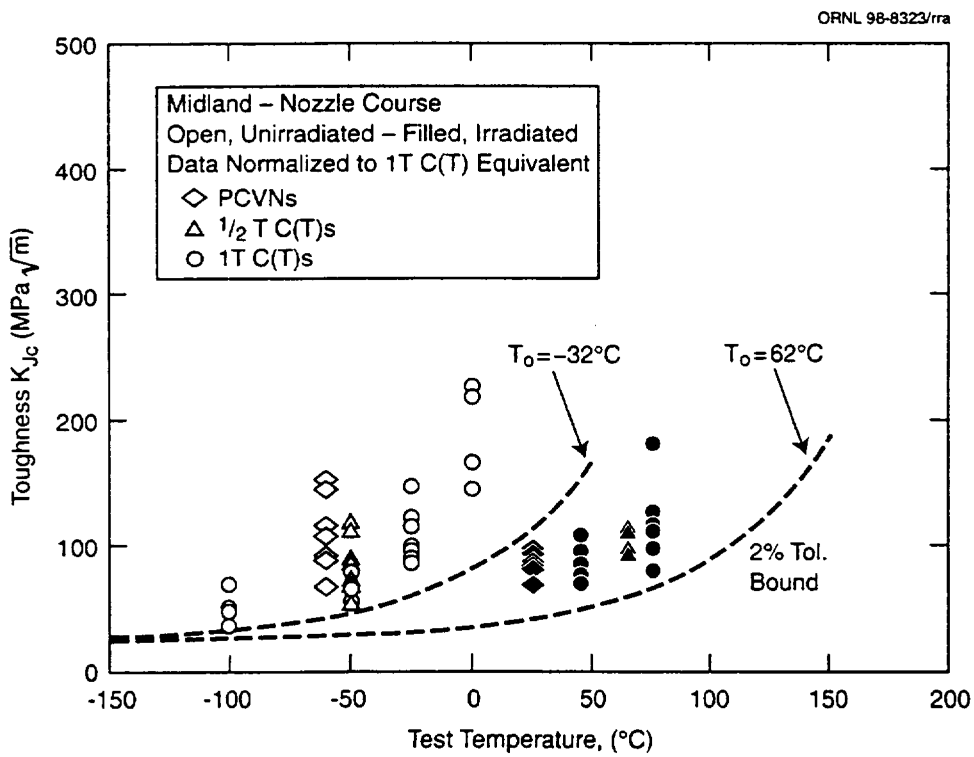

Figure 27. **Unirradiated and irradiated data for Midland nozzle course weld compared to the 2% tolerance bounds from the master curves.**

Table 17. Property changes due to irradiation

Fluence (n/cm^2)	ΔTT_{41J} (°C)	ΔT_o (°C)	*Regulatory Guide 1.99, Rev. 2* (°C)	$\Delta\sigma_{UTS}$ at room temperature (MPa)
Beltline				
0.5×10^{19}	45	78	81	104
1.0×10^{19}	103	81	100	134
Nozzle course				
0.5×10^{19}	63	NA	103	55
1.0×10^{19}	90	94	128	137

For the nozzle course weld material, significant deficiency appears to belong to the chemistry factor given in *Regulatory Guide 1.99.* The unexplained lack of nozzle course strengthening at 0.5×10^{19} n/cm^2 appears again in Figure 29.

5.4 Irradiation Effects on K_R Curves (R-Curves)

The comparison of R-curves is made difficult because R-curve properties are not always well represented by single-value numerical parameters that can be tabulated and compared. Nevertheless, two single-value properties that can be used to partially represent R-curves are (1) J_{Ic} that indicates toughness near the onset of slow-stable crack growth and (2) T-modulus for the rate of toughness development with crack growth, dJ/da, at the beginning of crack growth resistance development. There is no standard practice for the determination of dJ/da; hence, the T-modulus is a stochastic-type methodology for R-curve slope determination, made dimensionless by normalization using material flow strength and elastic modulus:

$$T = \frac{E}{\sigma_f^2}\left(\frac{dJ}{da}\right) , \tag{8}$$

where $\sigma_f = (\sigma_{ys} + \sigma_{UTS})/2$.

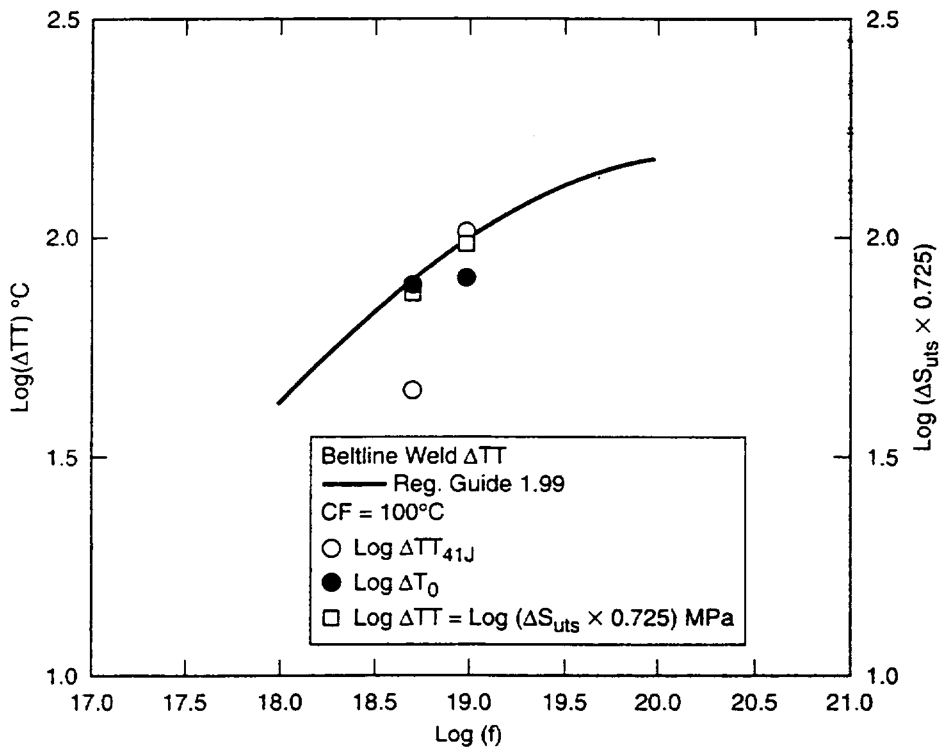

Figure 28. ***Regulatory Guide 1.99*** **predicted ΔTT curve calculated from chemistry factor and the experimentally measured ΔTT shifts by three methods for the beltline weld.**

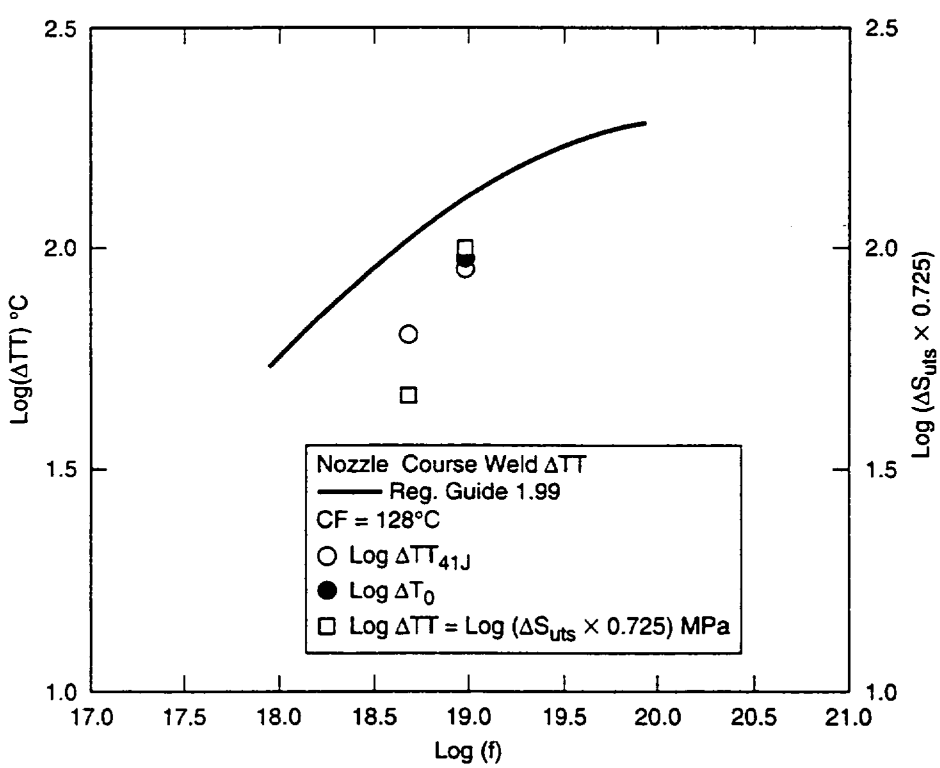

Figure 29. ***Regulatory Guide 1.99*** **predicted ΔTT curve calculated from chemistry factor for nozzle course weld versus the experimentally determined ΔTT shifts by three methods.**

R-curve slope, in the present case, is defined as the average R-curve slope between 0.2 and 1.5 mm (0.008 and 0.06 in.) of stable crack growth. Because there were only seven compact specimens irradiated for R-curve evaluations, all pre- and postirradiation comparisons are made at one selected upper-shelf temperature, namely 150°C (300°F). Table 18 presents the tabulated R-curve data. Only data from 20% side-grooved specimens are used here.

Focusing on J_{Ic} and T modulus at 150°C, it appears that the upper-shelf ductile tearing resistance of beltline weld metal has not been affected by irradiation up to 1×10^{19} n/cm^2. This is more accurately verified in Figure 30. However, beltline specimen MW11HD did not seem to fit the above assertion. In fact, the specimen suffered crack instability about halfway through the test at 177 MPa $\sqrt{m}$ crack drive.

Table 18. J_R curve properties

Test temperature (°C)	Code	J_{Ic} (in.-lb/in.^{2})	J_{Ic} (kJ/m^2)	Modulus (T)	Instability, K_c (MPa $\sqrt{m}$)	Average (J_{Ic})	Average (T)
Beltline weld material, unirradiated, 20% side grooved							
21	MW11MFA	870	152	71			
	MW11KEB	605	106	84			
	MW15GB	683	120	76			
	MW11FC	856	150	70		753	75
150	MW11IEB	693	121	41			
	MW9IFB	650	114	44			
	MW14C22	733	128	60		692	48
288	MW11MEA	449	79	32			
	MW11KFA	537	94	33		493	32
Beltline weld material, irradiated 1×10^{19} n/cm^2, 20% side grooved							
150	MW9HB	736	128	53			
	MW14B22	814	142	43			
	MW14A22	702	123	39			
	MW14C23	634	111	40			
	MW11HD	459	81	25	177	669	40
Nozzle course weld material, unirradiated, 20% side grooved							
21	NC31DB	658	115	47			
	NC34FG	587	103	57		622	52
150	NC34DB	534	93	39			
	NC34DA	467	82	43		500	41
288	I34M	359	63	32			
	NC31FB	335	59	39			
	NC31EA	334	59	37		343	36
Nozzle course weld material, irradiated 1×10^{19} n/cm^2, 20% side grooved							
150	NC34KA	503	88	23	180		
	NC31IA	484	85	35	187	493	29

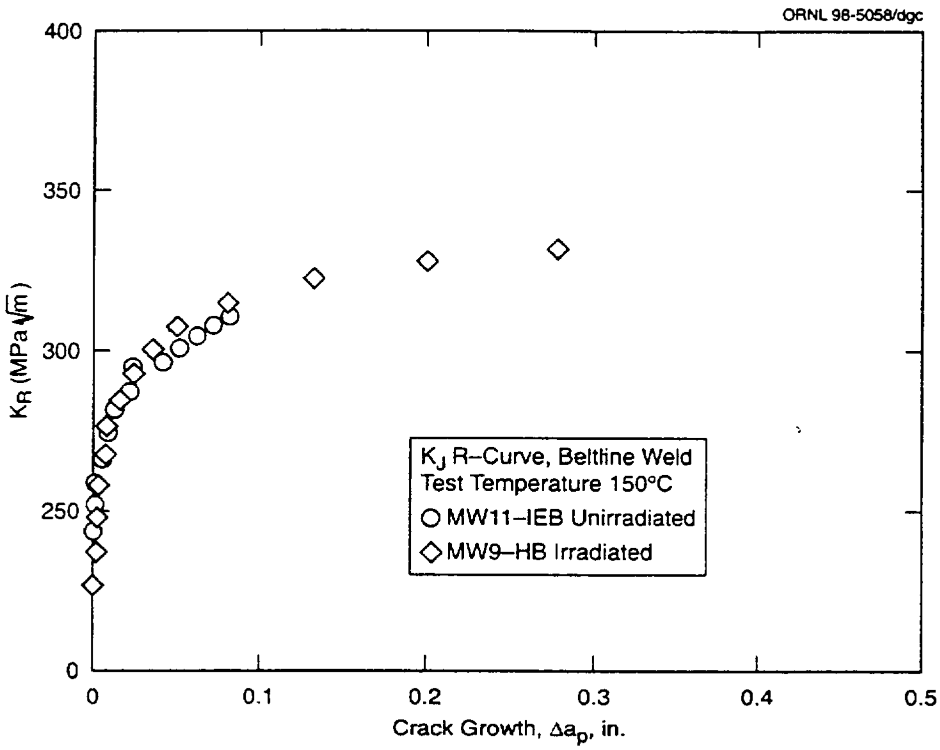

Figure 30. **Before and after irradiation (1.0×10^{19} n/cm^2) K_J R-curves on WF-70 beltline weld metal.**

This irradiated R-curve is compared to an unirradiated R-curve in Figure 31. Specimen MW11HD was clearly different in response to irradiation exposure, and the probable cause is its higher copper content. Table 2 reports high variability in beltline weld metal copper content, with the average copper content at about 0.25 wt %. However, specimen MW11HD came from a part of the beltline weld where copper ranged between 0.31 and 0.34 wt %. Load-displacement records provide further evidence that this specimen suffered ductile instability. Note the difference between Figures 32 and 33. Impending instability just beyond maximum load is evidenced in the form of small initial bursts of crack extension preceding the final separation.

Two nozzle course specimens were tested for R-curve, and, evidently because of the high copper content, both tests were terminated in ductile instabilities with test records that appeared similar to Figure 33.

Any suggestion that the three specimens mentioned could have failed by cleavage instability is not very likely, as suggested by Figure 34. The 150°C test temperature used on all specimens appears to be comfortably on upper shelf for WF-70 weld metals.

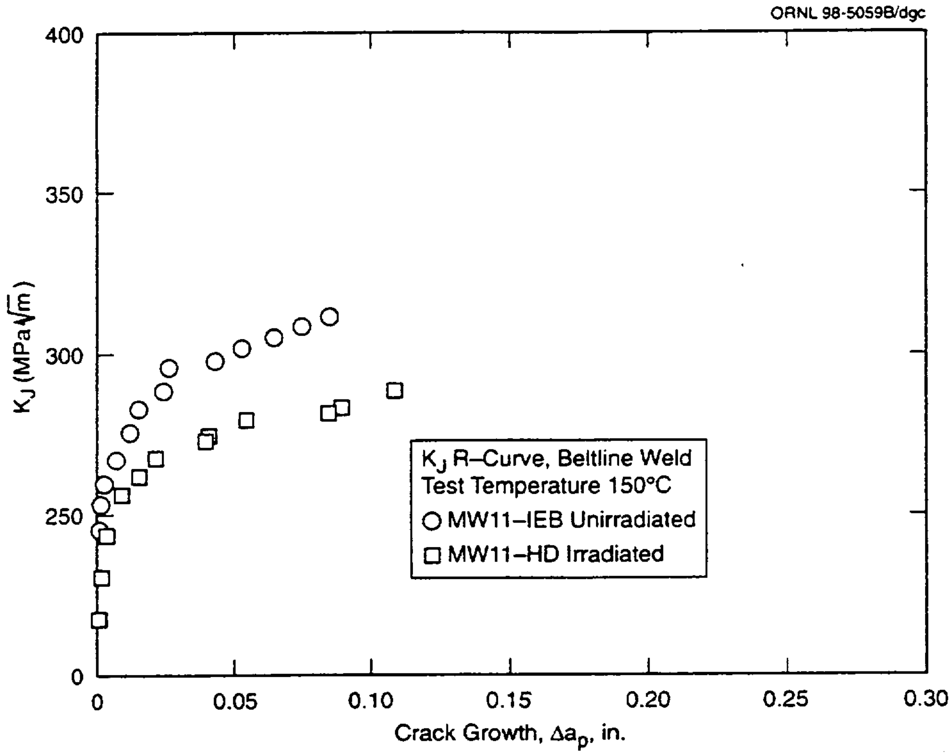

Figure 31. **The postirradiation K_J R-curve on one beltline weld specimen of high copper content compared to an unirradiated beltline specimen K_J R-curve.**

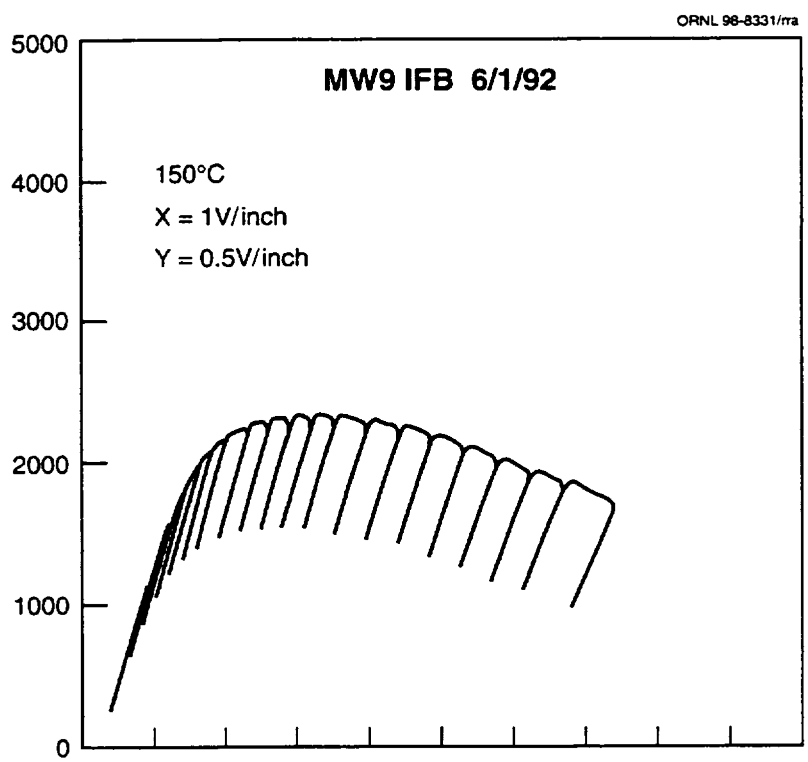

Figure 32. **The typical load versus crack mouth opening displacement record for unirradiated beltline weld metal, tested at 150°C.**

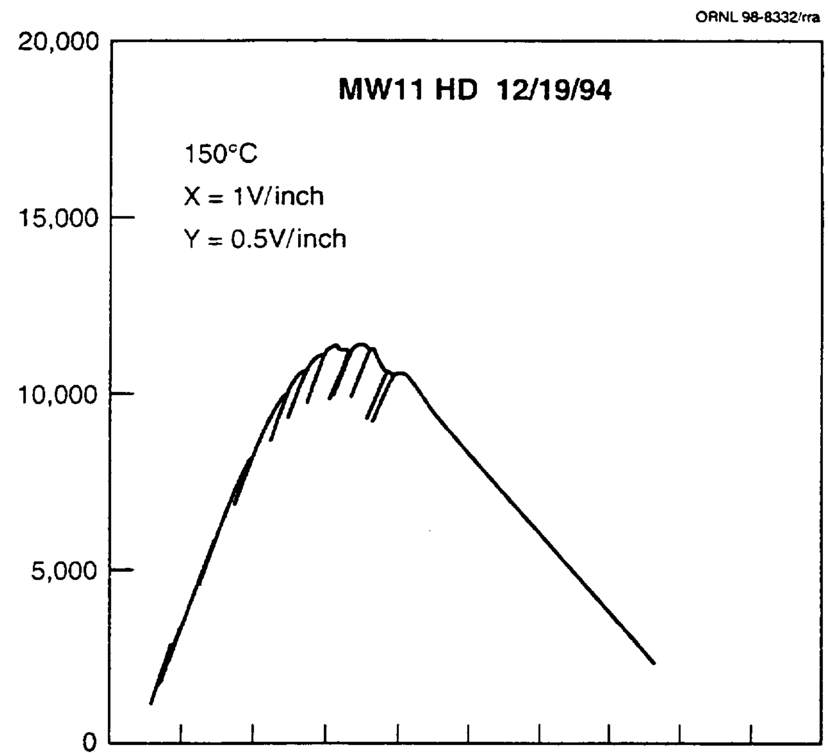

Figure 33. **A ductile instability type load versus crack mouth opening displacement record for an irradiated (to 1.0 × 10^{19} n/cm^2) beltline weld specimen taken from the region of highest copper content, tested at 150°C.**

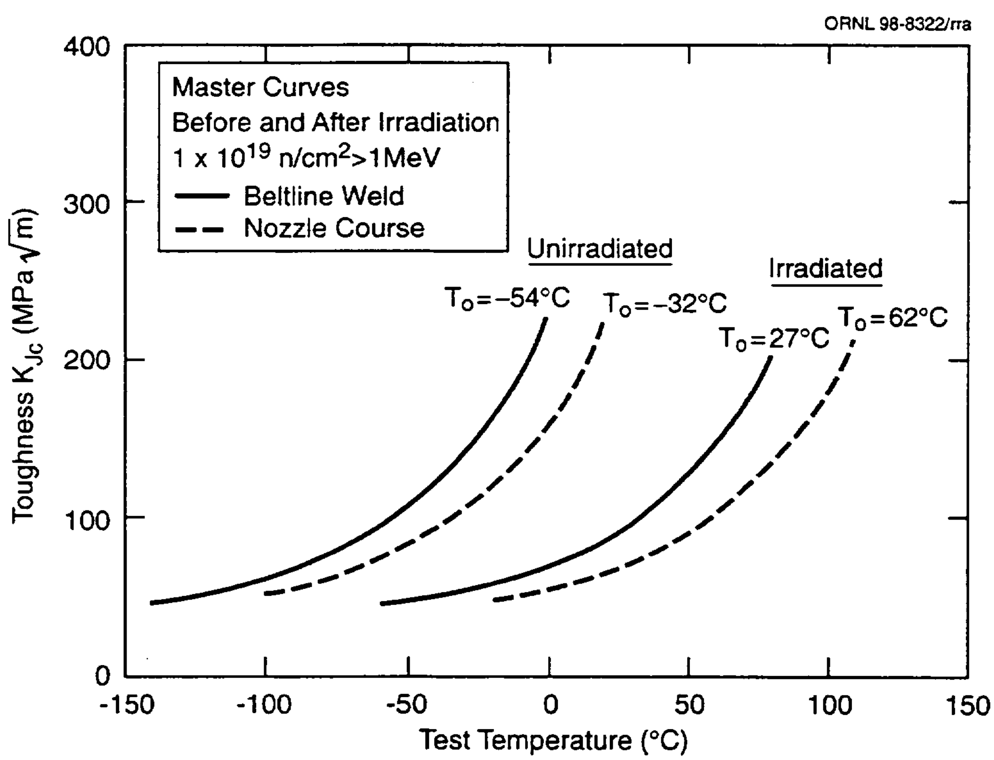

Figure 34. **Before and after irradiation master curves of both WF-70 weld metals; all are well below a 150°C test temperature.**

6. DISCUSSION

Postirradiation shape change that is commonly seen in CVN curves has been shown again in Figures 18 through 21. One issue of long-standing interest in HSSI research programs has been to determine if the transition curve shape based on fracture mechanics data will also change with temperature shift. Evidentally, the answer resides from upper-shelf energy reduction as the principal cause for the CVN shape change, and fracture mechanics methods have yet to show similar characteristics when upper-shelf R-curves fail to change after irradiation damage.

Figures 35 and 36 are used to illustrate how data can be evaluated for conformance to the universal master curve shape. Figure 35 represents the data scatter that had been observed with one of the two weld metals tested in the Fifth Irradiation Series.[18] The master curve shown defines the median K_{Jc} on data scatter after all K_{Jc} values have been adjusted to 1T equivalence. There were eight test temperatures, and the median K_{Jc} at each temperature is plotted against the master curve in Figure 36. Note that the test temperature on the abscissa has been normalized to reference temperature, T_o. These same two results are similarly evaluated in Figure 37 after irradiation to 1.5×10^{19} n/cm^2 (>1 MeV). The data trend as referenced to the master curve is about the same as it was in the unirradiated case.

Figures 38 and 39 make similar comparisons for the unirradiated and irradiated WF-70 beltline and nozzle course fracture toughness results at 1.0×10^{19} n/cm^2 (>1 MeV). Again, there is no evidence of curve shape change.

Omitted from Figure 38, however, was data obtained at 0°C corresponding to $T - T_o = 54$°C, even though there were 15 data generated at that temperature. The data had been analyzed for $K_{Jc(med)}$, and the value obtained had fit the master curve shape with apparently good accuracy. The problem was that the data distribution in this particular case had been influenced by certain well-disguised error sources. The test temperature of 0°C was only about 25°C short of the upper-shelf temperature for unirradiated material, and R-curve effects were beginning to influence the material cleavage type fracture toughness development patterns. R-curves are influenced by side grooving, as shown in Figure 40. Also, R-curves are not influenced by weakest-link type specimen size effects. Low upper-shelf steels develop onset of slow-stable crack growth at test temperatures that are only slightly above the reference temperature, T_o, so interfering R-curve effects had impacted the WF-70 weld data. Hence, the majority of the K_{Jc} values developed at 0°C were significantly biased. It is instructive to further examine what can happen to K_{Jc} data as upper-shelf temperature is approached.

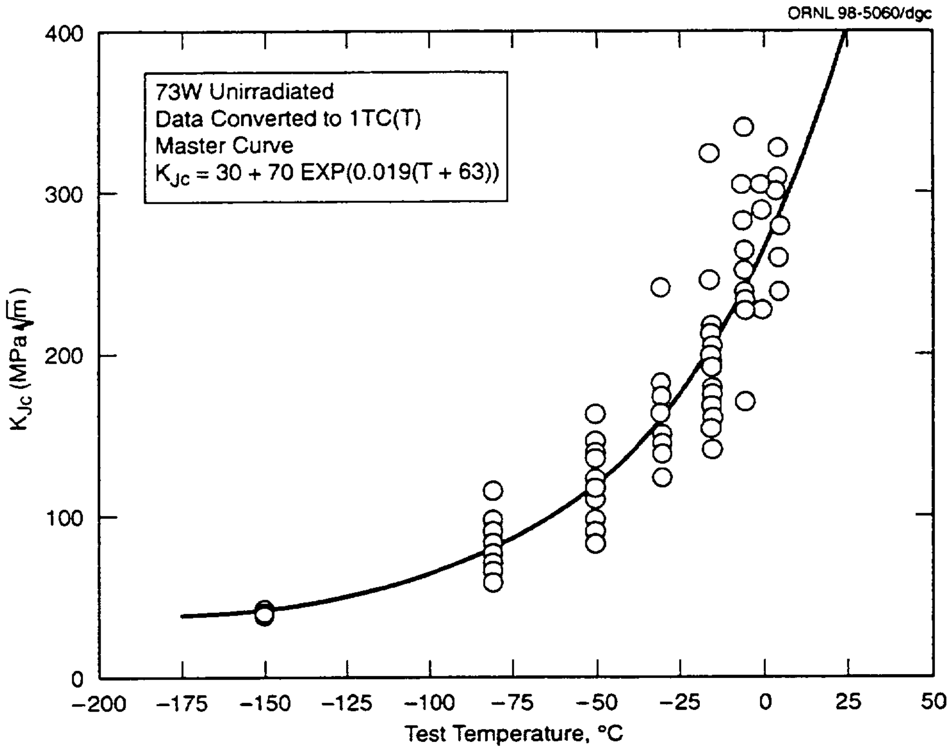

Figure 35. **Example of data scatter about the master curve (from the HSSI Fifth Irradiation Series).**

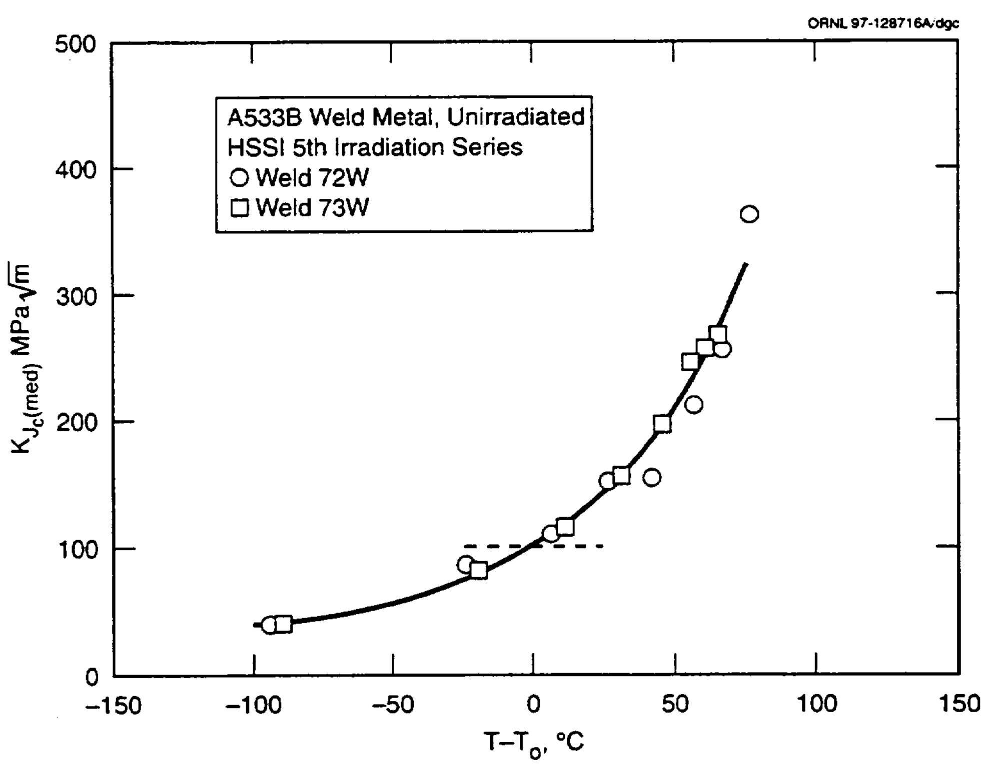

Figure 36. **Median fracture toughness for two materials plotted against the master curve.**

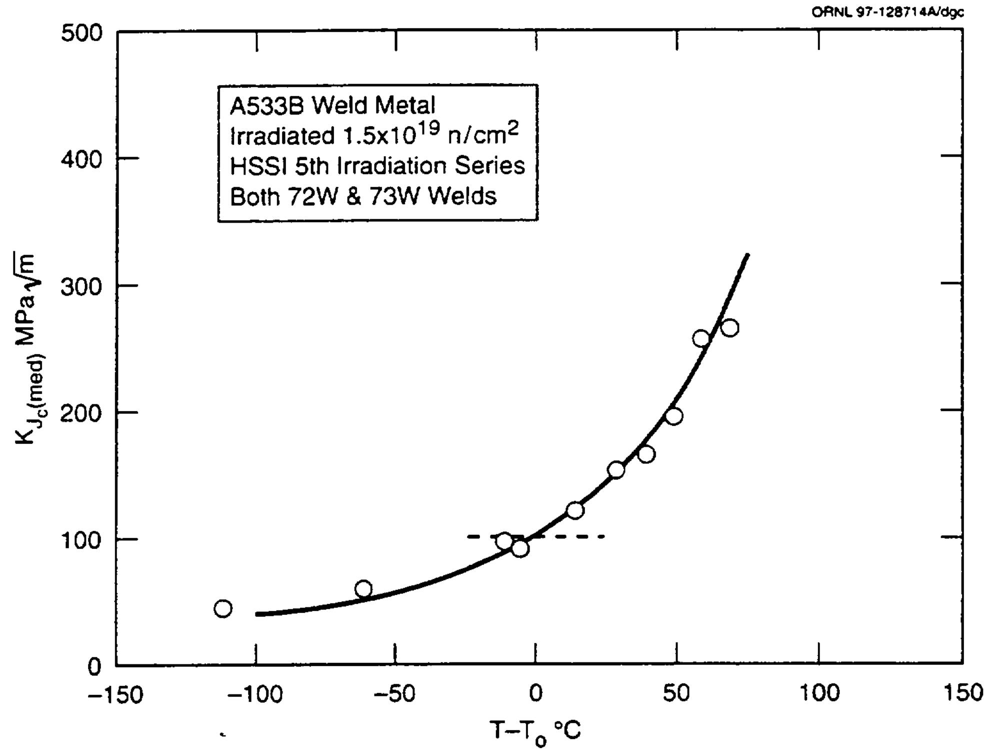

Figure 37. **The two materials shown in Figure 36 after irradiation to 1.5×10^{19} n/cm^2, again median K_{Jc} compared to the master curve.**

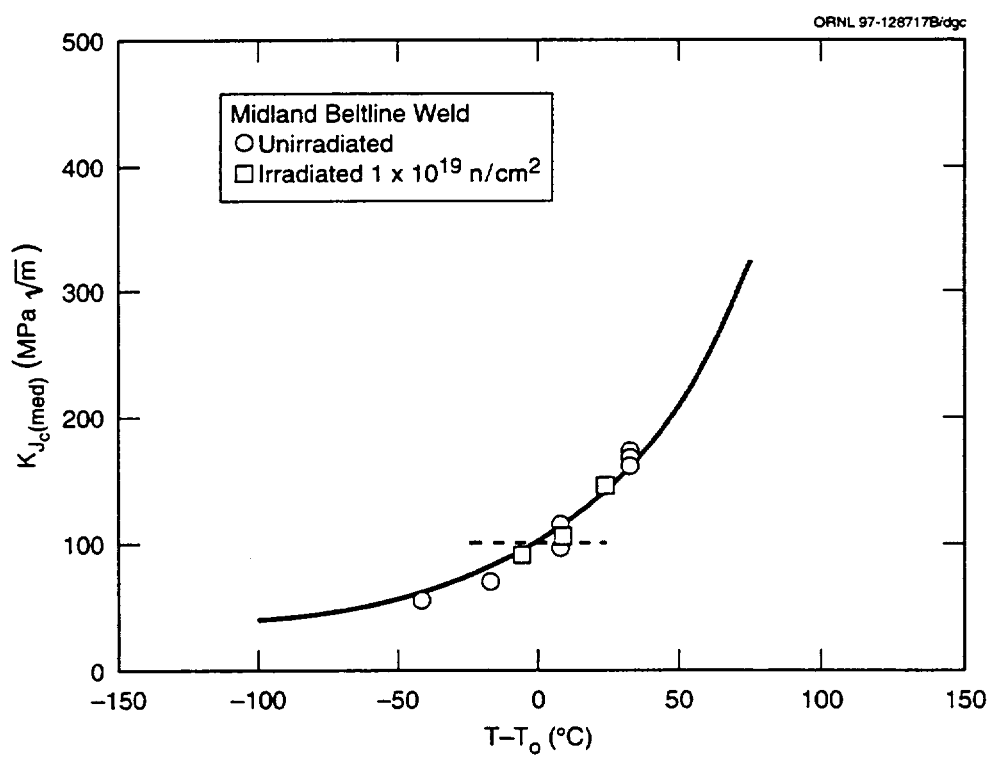

Figure 38. **Unirradiated and irradiated (1.0×10^{19} n/cm^2) median K_{Jc} beltline WF-70 weld metal plotted against the master curve.**

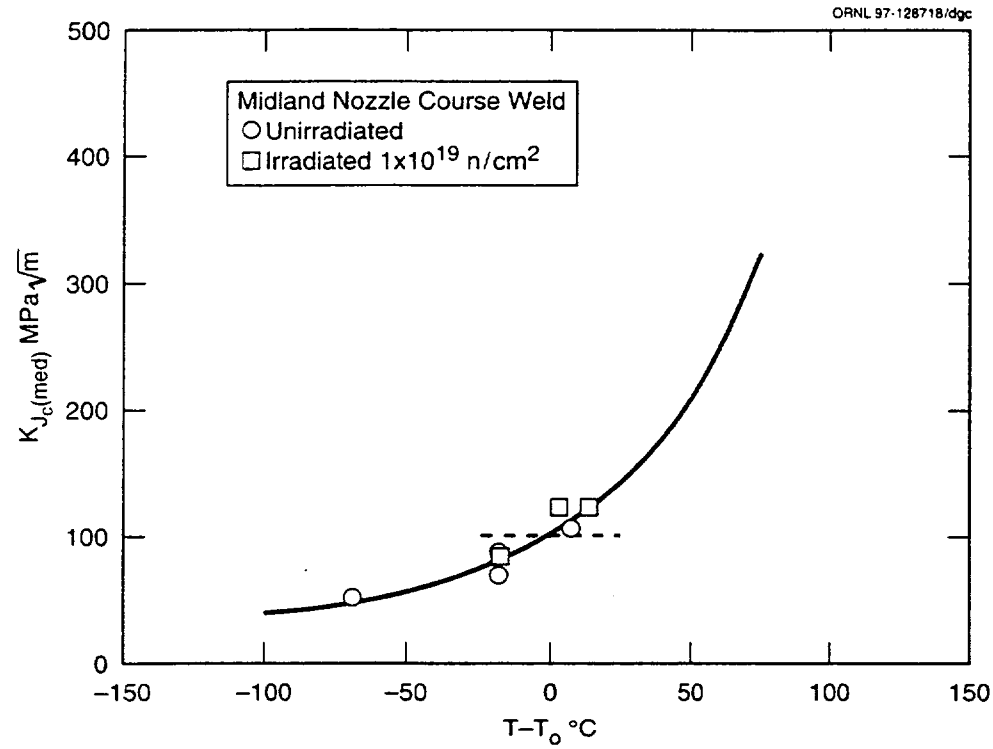

Figure 39. **Unirradiated and irradiated (1.0×10^{19} n/cm^2) nozzle course median K_{Jc} for WF-70 weld metal plotted against the master curve.**

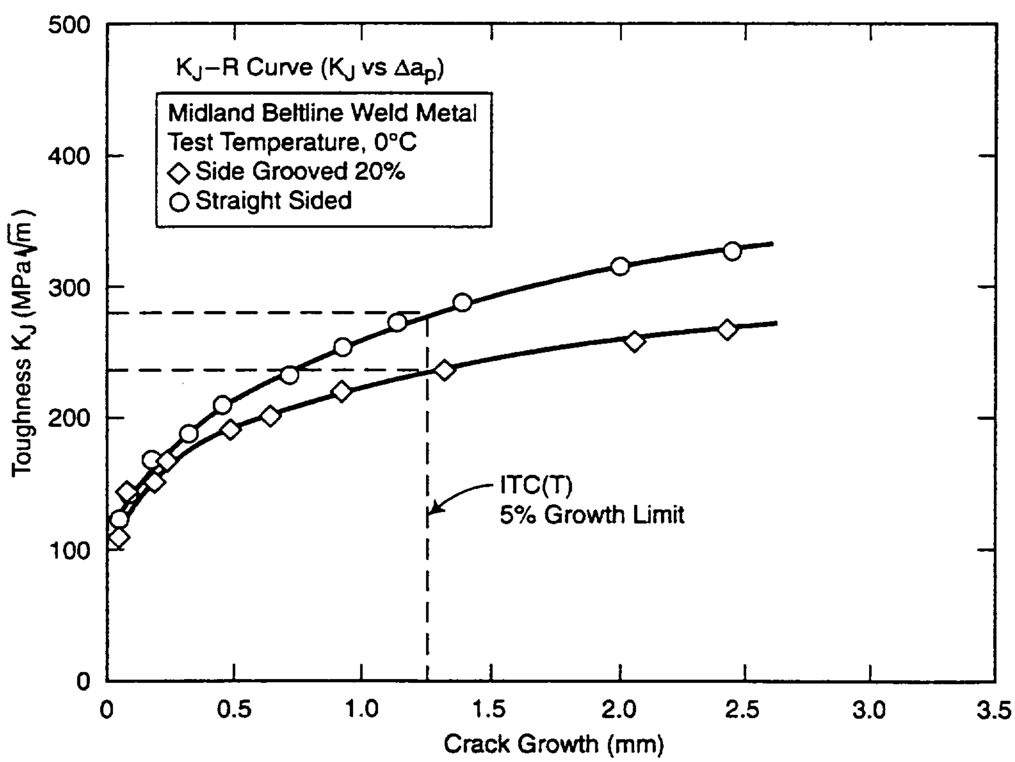

Figure 40. **Effect of side grooving on fracture toughness development as a function of slow-stable crack growth.**

R-curves were developed at 0, 150, and 288°C using side-grooved 1T specimens. Note in Figure 40 that considerable slow-stable growth is possible at 0°C, and at 0.05 b_o of slow-stable crack growth, side-grooved specimens can more readily reach a ductile instability K_J crack drive limit. Identification of such K_J instability values at the three previously mentioned test temperatures has led to the data indicated by filled squares and the K_R curve limit line shown in Figure 41. Faced with this evidence, one would naturally expect to see some data clustering near to or immediately above this limit line at 0°C. This did not happen. Of the 15 specimens tested at 0°C, 9 were 1T specimens and only 3 of these had been side grooved. Therefore, the upper R-curve shown in Figure 40 had controlled the path of growth resistance development in most cases. Two specimens were 1/2T compacts that suffered excessive loss of constraint, and neither could make a helpful contribution to a normal data scatter distribution. Four 2T compact specimens that had been tested at 0°C were not side grooved, and these also followed the high toughness R-curve crack growth resistance path shown in Figure 40. Here there was no evidence of a constraint control problem, but all K_{Jc}/K_J values were size adjusted to 1T equivalence, under conditions where the likelihood that specimen size effects had vanished due to being too near to upper shelf. Hence the size-adjusted K_{Jc} data exceed upper plateau R-curve fracture toughness capability of even the non-side-grooved 1T specimens.

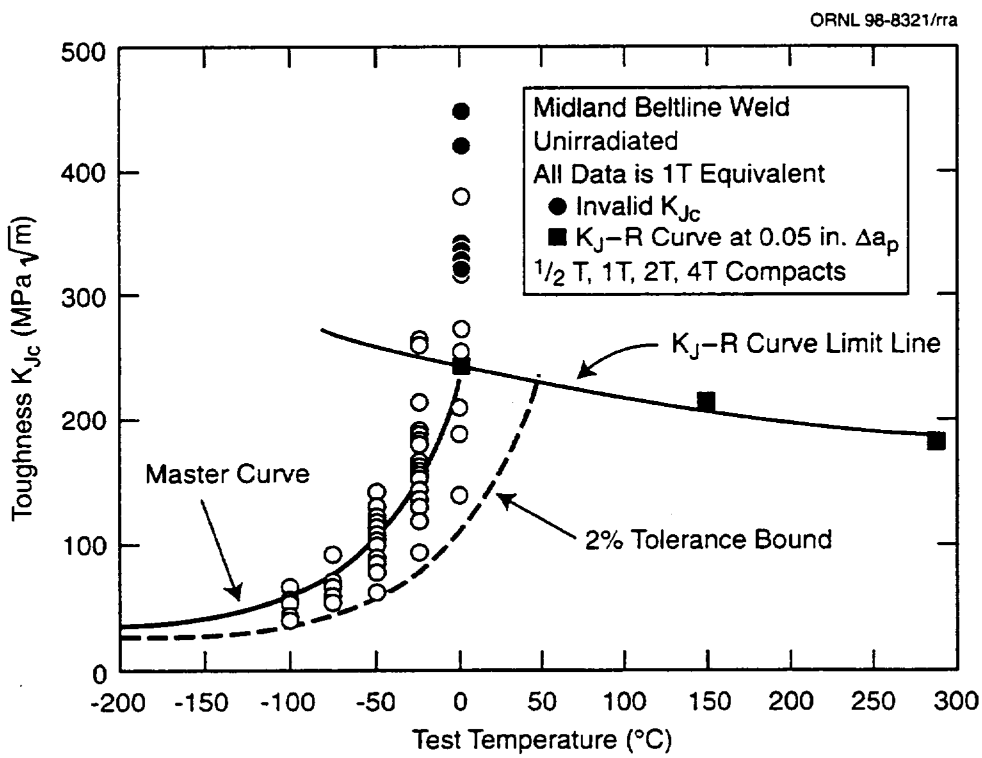

Figure 41. **Unirradiated beltline K_{Jc} data normalized to 1T equivalence; the master curve and 2% tolerance bound and a K_J limit line for side-grooved specimens.**

This experience clearly demonstrates problems that can arise when master curve data development is taken too close to upper-shelf temperatures. These problems are associated with the superposition of R-curve properties on K_{Jc} data distributions. Cleavage-controlled material characteristics tend to weaken or vanish in this temperature range. Consequently, data will begin to deviate away from the true master curve trend.

7. SUMMARY AND CONCLUSIONS

WF-70 weld metal obtained from the nozzle course shell and the beltline shell of the Midland Unit 1 reactor has been evaluated, covering most of the mechanical properties of relevance to service performance information needs. Baseline material characterization included chemical composition, tensile properties, Charpy V-notch transition curves, and drop-weight NDT determinations. These baseline determinations indicated negligible difference between beltline and nozzle course WF-70 weld metals other than showing a distinct difference in copper content. Fracture mechanics–based toughness evaluations in the form of transition temperature and R-curve tests were able to reveal that the two welds were in fact different prior to irradiation experiments and should be treated as such in irradiation damage evaluations.

The RT_{NDT} transition temperature of unirradiated WF-70 weld metal as evaluated by ASME Code practices was shown to be overly conservative relative to the fracture mechanics–based K_{Jc} data developed on WF-70 weld metal. Postirradiation positioning of the ASME lower-bound curve showed essentially similar misrepresentation of the irradiated data. However, the transition temperature shift was suitably quantified by the shift of Charpy V-notch transition temperature curves as referenced to the 41-J energy level. The misfit here came from the ASME Code application intended to introduce a safe operating margin for LUS steels by assuming that safe margin can be achieved using conservative transition temperature representation. The evidence developed in the present experiment has shown that LUS steels do not necessarily require such conservative transition temperature manipulations. Adequacy of the upper-shelf fracture toughness appears to be the important issue and this problem is not remedied through transition temperature manipulation.

Use of the master curve concept allowed more accurate fitting of transition range data developed by fracture mechanics test methods. The nozzle course WF-70 material with higher copper content exhibited only 13°C more fracture toughness transition temperature shift than the beltline weld.

Although the Charpy upper-shelf energy decreases of nozzle course and beltline weld metals were relatively small due to irradiation to 1×10^{19} n/cm^2 (>1 MeV), the effect on R-curve properties showed a more pronounced influence on the (higher copper content) nozzle course weld metal. With the average copper content of the beltline weld, there was no influence of irradiation on R-curve behavior. However, the weld metal with copper in the 0.30 to 0.40 wt % range showed significant irradiation damage to the upper-shelf (R-curve) resistance against slow-stable crack growth. In fact, three 1T compact specimens taken from high-copper regions showed ductile instabilities at about 175 MPa $\sqrt{m}$ (159 ksi $\sqrt{in.}$) crack drive. No ductile instability evidence was observed in any of the unirradiated material tests.

Nozzle course WF-70 weld metal with 0.4 wt % copper had far less ΔT shift as predicted by *Regulatory Guide 1.99* than the ΔT values measured by any of the three measurement criteria. This suggests that Midland nozzle course weld metal behaved according to a lower chemistry factor than the *Regulatory Guide* reported value. Eason et al.[19] have proposed a new relationship based on a Charpy V data base that was more than double that used to develop *Regulatory Guide 1.99 (Rev. 2)*. The Eason et al. ΔT is reduced by 19°C (34°F), which appears to be more consistent with the experimental result indicated herein.

The present experiment was unique from the standpoint of applying the master curve evaluation method to a low upper-shelf material. This study showed how transition range properties of K_{Jc} data distributions change as upper-shelf temperatures are approached. Hence, considerable care should be used in applying master curve concepts to low upper-shelf materials. Attention should be given to the proximity of test temperature to the upper-shelf temperature, where the tip-off is the extent of slow-stable crack growth prior to K_{Jc} cleavage instability events. The superposition of R-curve effects on transition range K_{Jc} data distributions suggests that certain awareness is needed when applying master curve indicated fracture toughness to low upper-shelf steels.

8. REFERENCES

1. *Material Documentation Report for the Weld Material Removed from the Consumers Power (Midland) Reactor Vessel* (620-0012-51), BAW-2070, Babcock and Wilcox, January 1989.

2. *ASME Boiler and Pressure Vessel Code, An American National Standard*, Section III, Division I-NB, Article 2330, American Society of Mechanical Engineers, New York, 1992.

3. R. K. Nanstad, D. E. McCabe, R. L. Swain, and M. K. Miller, *Chemical Composition and RT_{NDT} Determinations for Midland Weld WF-70*, USNRC Report NUREG/CR-5914 (ORNL-6740), December 1992.

4. K. K. Yoon, *Fracture Toughness Characterization of WF-70 Weld Metal*, BAW-2202, Babcock and Wilcox, September 1993.

5. ASTM Standard E 208-95a, "Conducting Drop-Weight Test to Determine Nil-Ductility Transition Temperature of Ferritic Steels," in *Annual Book of ASTM Standards*, Vol. 03.01, American Society for Testing and Materials, 1996.

6. ASTM Standard E 185-82, "Conducting Surveillance Tests for Light-Water Cooled Power Reactor Vessels," in *Annual Book of ASTM Standards*, Vol. 03.01, American Society for Testing and Materials, 1996.

7. ASTM Standard E 399-90, "Plane-Strain Fracture Toughness of Metallic Materials," in *Annual Book of ASTM Standards*, Vol. 03.01, American Society for Testing and Materials, 1996.

8. ASTM Standard E 1820-96, "Measurement of Fracture Toughness," in *Annual Book of ASTM Standards*, Vol. 03.01, American Society for Testing and Materials, 1998.

9. ASTM Standard E 1921-97, "Determination of Reference Temperature, T_o, for Ferritic Steels in the Transition Range," in *Annual Book of ASTM Standards*, Vol. 03.01, American Society for Testing and Materials, 1998.

10. Welding Research Council, "PVRC Recommendations on Toughness Requirements for Ferritic Materials," PVRC Ad Hoc Group on Toughness Requirements, WRC Bulletin 175, New York, August 1972.

11. Electric Power Research Institute, "Flaw Evaluation Procedures: ASME Section XI," EPRI report NP-719-SR, New York, August 1978.

12. K. Wallin, "The Scatter in K_{Ic}-Results," *Engineering Fracture Mechanics*, 19(6), 1085-1093 (1984).

13. D. E. McCabe, R. K. Nanstad, S. K. Iskander, and R. L. Swain, *Unirradiated Material Properties of Midland Weld WF-70*, USNRC Report NUREG/CR-6249 (ORNL/TM-1277), October 1994.

14. J. D. Landes, D. E. McCabe, and H. A. Ernst, "Geometry Effects on the R-Curve," pp. 123-143 in *Nonlinear Fracture Mechanics: Volume II - Elastic-Plastic Fracture, ASTM STP 995*, American Society for Testing and Materials, 1989.

15. ASTM Standard E 1221-88, "Determining Plane-Strain Crack-Arrest Fracture Toughness, K_{Ia}, of Ferritic Steels," in *Annual Book of ASTM Standards*, Vol. 03.01, American Society for Testing and Materials, 1996.

16. ASTM Standard E 23-93a, "Notched Bar Impact Testing of Metallic Materials," in *Annual Book of ASTM Standards*, Vol. 03.01, American Society for Testing and Materials, 1993.

17. J. G. Merkle, K. Wallin, and D. E. McCabe, *Technical Basis for an ASTM Standard on Determining the Reference Temperature, T_o, for Ferritic Steels in the Transition Range*, USNRC Report NUREG/CR-5504 (ORNL/TM-13631), December 1998

18. R. K. Nanstad, F. M. Haggag, D. E. McCabe, S. K. Iskander, K. O. Bowman, and B. H. Menke, *Irradiation Effects of Fracture Toughness of Two High-Copper Submerged-Arc Welds, HSSI Series 5*, USNRC Report NUREG/CR-5913, Vol. 1 (ORNL/TM-12156/V1), October 1992.

19. E. D. Eason, J. E. Wright, and G. R. Odette, "Improved Embrittlement Correlations for Reactor Pressure Vessel Steels, NUREG/CR-6551 (MCS-970501), November 1998

Appendix A

Tensile Properties

Beltline Weld (Unirradiated and Irradiated)

Nozzle Course Weld (Unirradiated and Irradiated)

Charpy Data

Charpy Plots

Hyperbolic Curve

Coefficients

Beltline and Nozzle Course Weld Data, Capsules 10.01 and 10.02

Beltline Weld Data, Capsule 10.05

Nozzle Course Weld Data, Capsule 10.05

Beltline weld tensile properties (unirradiated and irradiated)

Specimen	Test temperature		Yield strength		Ultimate strength		Elongation (%)
	°C	°F	MPa	ksi	MPa	ksi	
Unirradiated							
13101A	24	75	507	73.5	609	88.3	18
13102B	24	75	514	74.5	618	89.6	18
13105A	288	550	482	69.9	609	88.3	15
13106B	288	550	479	69.5	609	88.4	15
13104A	150	320	478	69.3	585	84.9	15
13103B	150	320	474	68.7	583	84.6	15
13107A	–25	–13	558	81.0	672	97.5	11
13107B	–25	–13	551	79.9	669	97.1	20
13109A	–50	–58	566	82.1	689	99.9	20
13110A	–50	–58	570	82.7	698	101.3	20
13111A	–100	–148	622	90.2	760	110.3	22
13112B	–100	–148	625	90.6	767	111.3	22
MW9-MN4	–150	–238	737	106.9	851	123.4	25
Scoping capsules, irradiated 0.5 × 10^{19} n/cm^2							
MW9-MA5	25	77	630	91.4	722	104.7	25
MW9-MB1	25	77	637	92.4	719	104.3	24
MW9-MA3	100	212	596	86.4	685	99.3	23
MW9-MA4	100	212	593	86.0	679	98.5	23
MW9-MA1	150	302	582	84.4	669	97	22
MW9-MA2	150	302	582	84.4	669	97	22
Capsule 10.06, irradiated 1.0 × 10^{19} n/cm^2							
13I-01B	25	77	636	92.2	736	106.8	
13I-02B	25	77	658	95.4	756	109.7	
13J-03B	150	302	598	86.7	694	100.7	
13J-04B	150	302	591	85.7	687	99.6	

Nozzle course weld tensile properties (unirradiated and irradiated)

Specimen	Test temperature		Yield strength		Ultimate strength	
	°C	°F	MPa	ksi	MPa	ksi
Unirradiated						
341D1	24	75	547	79.4	655	95
341D2	24	75	546	79.2	654	94.8
341D5	288	550	486	70.5	589	85.4
341D6	288	550	483	70.1	586	85.0
341D3	150	320	496	71.9	594	86.2
341D4	150	320	475	68.9	579	84.0
341D7	−50	−58	578	83.8	712	103.3
341D8	−50	−58	585	84.9	716	103.8
341C1	−75	−103	651	94.4	752	109.1
341C3	−75	−103	590	85.6	778	112.9
341C5	−100	−148	673	97.7	818	118.7
341C8	−100	−148	627	91.0	821	119.1
Scoping capsules, irradiated 0.5×10^{19} n/cm^2						
NC34BI1	40	104	606	87.9	722	104.7
NC34AI5	40	104	555	80.5	687	99.6
NC34AI3	115	240	523	75.8	656	95.2
NC34AI4	115	240	517	75.0	657	95.3
NC34AI1	165	330	517	75.0	645	93.5
NC34AI2	165	330	515	74.6	651	94.4
Capsule 10.06, irradiated 1.0×10^{19} n/cm^2						
NC31P12	25	77	701	101.7	791	114.8
NC31P16[a]						
NC31P06	150	302	617	89.5	705	102.3
NC31P11	150	302	652	94.6	735	106.6
NC31P10	288	550	635	92.1	729	105.8
NC31P08	288	550	627	90.9	704	102.1

[a]Failed test.

DATA SOURCE: CC ANALYSIS SETS
Y VARIABLE: ENERGY

NOTE: NONE

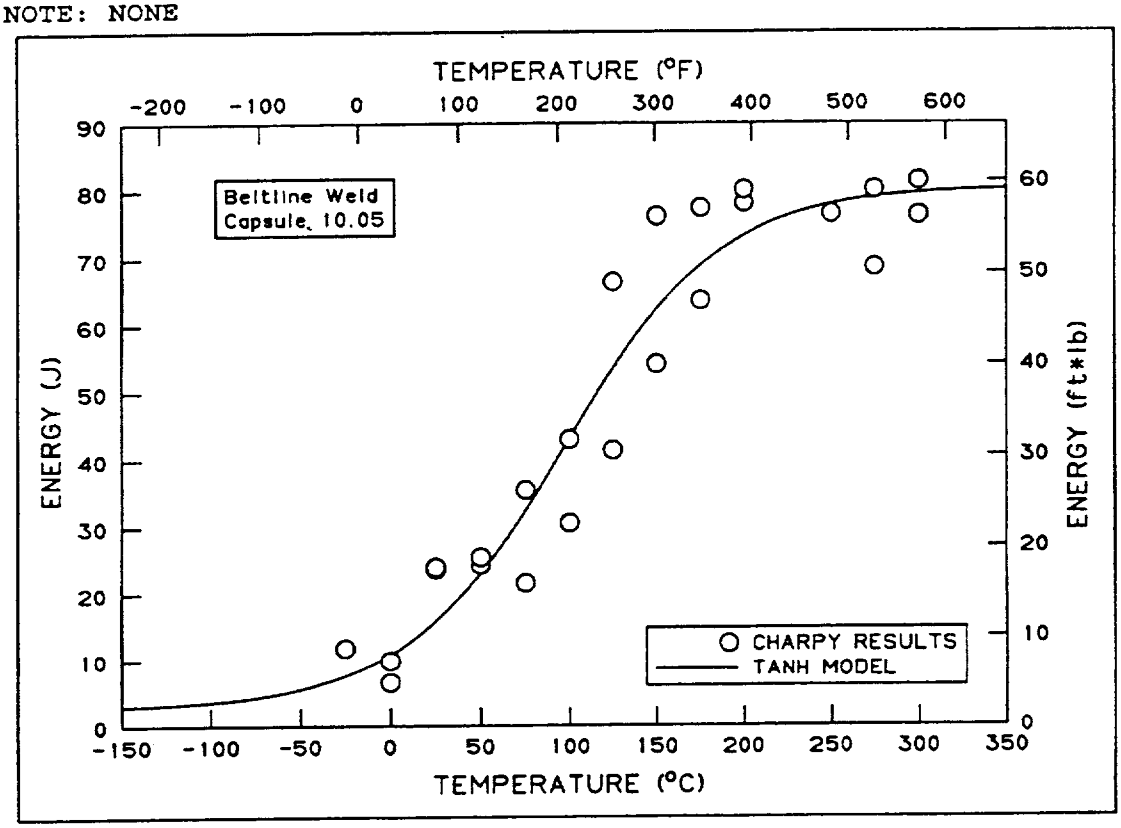

DATA SOURCE: AA ANALYSIS SETS
Y VARIABLE: ENERGY

NOTE: NONE

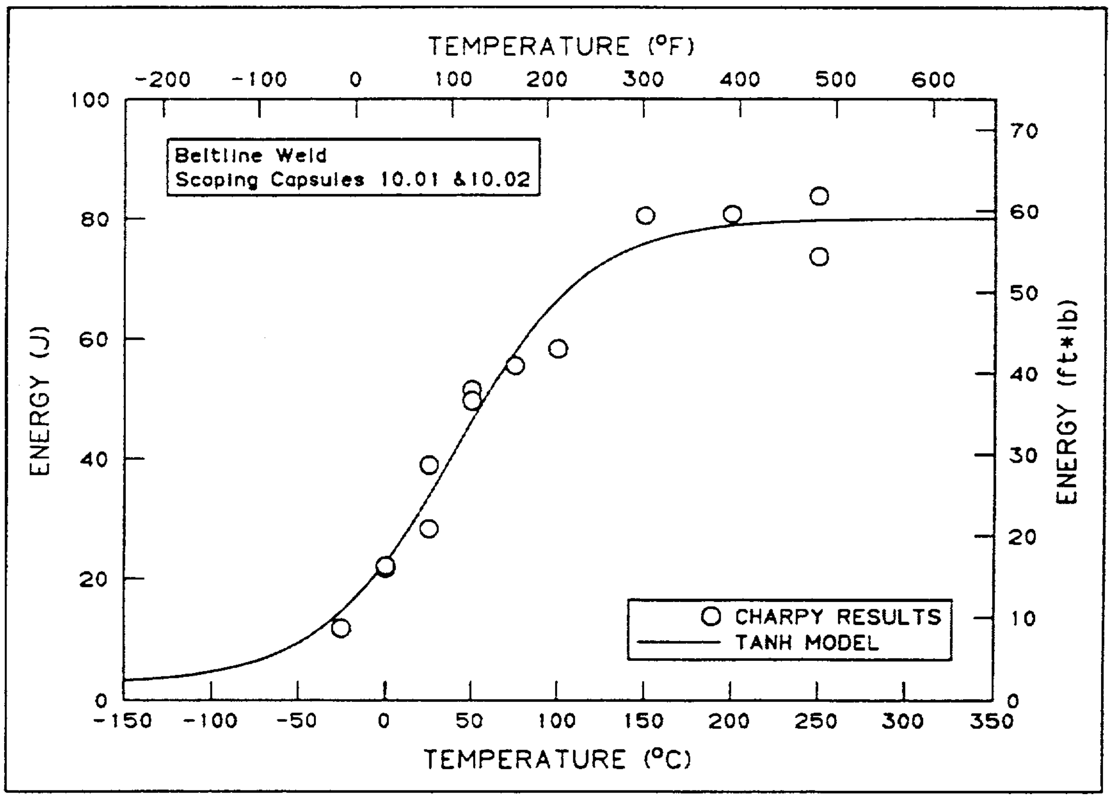

DATA SOURCE: BB ANALYSIS SETS
Y VARIABLE: ENERGY

NOTE: NONE

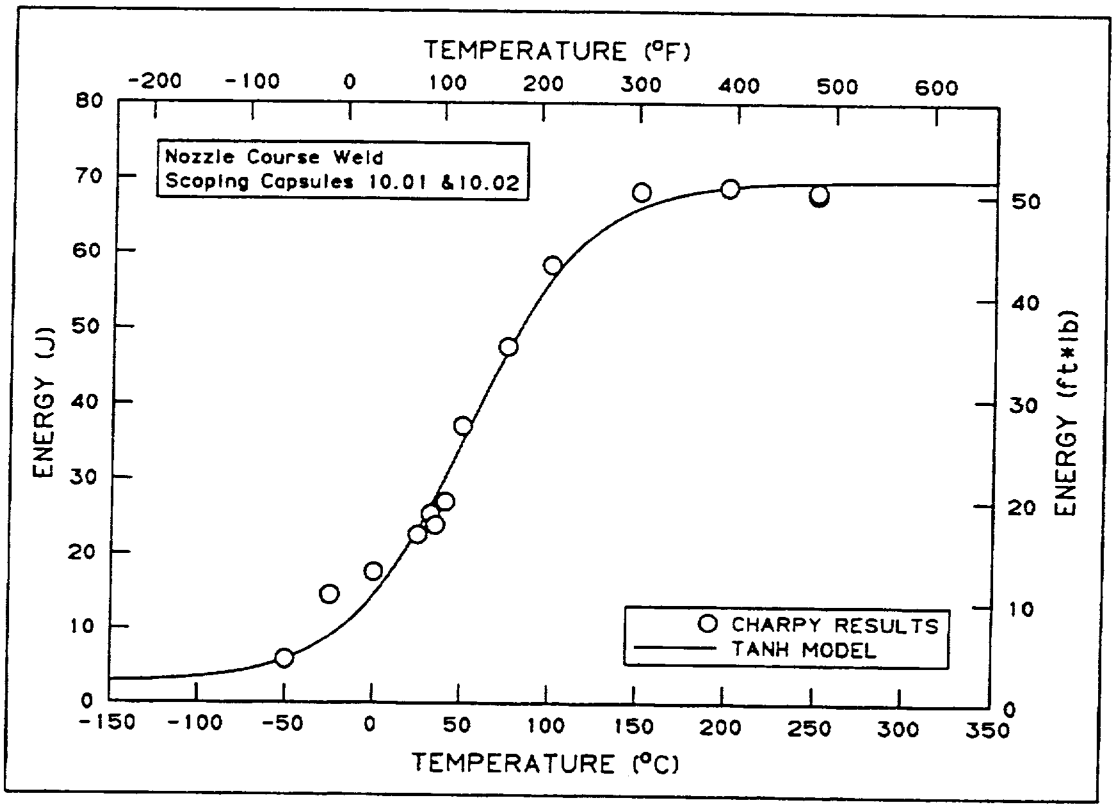

DATA SOURCE: DD ANALYSIS SETS
Y VARIABLE: ENERGY

NOTE: NONE

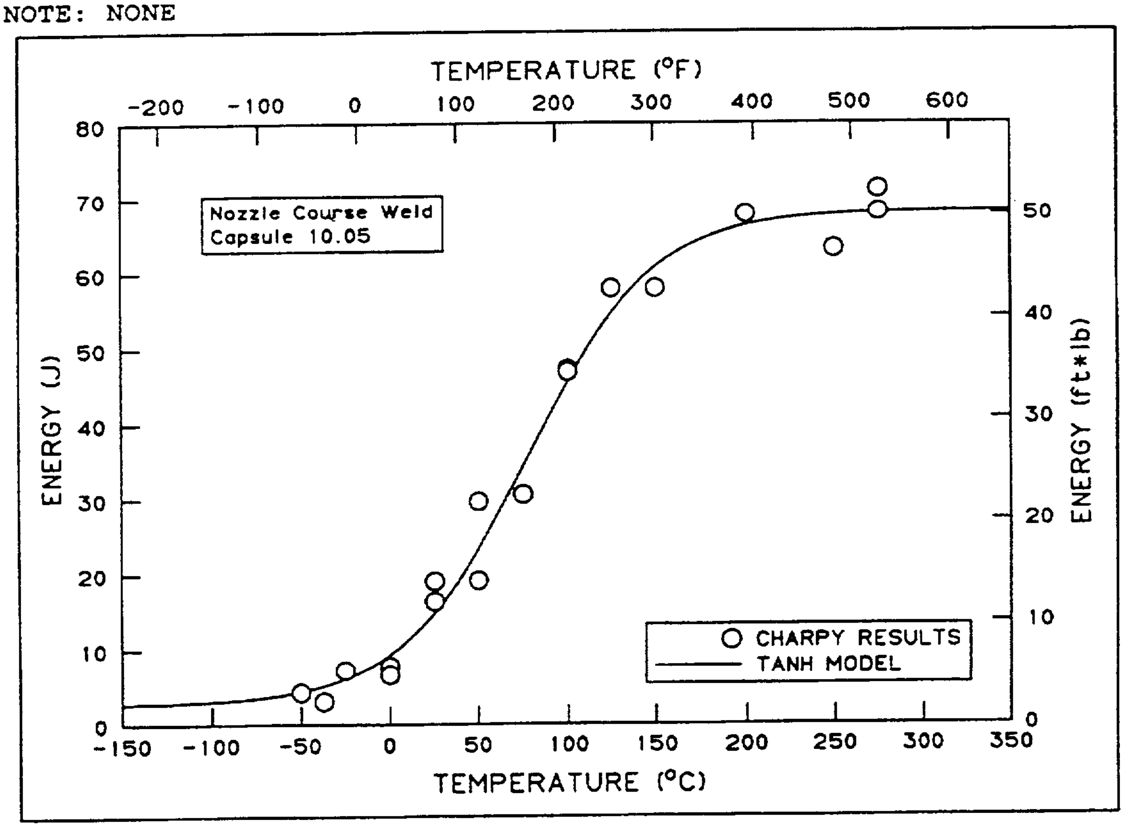

Hyperbolic Curve Fits to Charpy Data

$$E = A + B * \tanh[(T - T_o)/C] ,$$

where E is Charpy V-notch energy and T_o is temperature at mid-transition.

Coefficients

	Beltline				Nozzle course			
	Scoping capsule		Capsule 10.05		Scoping capsule		Capsule 10.05	
	SI	Eng.	SI	Eng.	SI	Eng.	SI	Eng.
A	41.35	30.5	36.25	26.75	36.25	26.75	41.55	30.65
B	38.65	28.5	33.55	24.75	33.55	24.75	38.85	28.65
C	76.6	122.3	69.95	122.3	68.0	122.4	89.75	161.55
T_o	40.3°	104.5°	57.7°	126.9°	52.7°	126.9°	96.3°	205.3°

Charpy test results on specimens from scoping capsules 10.01 and 10.02 (0.5×10^{19} n/cm^2)

Specimen	Test temperature		Energy		Shear (%)
	(°C)	(°F)	(J)	(ft-lb)	
Beltline weld					
MW9MB5	–25	–13	11.8	8.7	5
MW9MF1	0	32	21.7	16	10
MW9MD2	0	32	22.1	16.3	10
MW9MD1	25	77	28.3	20.9	30
MW9MC4	25	77	38.9	28.7	30
MW9MC3	50	122	51.4	37.9	45
MW9MC2	50	122	49.6	36.6	50
MW9MD5	75	167	55.5	40.9	45
MW9MC5	100	212	79	58.3	100
MW9MC1	150	302	80.5	59.4	100
MW9MD4	200	392	80.8	59.6	100
MW9MF2	250	482	83.9	61.9	100
MW9MB4	250	482	73.6	54.3	100
Nozzle course weld					
NC34EI1	–50	–58	5.8	4.3	0
NC34DI5	–25	–13	14.5	10.7	5
NC34DI4	0	32	17.6	13	10
NC34KI5	25	77	22.6	16.7	25
NC34DI3	32.2	90	25.4	18.7	20
NC34EI3	35	95	23.9	17.6	40
NC34EI5	40.6	105	27	19.9	40
NC34KI4	50	122	37.1	27.4	30
NC34EI2	75	167	47.6	35.1	45
NC34EI4	100	212	58.4	43.1	70
NC34BI5	150	302	68.3	50.4	100
NC34DI1	200	392	68.9	50.8	100
NC34DI2	250	482	67.9	50	100
NC34BI4	250	482	68.3	50.4	100

Charpy test results on specimens from Capsule 10.05, beltline weld (1.0×10^{19} n/cm^2)

Specimen	Test temperature		Energy		Lateral expansion (mils)	Shear (%)
	(°C)	(°F)	(J)	(ft-lb)		
MW11BB1	–25	–13	11.8	8.7	6	0
MW11AJ2	0	32	6.6	4.9	4	0
MW11AA3	0	32	9.9	7.3	5	5
MW11AB2	25	77	23.7	17.5	10	20
MW11AB4	25	77	24	17.7	11	20
MW11BF4	50	122	24.4	18	12	25
MW11AA2	50	122	25.5	18.8	15	35
MW11AF5	100	212	43	31.7	2	80
MW11AG4	150	302	76.2	56.2	35	100
MW11AG5	200	392	78.1	57.6	33	100
MW11BF1	250	482	76.5	56.4	38	100
MW9AC3	75	167	35.5	26.2	21	40
MW9AI1	75	167	21.6	15.9	13	15
MW9AI4	100	212	30.6	22.6	17	35
MW9BF5	125	257	66.4	49	32	90
MW9AI3	125	257	41.4	30.5	26	40
MW9AI2	150	302	54.2	40	31	80
MW9AI5	175	347	63.6	46.9	33	90
MW9AC1	175	347	77.4	57.1	34	100
MW9AC2	200	392	80.1	59.1	30	100
MW9BF2	275	527	80.1	59.1	34	100
MW9BJ1	275	527	68.6	50.6	35	100
MW9AC4	300	572	76.3	56.3	44	100
MW9AC5	300	572	81.4	60.0	38	100

Charpy test results on specimens from Capsule 10.05, nozzle course weld (1.0×10^{19} n/cm^2)

Specimen	Test temperature		Energy		Shear (%)
	(°C)	(°F)	(J)	(ft-lb)	
NC31AB5	–50	–58	4.3	3.2	0
NC31AA2	–37	–36	3.1	2.3	0
NC31BF1	–25	–13	7.2	5.3	0
NC31BA2	0	32	7.7	5.7	5
NC31AF4	0	32	6.6	4.9	0
NC31BB3	25	77	16.3	12	20
NC31AH4	50	122	19.1	14.1	15
NC31AB1	75	167	30.5	22.5	70
NC31BB5	100	212	47.2	34.8	80
NC31BB4	125	257	57.9	42.7	95
NC31AB2	200	392	67.8	50	100
NC31AA4	250	482	63.2	46.6	100
NC31AB3	275	527	71.2	52.5	100
NC31AH2	275	527	68.1	50.2	100
NC34BB2	25	77	19	14	10
NC34AB4	50	122	29.6	21.8	30
NC34AE4	75	167	30.5	22.5	45
NC34AB2	100	212	46.9	34.6	60
NC34AE5	150	302	57.9	42.7	95

Appendix B

Scoping Capsules 10.01 and 10.02

Irradiation by Materials Engineering Associates

Irradiation Period:

July 20 to September 26, 1993
1421 effective full-power hours - core edge position 44
Rotation on August 9, 1993

Reactor:

University of Buffalo Reactor
Buffalo Materials Research Center
State University of New York
Buffalo, New York

Shipped to ORNL:

November 5, 1993

Capsule Contents:

Scoping Capsule 10.01, UBR-93B

Specimen	Number	Material
CVN	20	Beltline
1/2T C(T)	4	Beltline
Tensile	8	Beltline

Scoping Capsule 10.02, UBR-93A

Specimen	Number	Material
CVN	14	Nozzle
CVN	6	Beltline
1/2T C(T)	2	Nozzle
1/2T C(T)	2	Beltline
Tensile	8	Nozzle

Temperature:

Temperatures during irradiation were reported to be within ±15°F of the target temperature of 550°F.

Neutron Dosimetry:

Neutron dosimeters supplied to MEA for Capsule UBR-93A were returned to ORNL after irradiation. Results are not known. MEA independently has verified that the fluence target of 0.5×10^{19} n/cm^2 (E > 1 MeV) was attained by the 1420.9-h exposure.

ORNL 98-6904/dgc

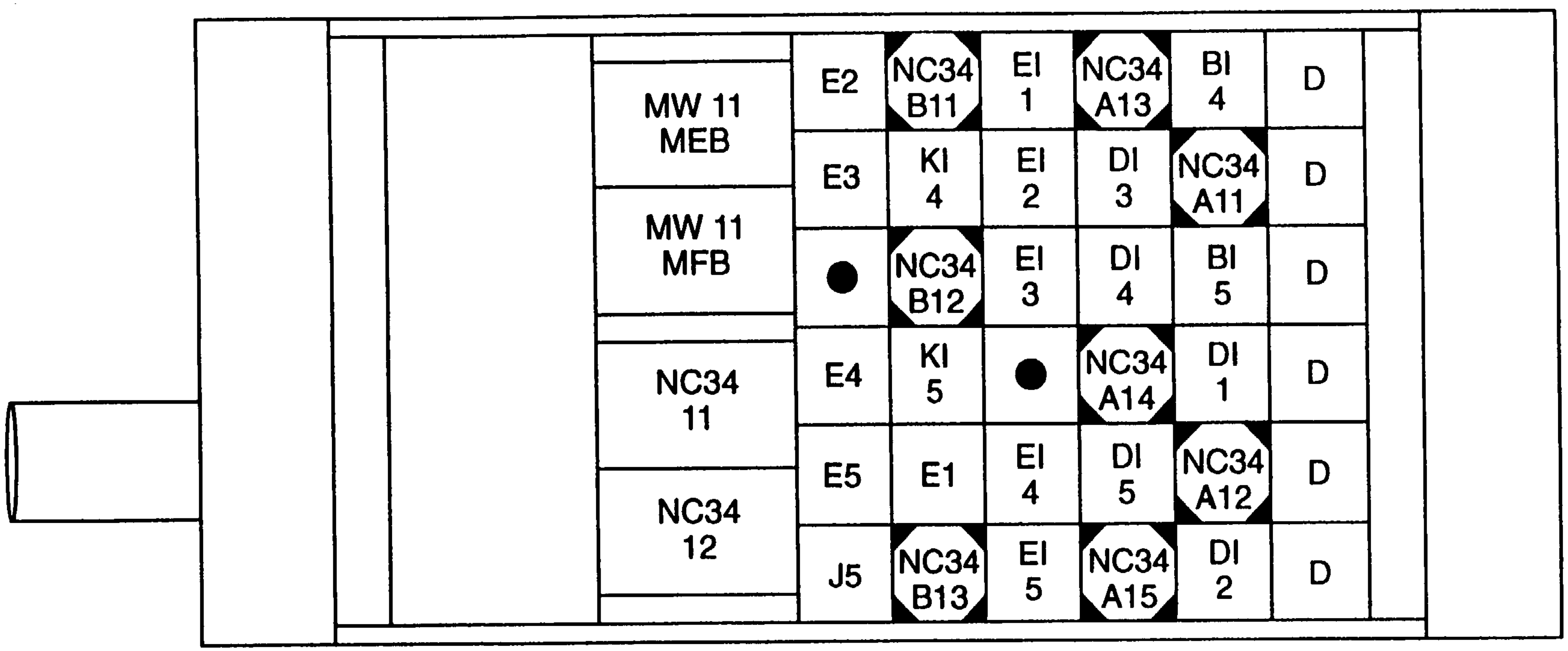

D = Dummy Cv

INDEX FOR RECORDER PRINT NUMBER VS CAPSULE/THERMOCOUPLE NUMBER VS. SPECIMEN NUMBER

(PERIOD: 20 JUNE - 28 SEPTEMBER 1993)

Capsule Number UBR-93A

Print No.	Capsule Thermocouple No.	Specimen No.	Comments
1	1	DI 2	
2	2	NC34 A15	
3	3	NC34 B13	
4	4	J5	
5	5	B1 4	
6	6	NC34 B11	
7	7	NC34 A13	
8	8	E2	
9	9	E4	
10	10	NC34 B12	
11	11	EI 3	
12	12	NC34 A14	
13	13	MW11 MEB	
14	14	NC34 12	
15	15	MW11 MFB	
1 (Recorder 2)	16	MW11 MFB	(1)(2)
2 (Recorder 2)	17	NC34 11	(1)
-	18	EI 1	STC
-	19	B1 4	CTC

Capsule Number UBR-93B (Ref. 1)

Print No.	Capsule Thermocouple No.	Specimen No.	Comments
16	1	C2	
17	2	MW9 MA5	
18	3	MW9 MB3	
19	4	J3	
20	5	B4	
21	6	MW9 MB1	
22	7	MW9 MA3	
23	8	F4	
24	9	G4	
25	10	MW9 MB2	
26	11	D3	
27	12	MW9 MA4	
28	13	MW9 NE1	
29	14	MW11 1FA	
30	15	MW9 NE2	
16 (Recorder 2)	16	MW9 NE2	(1)(3)
17 (Recorder 2)	17	MW11 1EA	(1)
-	18	D1	STC
-	19	B4	CTC

Comment (1): Discontinued continuous recording on 6 July 1993 ; no longer needed.
(2): Attached to same specimen as Recorder Print 15
(3): Attached to same specimen as Recorder Print 30

Schematic Drawing- Showing the Specimen Orientation of 1/2 TCT's and CVN's in the MEA Capsules.

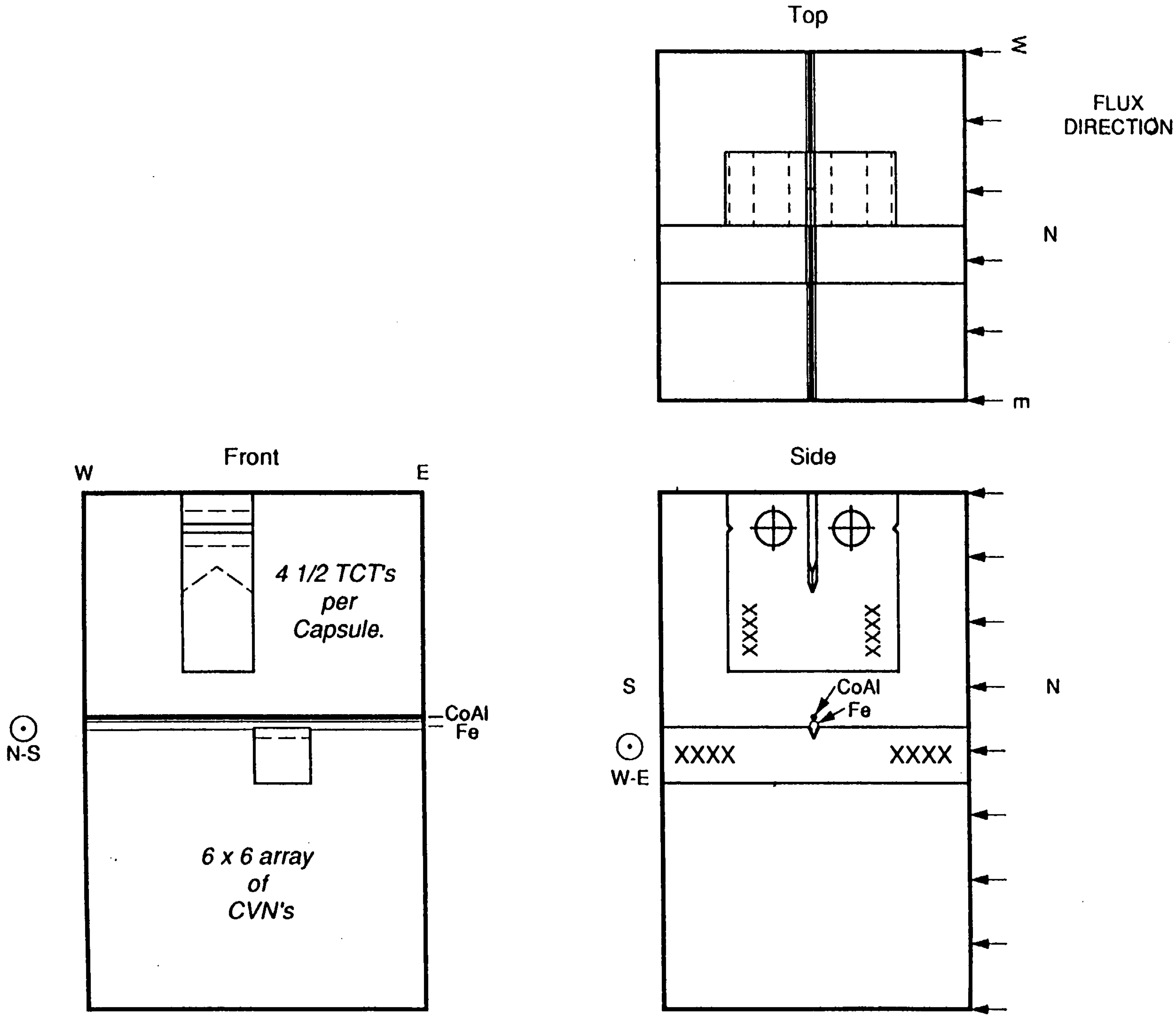

Appendix C

Capsule 10.05

Construction: ORNL

Exposure: Ford Nuclear Reactor

Irradiation Period:

May 12, 1992, to March 5, 1993
3595 effective full-power hours - core edge

Reactor:

Ford Nuclear Reactor
Phoenix Materials Laboratory
2301 Bonisteel Boulevard
Ann Arbor, Michigan 48109

Shipped to ORNL:

May 18, 1994

Capsule Contents:

Charpys, 1/2T, 1T, C(T) specimens
See Figures C1 to C17
See Table C1

Irradiation Information:

Average temperature, Table C2
Thermocouple locations, Page C-23
Capsule location, Figure C19, Page C-25
Fluence Distribution, Table C3

Table C1.

Specimens	Number	Material	Block locations[a]
Tenth Irradiation			
1T C(T)	25	Beltline	A2, A3, B2, B3, C3
1/2T C(T)	24	Beltline	D2
1/2T C(T)	6	72W[b]	D2
1/2T C(T)	6	73W[b]	D2
CVN	24	Beltline	C2, C3
CVN	24	Nozzle	C2, C3
PCVN	10	Beltline	C2, C3
PCVN	10	Nozzle	C2, C3
Annealing Program			
1T C(T)	8	Beltline	A1, A4, B1, B4, D1, D4
CVN	30	Nozzle	C1, C4, D1, D4
CVN	75	Beltline	A1, B1, C4
CVN	30	72W[b]	A4, D4
CVN	58	72W[b]	A4, B4, C4
CVN	12	Repair weld	C1
CVN	45	HSST Plate 02	A1, A4, B1, B4, C1
CVN	18	Cladding	B4, D4, C1
PCVN	6	Cladding	D4
CVN	12	HFIR	D1
CVN	12	A 508	D1

[a]See Figures C1 through C17.
[b]From HSSI Fifth Irradiation Series.

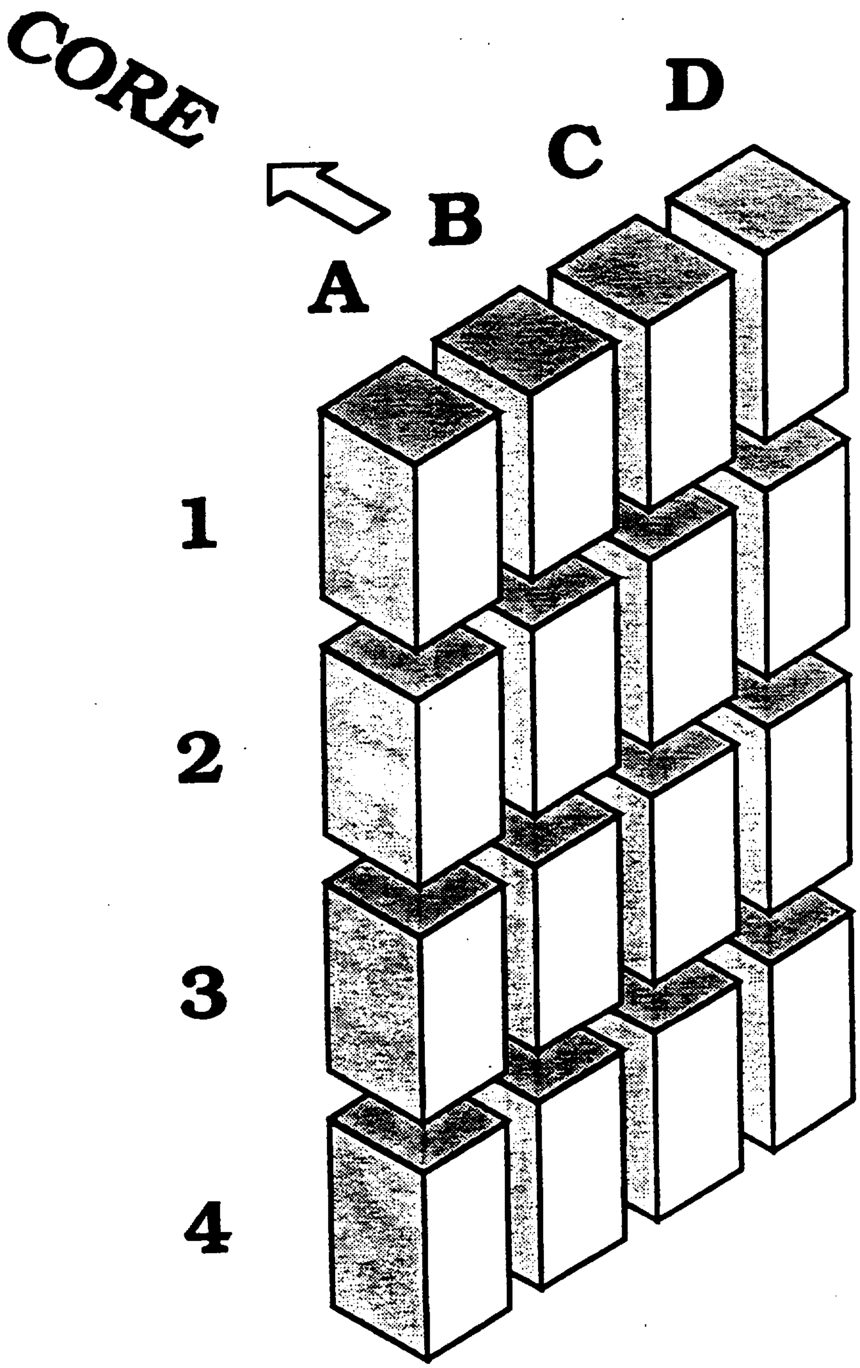

Arrangement of specimen blocks for capsule 5 of the HSST 10th irradiation series.

SPECIMEN LAYOUT BLOCK A1

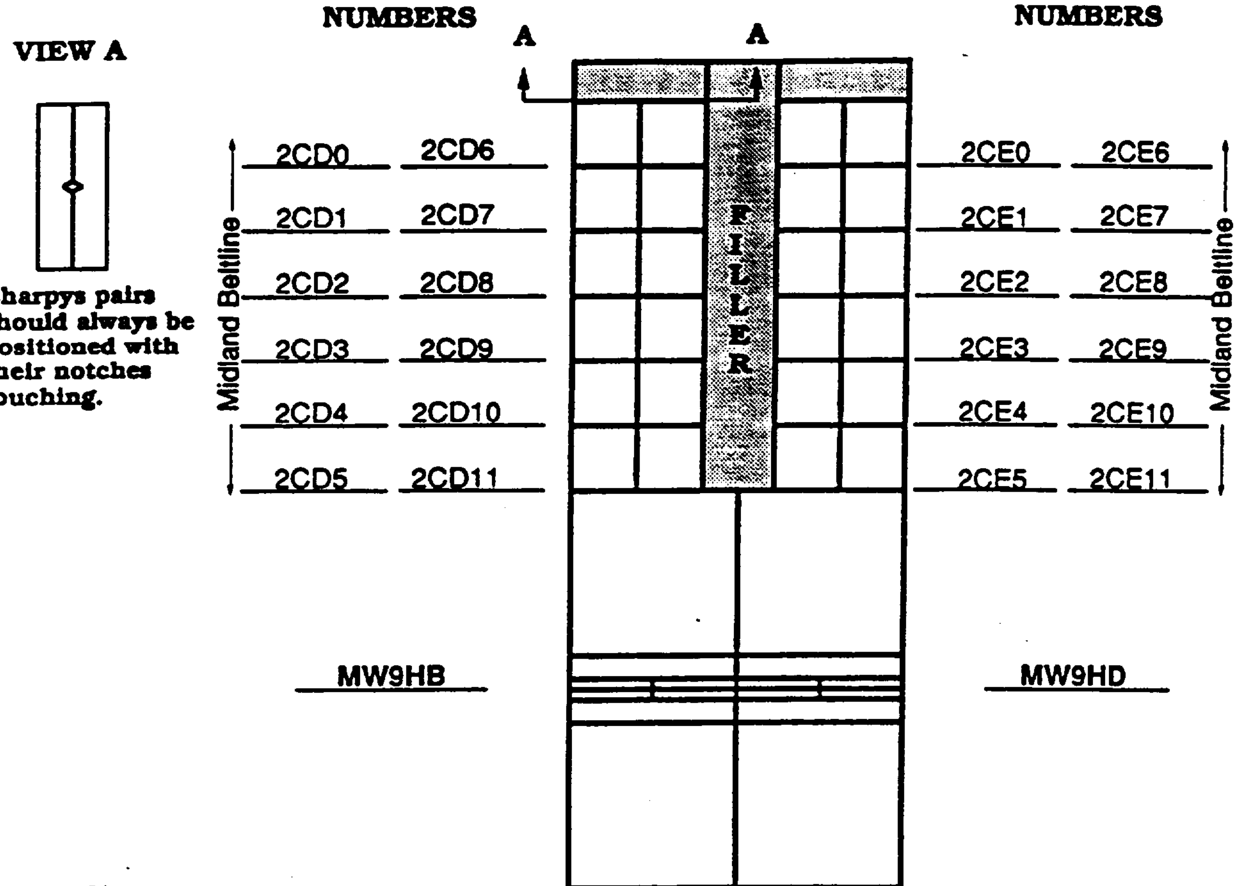

Charpys pairs should always be positioned with their notches touching.

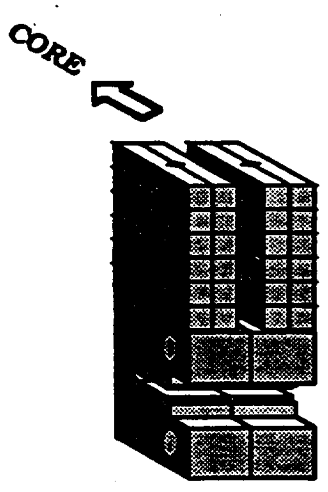

Each block contains:

24 charpy specimens 6x4

2 1TCTs

SPECIMEN LAYOUT BLOCK A2

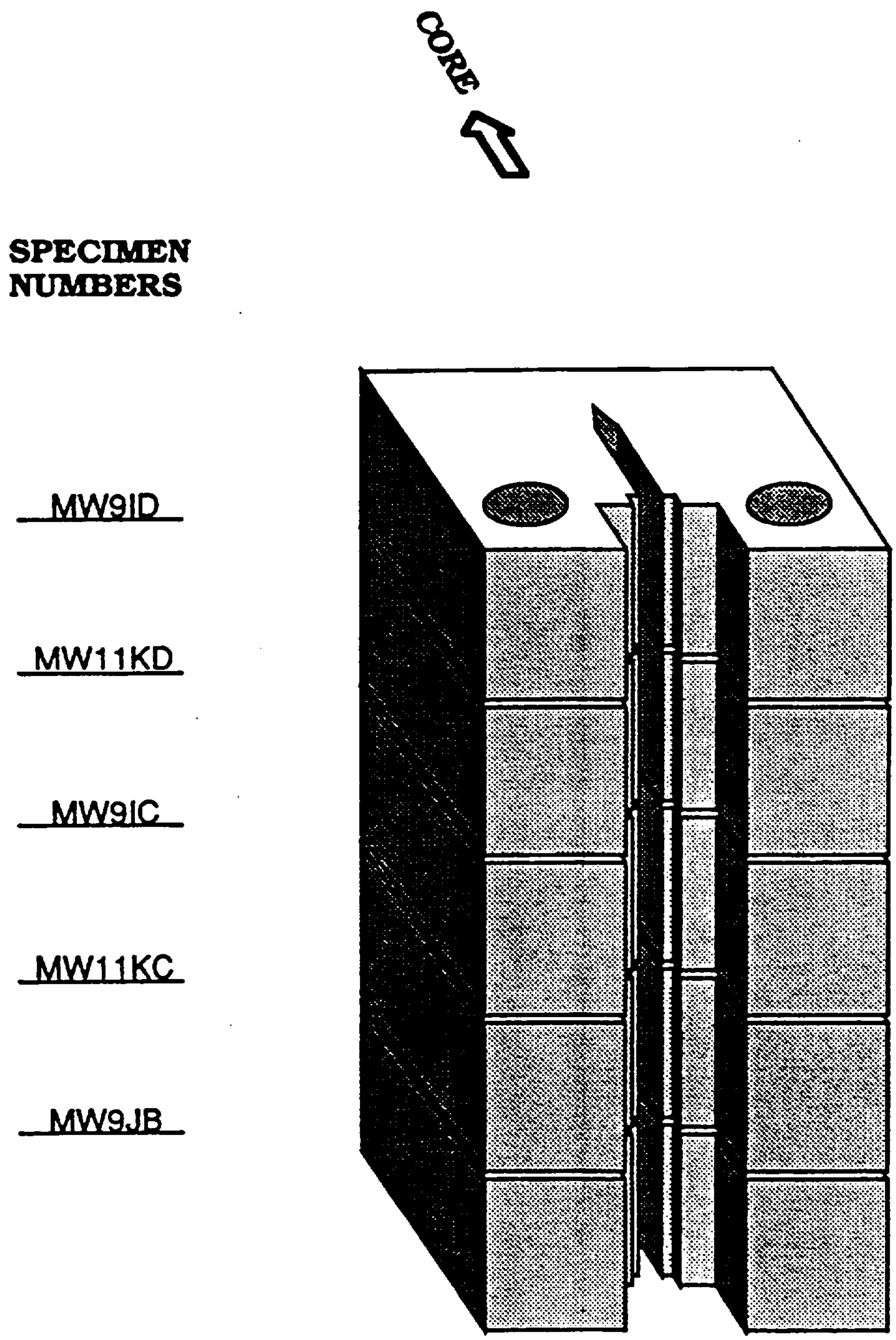

SPECIMEN LAYOUT BLOCK A3

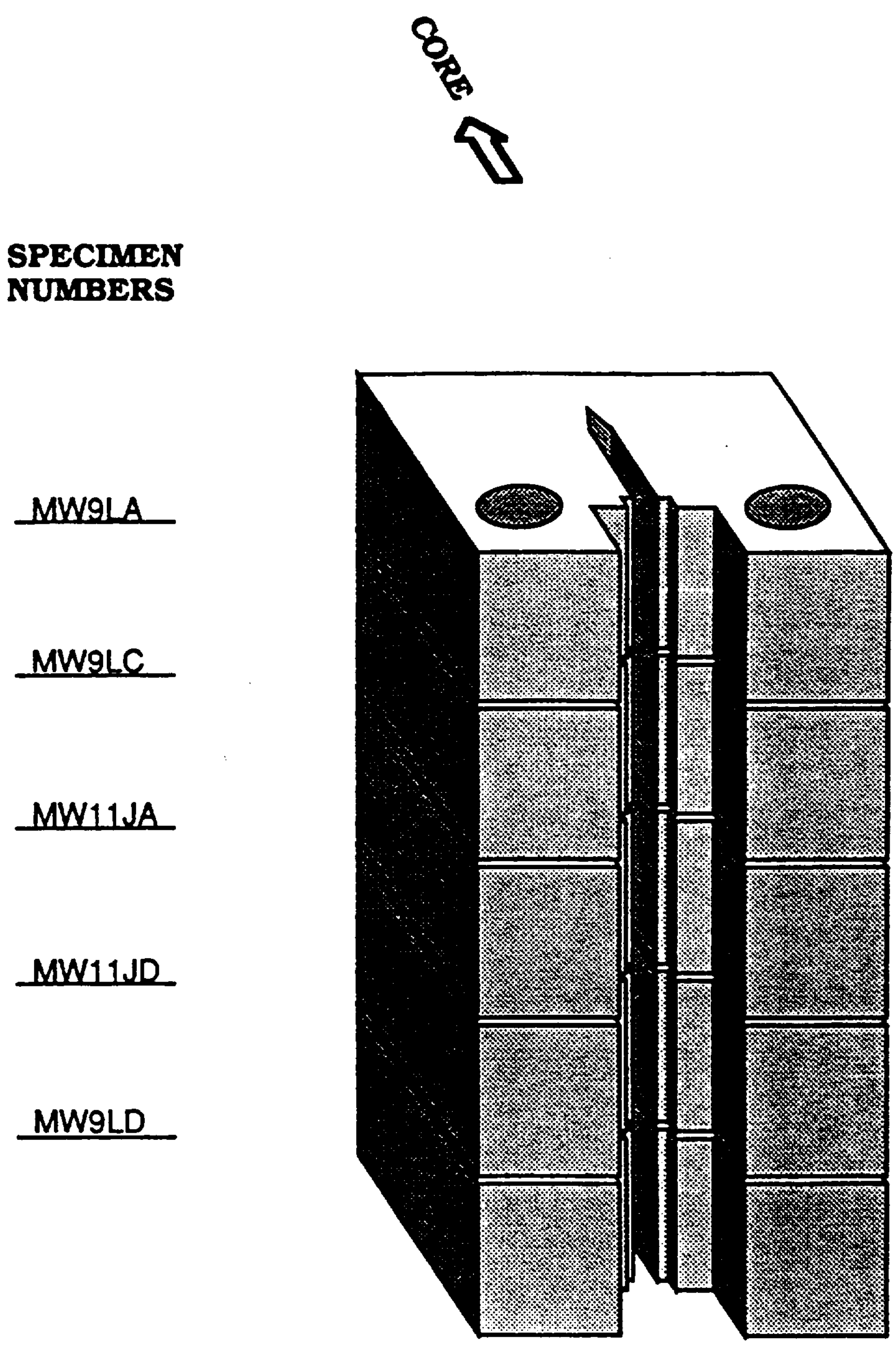

SPECIMEN LAYOUT BLOCK A4

VIEW A

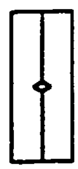

Charpys pairs should always be positioned with their notches touching.

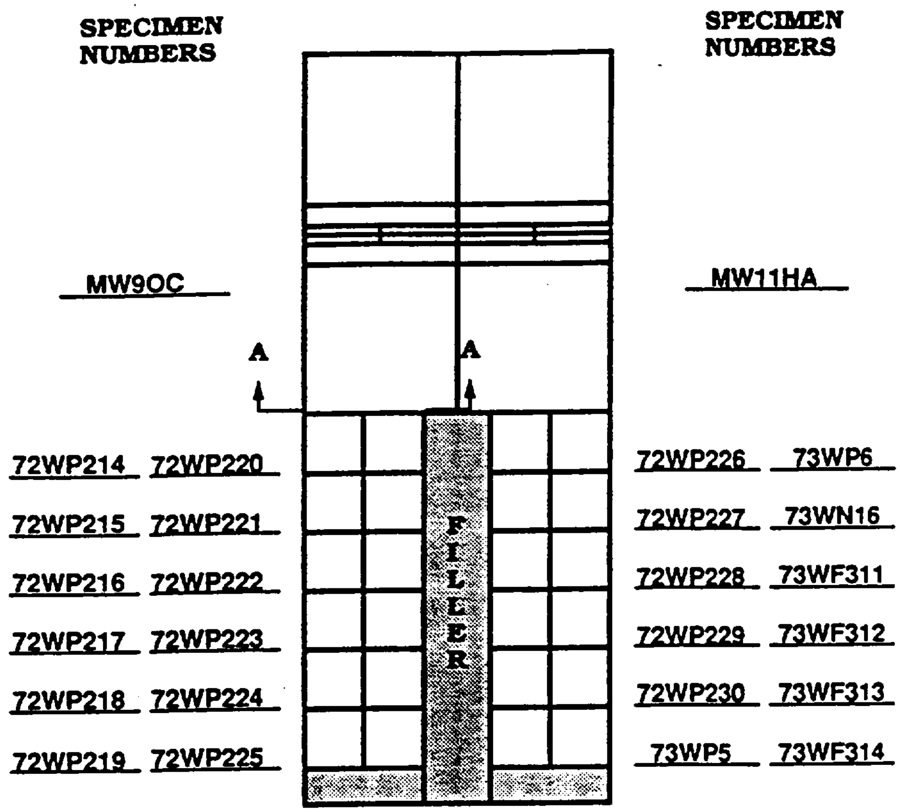

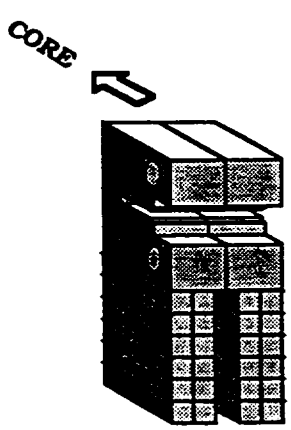

Each block contains:

2 1TCTs

24 charpy specimens 6x4

SPECIMEN LAYOUT BLOCK B1

VIEW A

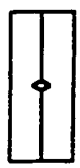

Charpys pairs should always be positioned with their notches touching.

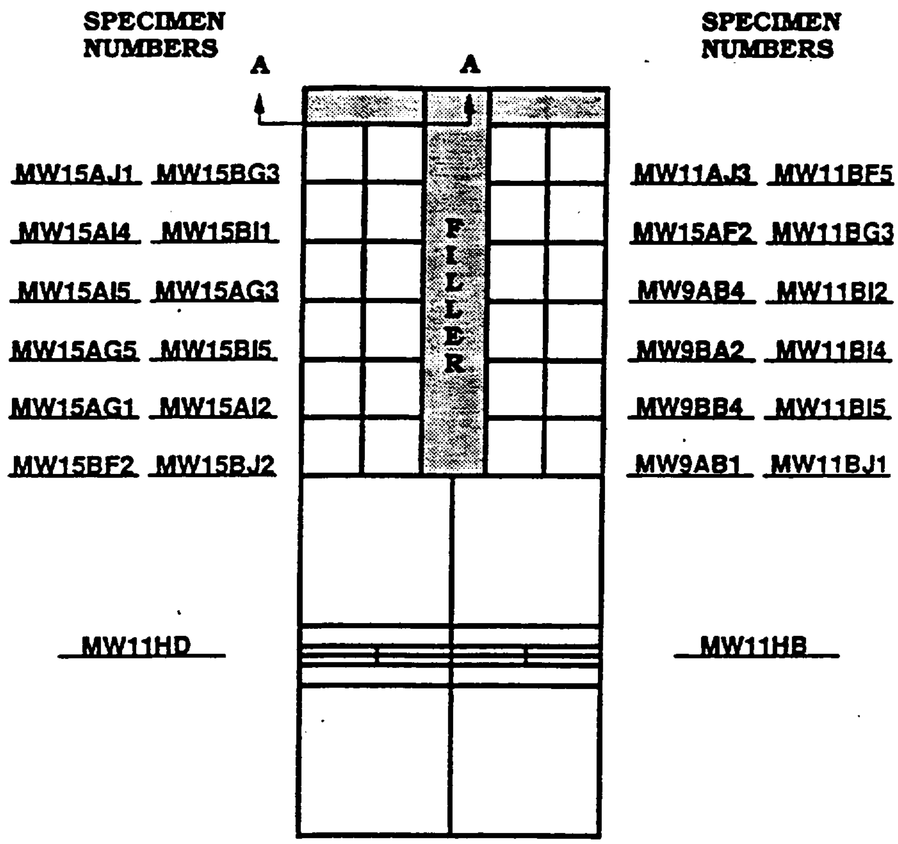

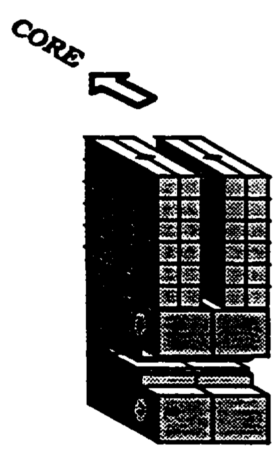

Each block contains:

24 charpy specimens 6x4

2 1TCTs

SPECIMEN LAYOUT BLOCK B2

CORE

SPECIMEN NUMBERS

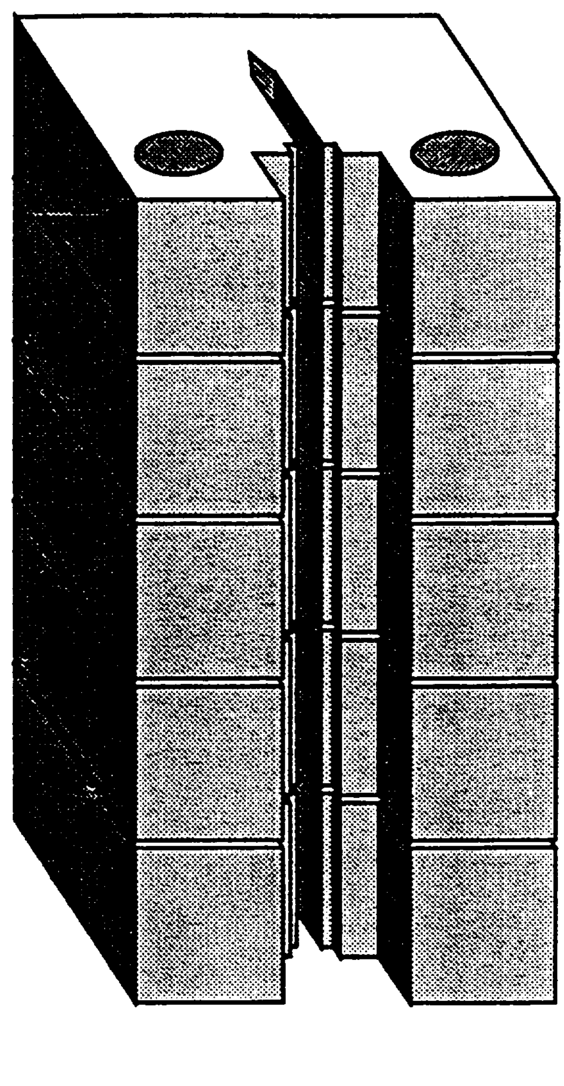

MW9JA

MW11IC

MW9JC

MW11ID

MW9KB

SPECIMEN LAYOUT BLOCK B3

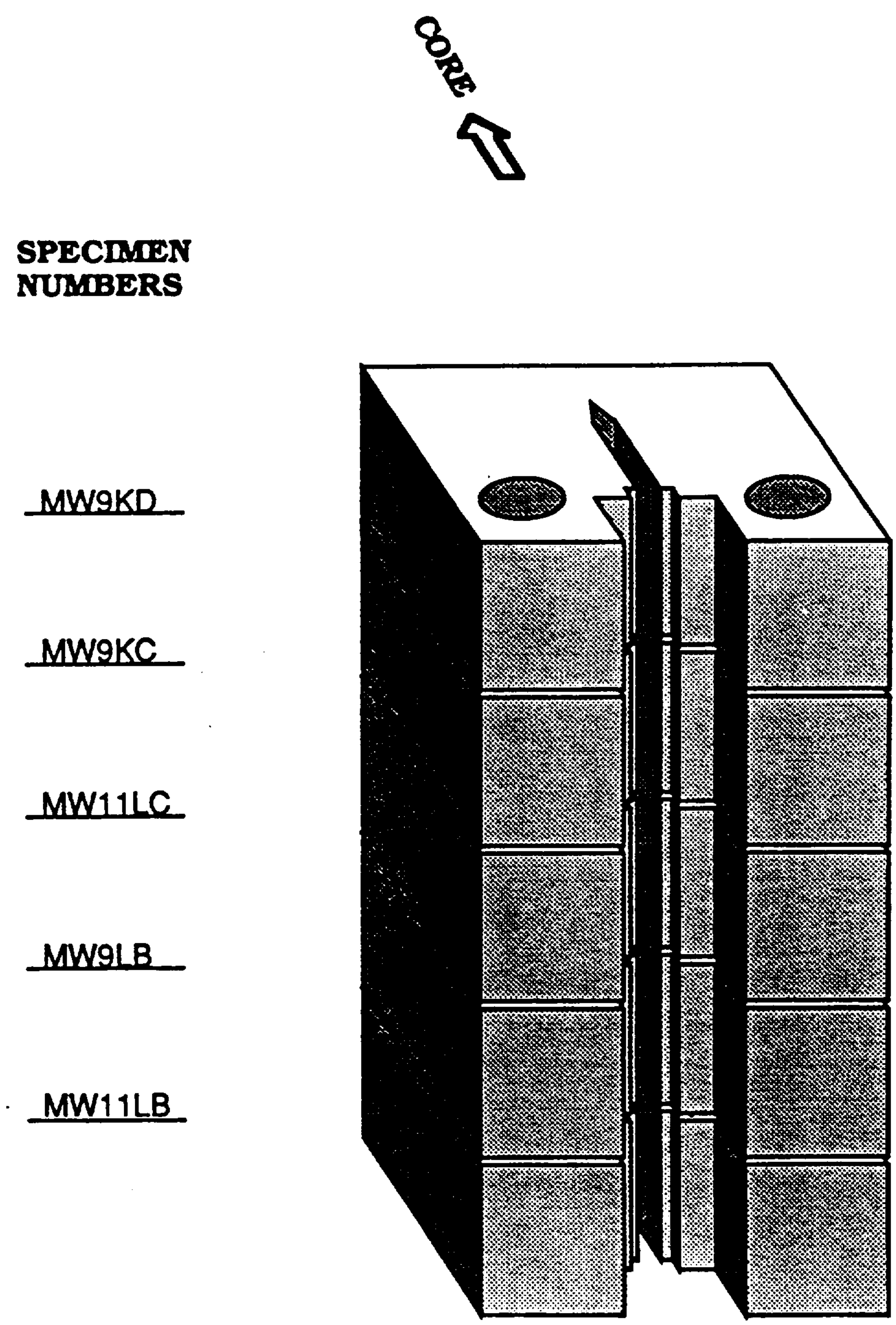

SPECIMEN LAYOUT BLOCK B4

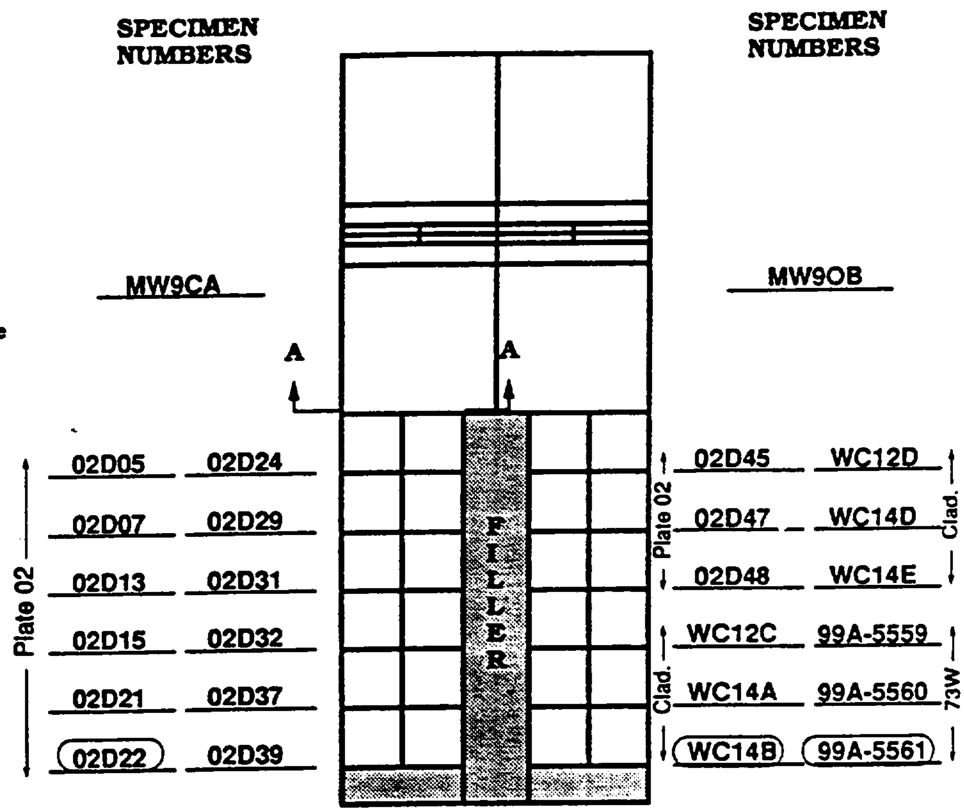

VIEW A

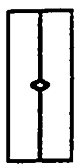

Charpys pairs should always be positioned with their notches touching.

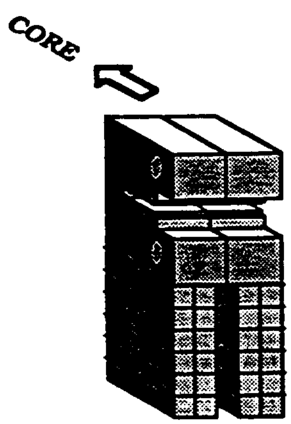

= Magnetic Field Tested

Each block contains:

2 1TCTs

24 charpy specimens 6x4

SPECIMEN LAYOUT BLOCK C1

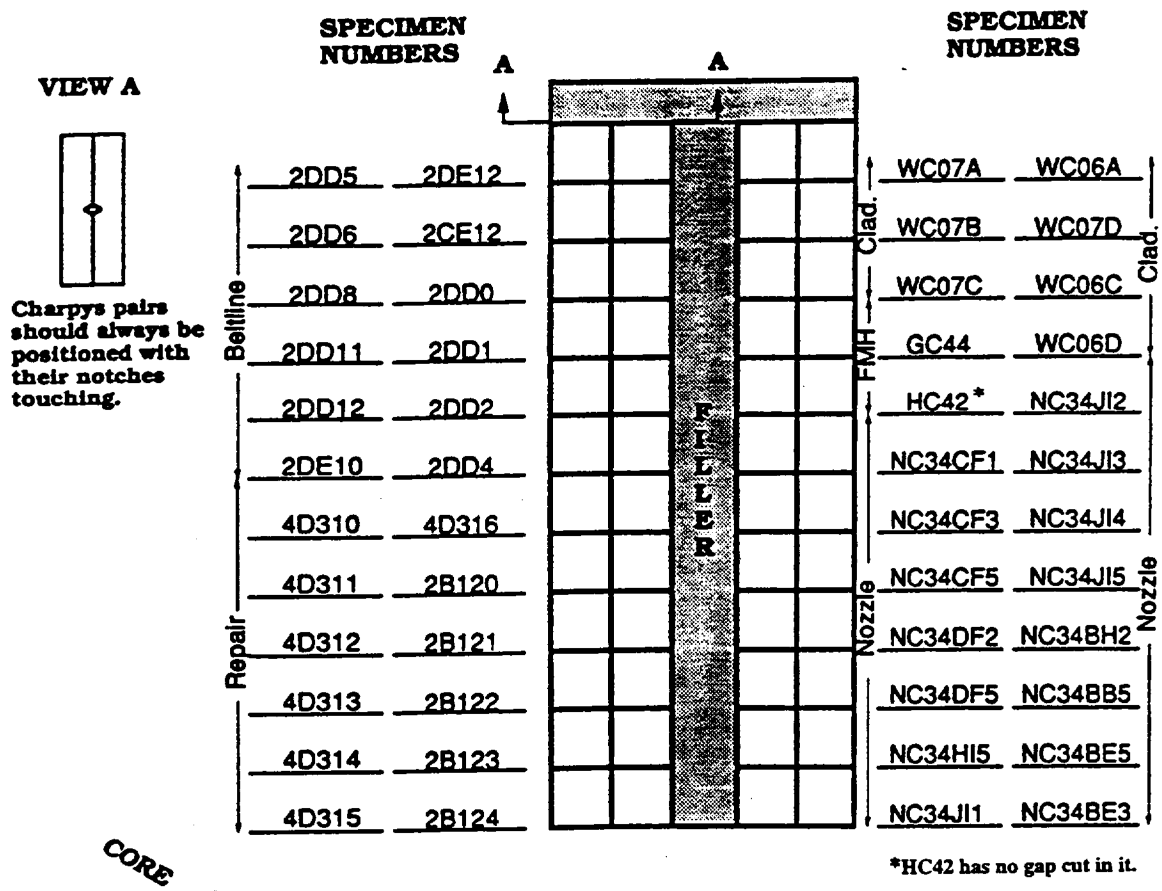

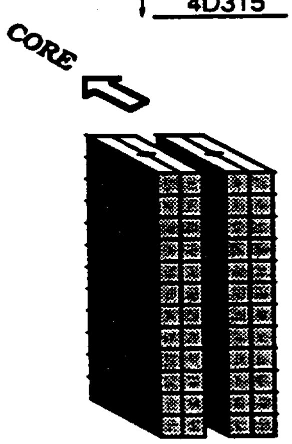

Each block contains:

48 charpy specimens 6x4

SPECIMEN LAYOUT BLOCK C2

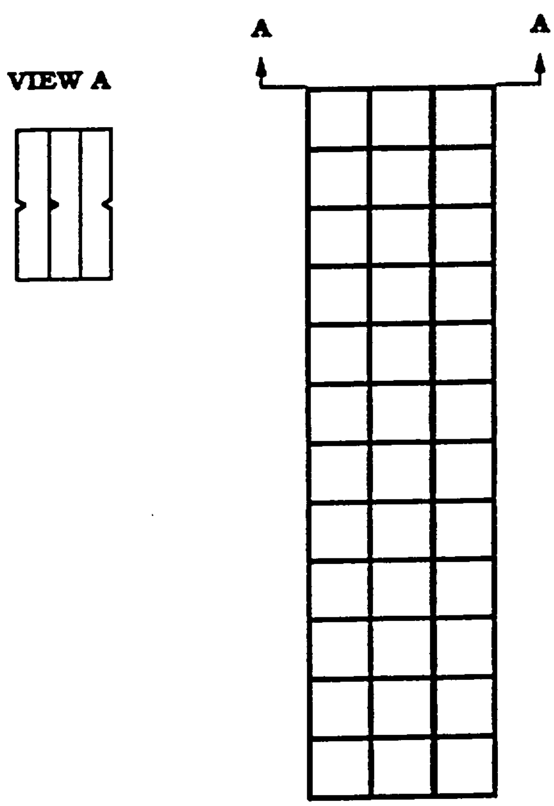

SPECIMEN NUMBERS

LEFT	MIDDLE	RIGHT
NC31AA2	NC31DF4	MW9AC1
NC31AA4	2DE0	MW9AC2
NC31AB1	NC34AA5	MW9AC3
NC31AB2	2DE2	MW9AC4
NC31AB3	NC34BH4	MW9AC5
NC31AB5	2DE1	MW9AI1
NC31AF4	NC34CF4	MW9AI2
NC31AH2	2DE3	MW9AI3
NC31AH4	NC34AA1	MW9AI4
NC31BA2	2DE4	MW9AI5
NC31BB3	MW11BF4	MW9BF2
NC31BB4	NC34BB4	MW9BF5

Nozzle

Precracked

Beltline

Beltline

Nozzle

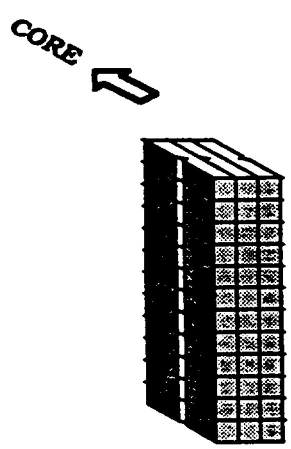

Each block contains:

36 charpy specimens 6x4

SPECIMEN LAYOUT BLOCK C3

VIEW A

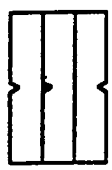

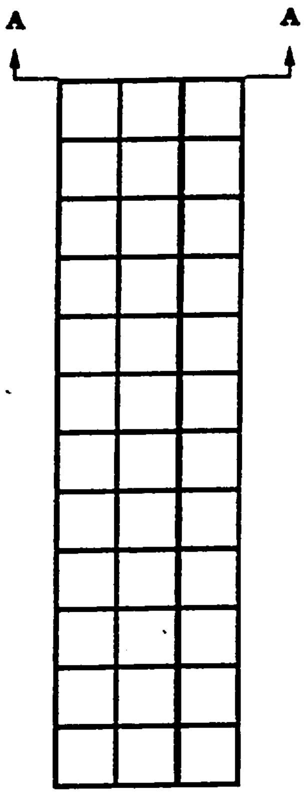

SPECIMEN NUMBERS

LEFT	MIDDLE	RIGHT
NC31BB5	NC31BA4	MW9BJ1
NC31BF1	2DE5	MW11AA2
NC34BB2	NC31BB1	MW11AA3
NC31BF4	2DE6	MW11AB2
NC31BF5	NC31BH3	MW11AB4
NC31BH1	2DE7	MW11AF5
NC34AB2	NC34BE1	MW11AG4
NC34AB4	2DE8	MW11AG5
NC34AE4	NC31BH5	MW11AJ2
NC34AE5	2DE9	MW11BB1
NC34AF1	MW11BF1	MW11BB4
NC34AF2	NC31BF3	MW11BB5

Nozzle

Precracked

Beltline

Beltline

Nozzle

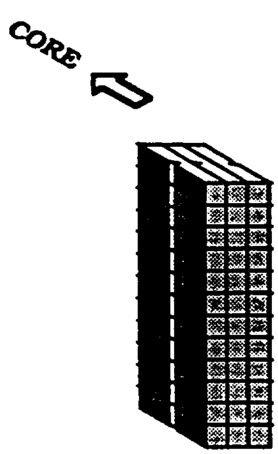

Each block contains:

36 charpy specimens 6x4

SPECIMEN LAYOUT BLOCK C4

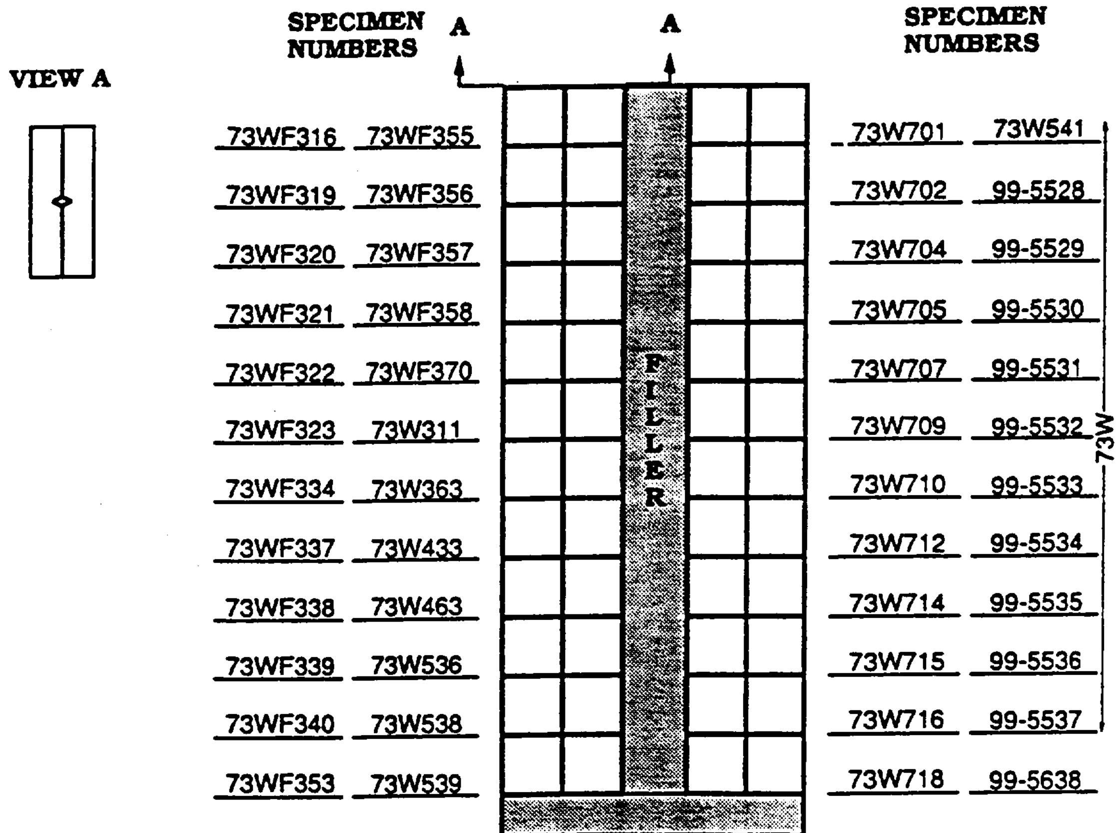

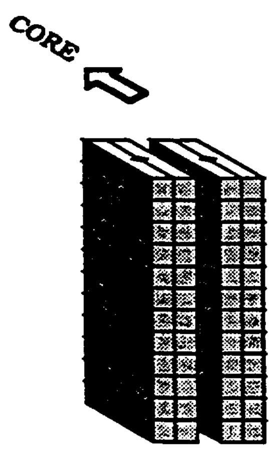

Each block contains:

48 charpy specimens 6x4

SPECIMEN LAYOUT BLOCK D1

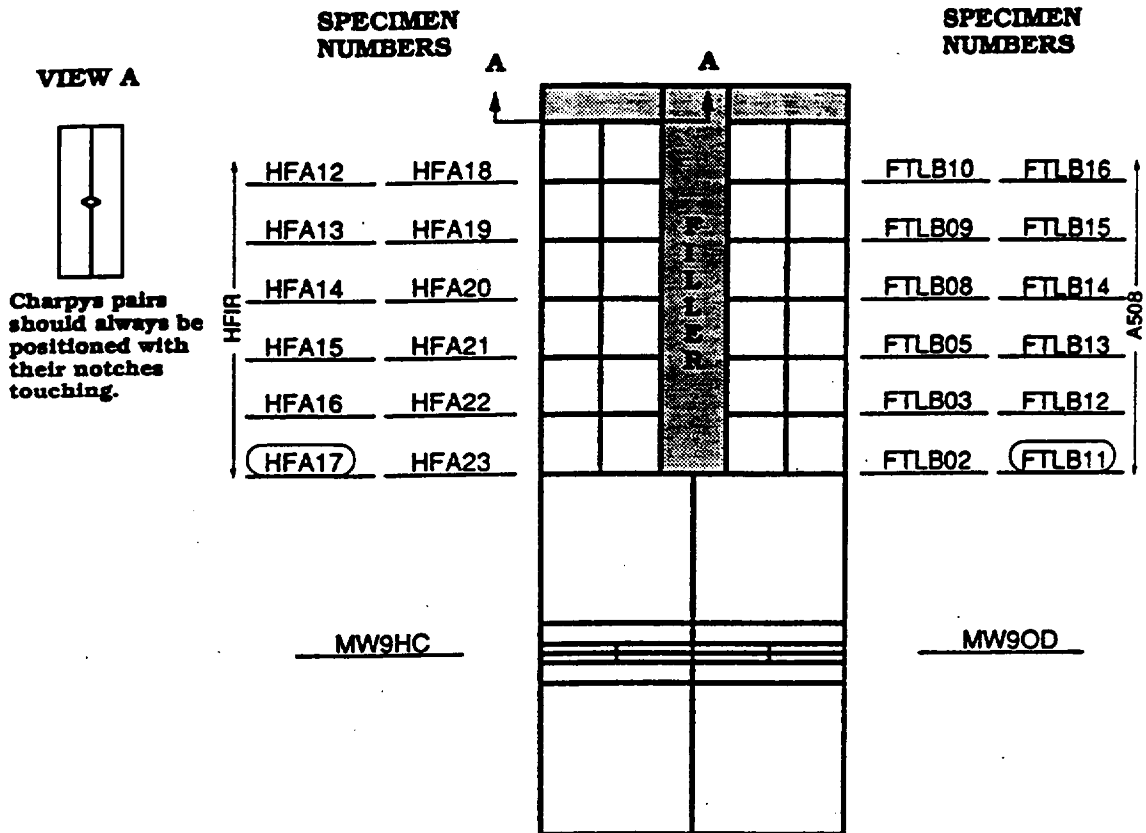

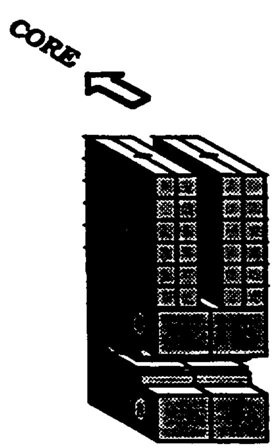

= Magnetic Field Tested

Each block contains:

24 charpy specimens 6x4

2 1TCTs

SPECIMEN LAYOUT BLOCK D2

SPECIMEN NUMBERS

LEFT BACK	LEFT FRONT
72PH13	72PH10
73QH04	73QH03
72PH05	72PH04
73QH05	73QH12
MW9HEA	MW11HEB
MW11LFB	MW9IEA
MW9LEB	MW11MCA
MW11JFB	MW9KFB
MW9HFA	MW11HFB
MW11KFAB	MW9JEA

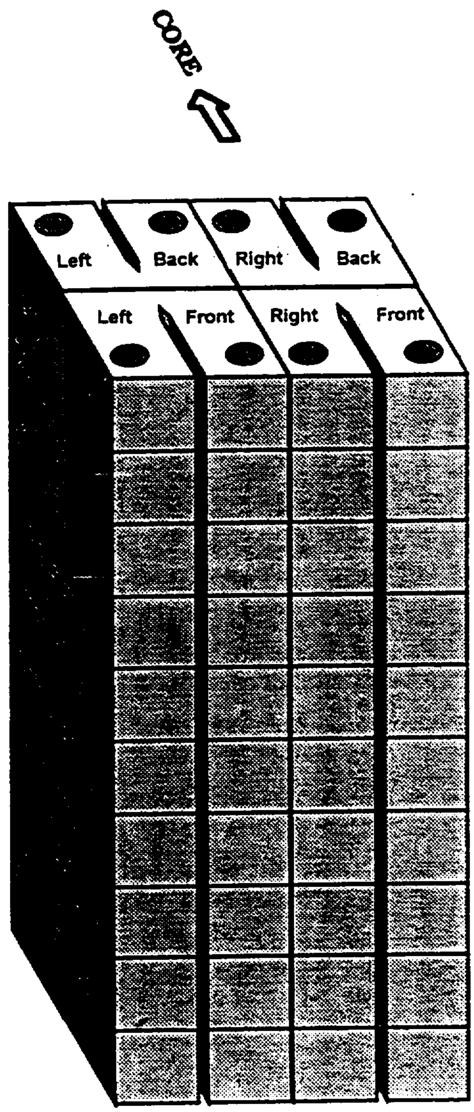

SPECIMEN NUMBERS

RIGHT BACK	RIGHT FRONT
72PH09	73QH11
73QH02	72PH14
72PH08	73QH10
73QH14	72PH07
MW9CEA	MW9OFA
MW11LEB	MW11JFA
MW9IFA	MW9JFB
MW11IFB	MW11HEA
MW9LFA	MW9JEB
MW11MDB	MW9HEB

SPECIMEN LAYOUT BLOCK D3

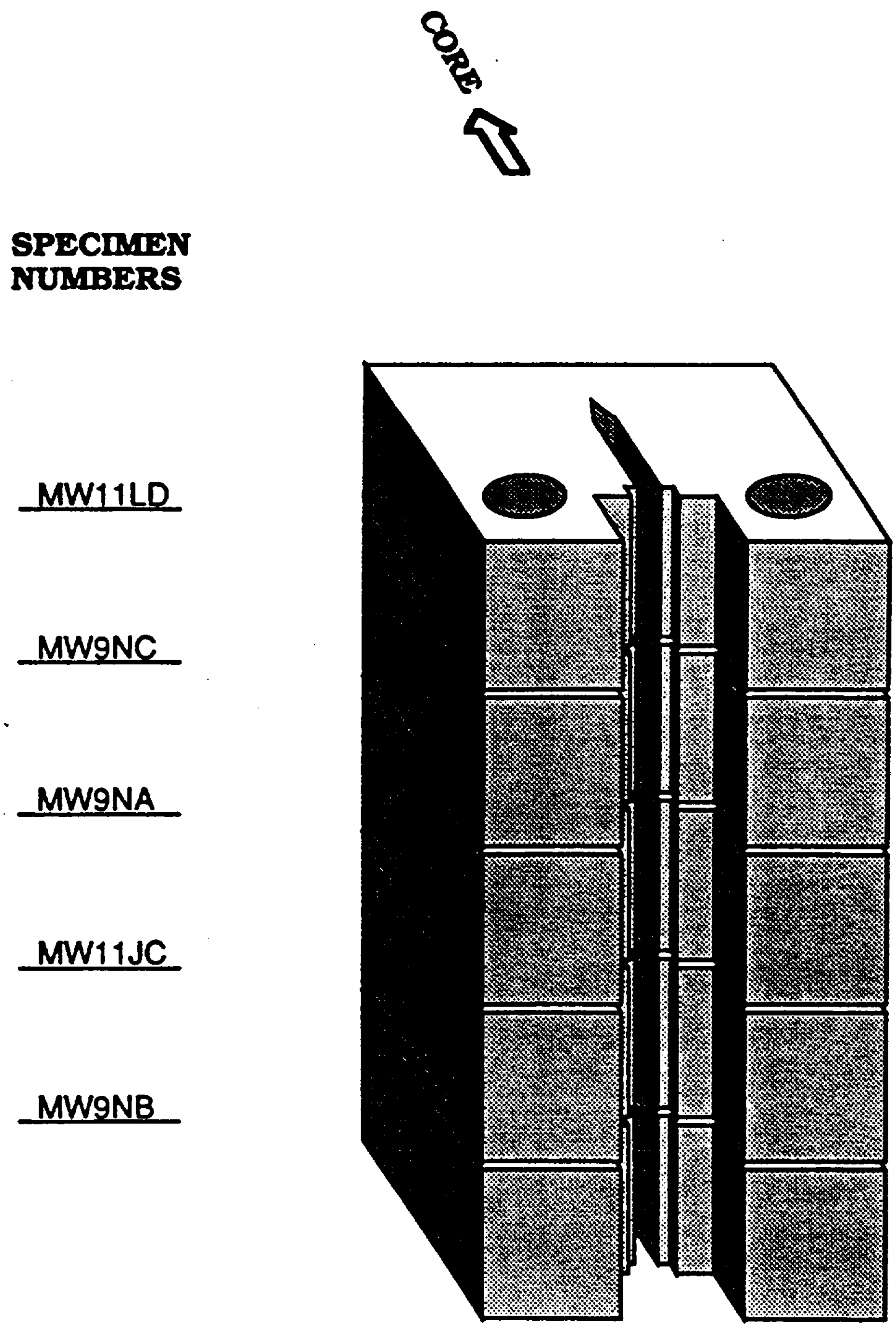

SPECIMEN LAYOUT BLOCK D4

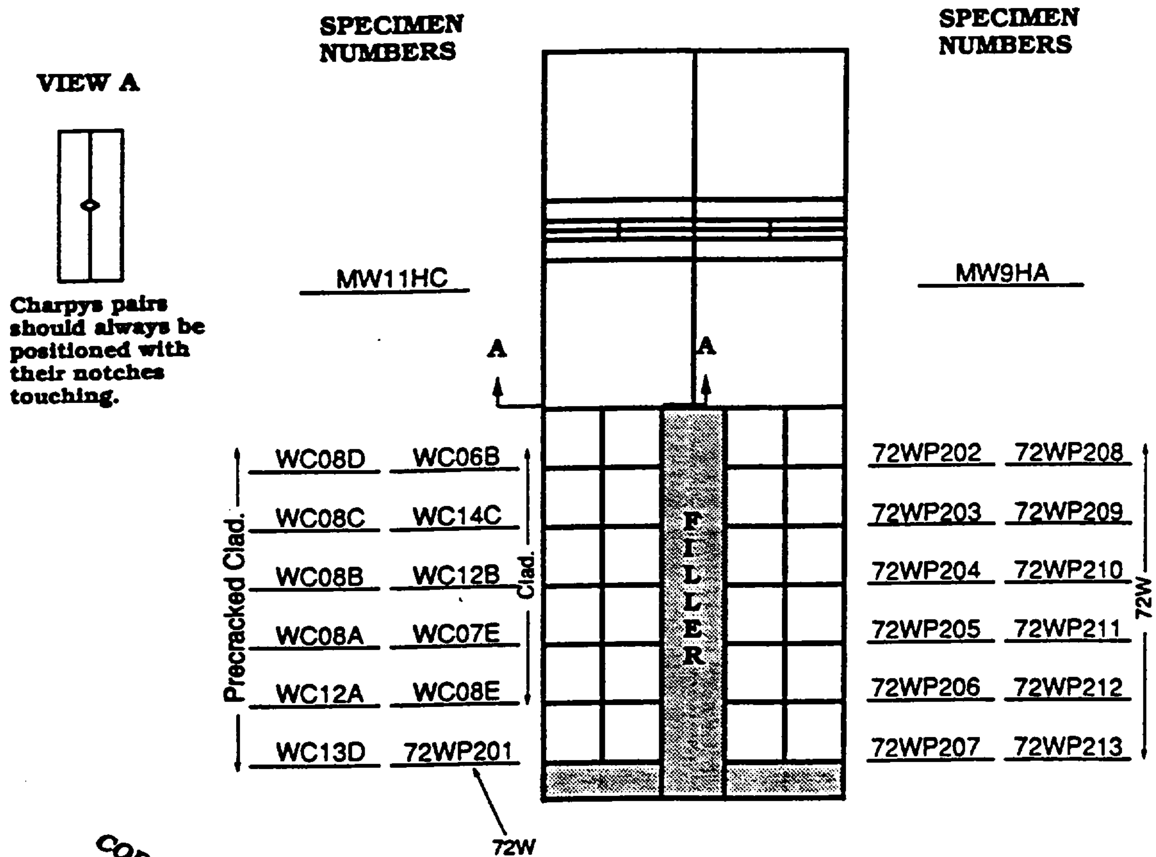

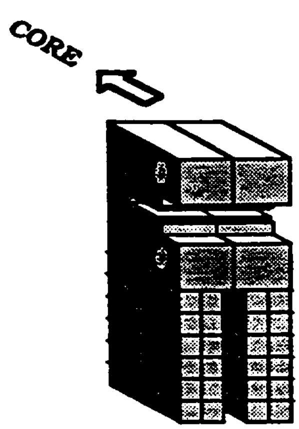

Each block contains:

2 1TCTs

24 charpy specimens 6x4

Table C2. Temperature control (thermocouple locations, Figure C18) for HSSI Capsule 10.05

TE	Zone	Average (°C)	Standard deviation	TE	Zone	Average (°C)	Standard deviation
1	1	283.99	1.09E-05	24	4	294.37	1.496429
2	2	284	0.029354	25	5	287.99	0.911097
3	3	284	0.034993	26	4	290.5	2.103396
4	4	284.67	1.495594	27	4	289.69	1.780189
5	5	284.67	1.152184	28	4	286.74	1.94324
6	6	284	0.021794	29	5	281.06	1.179192
7	7	284.17	0.511899	30	5	286.29	0.681282
8	8	284.01	0.069346	31	4	290.8	1.002039
9	9	284	0.034993	32	8	295.2	0.787988
10	3	264.57	0.880848	33	7	297.3	0.867276
11	2	273.86	0.472558	34	6	283.07	0.416653
12	2	270.57	0.87385	35	5	286.51	0.461799
13	1	265.97	1.185937	36	6	286.79	0.433397
14	1	286.06	0.408271	37	8	295.6	0.665519
15	3	287.8	0.357453	37	9	295.6	0.695059
16	2	288.27	0.161702	38	9	294.44	0.658037
17	3	294.67	0.416214	39	9	286.73	0.486451
18	5	293.79	0.568299	40	8	290.81	0.219565
19	6	289.26	0.134536	41	7	289.4	0.500666
20	5	285.11	0.568967	42	7	263.62	0.758272
21	2	291.65	0.526099	43	9	263.06	1.416963
22	1	294.69	1.081014	44	8	271.86	1.639209
23	4	293.23	1.430923	45	8	270.32	0.644804

VIEW LOOKING TOWARDS CORE
HSSI-10-5
THERMOCOUPLE LOCATIONS

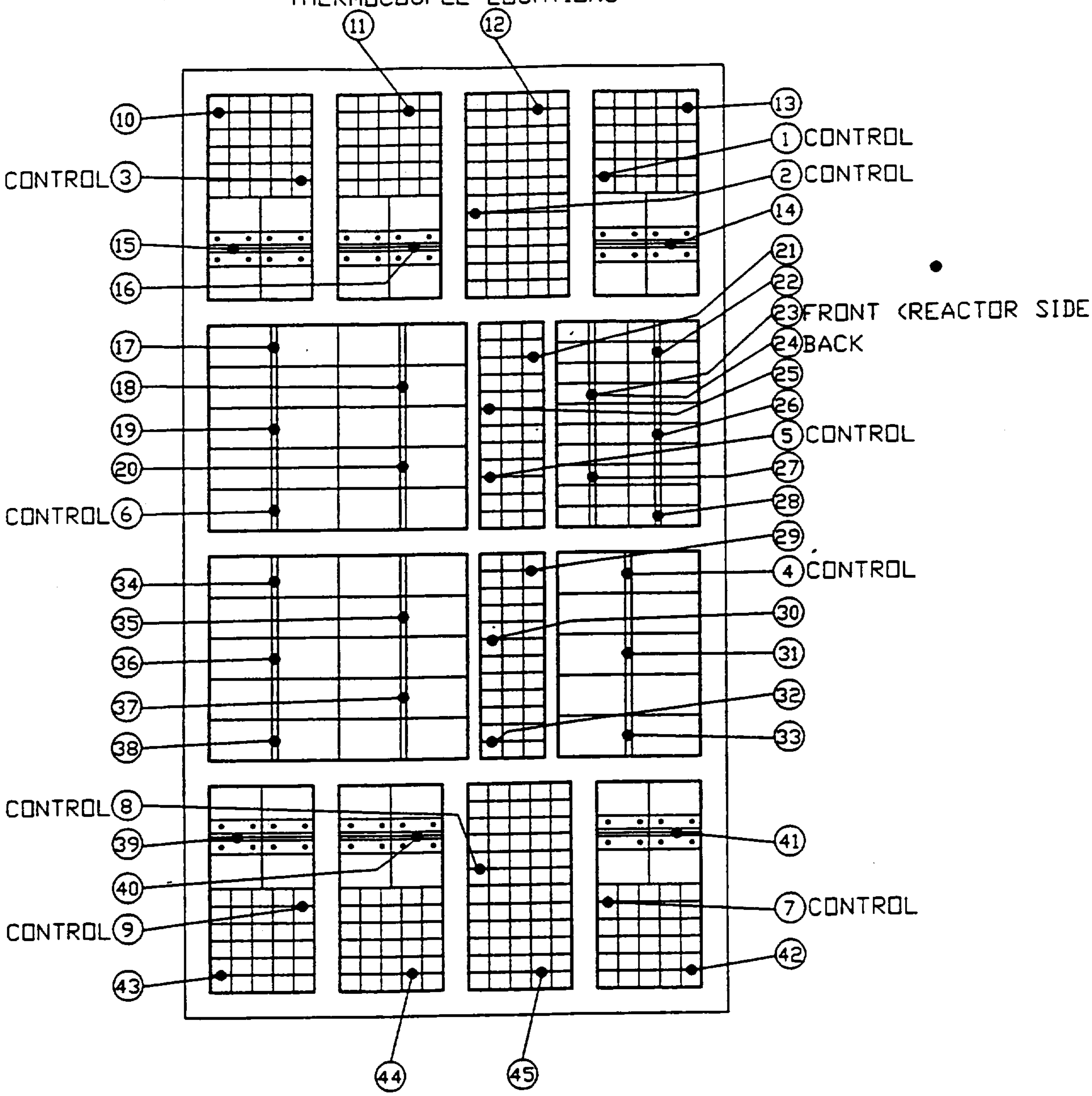

Table C3. Fluence distribution for Capsule 10.05
(>1 MeV)

Block	Charpy specimens	1T C(T) specimens	1/2T C(T) specimens
A1	5.45×10^{18} n/cm^2	0.73×10^{19} n/cm^2	
B1	7.27×10^{18} n/cm^2	0.98×10^{19} n/cm^2	
C1	9.48×10^{18} n/cm^2		
D1	8.16×10^{18} n/cm^2	1.09×10^{19} n/cm^2	
A2		0.92×10^{19} n/cm^2	
B2		1.22×10^{19} n/cm^2	
C2	1.30×10^{19} n/cm^2		
D2			1.23×10^{19} n/cm^2
A3		0.90×10^{19} n/cm^2	
B3		1.19×10^{19} n/cm^2	
C3	1.28×10^{19} n/cm^2		
D3		1.31×10^{19} n/cm^2	
A4	4.84×10^{18} n/cm^2	0.68×10^{19} n/cm^2	
B4	6.46×10^{18} n/cm^2	0.91×10^{18} n/cm^2	
C4	8.63×10^{18} n/cm^2		
D4	7.25×10^{18} n/cm^2	1.01×10^{19} n/cm^2	
Average	0.86×10^{19} n/cm^2	1.04×10^{19} n/cm^2	1.23×10^{19} n/cm^2

ORNL 98-6906/dgc

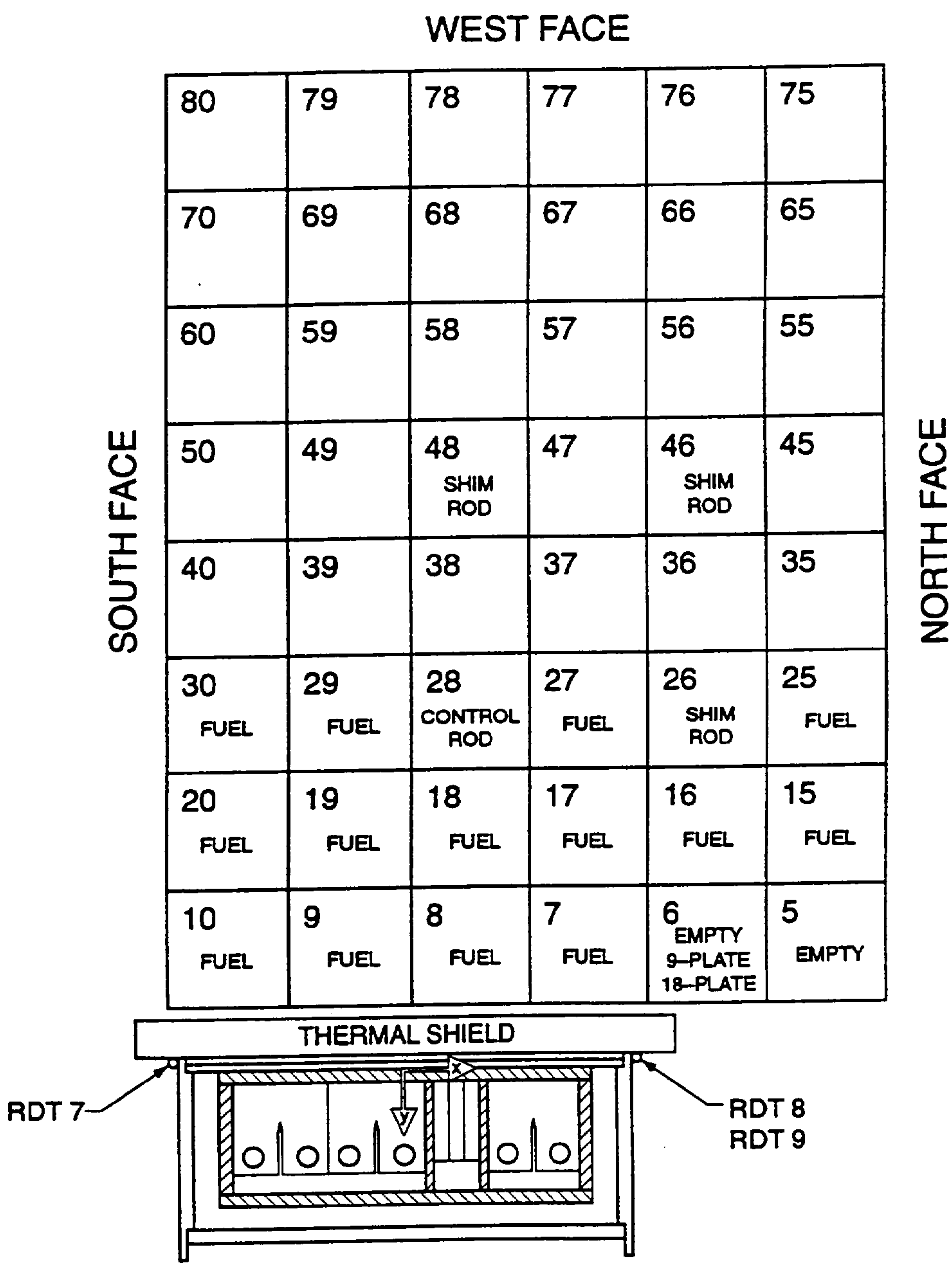

Fig. C19. Location of the HSSI 10.05 capsule relative to the reactor core; horizontal cross section.

Appendix D

Capsule 10.06

Construction: ORNL

Exposure: Ford Nuclear Reactor

Irradiation Period:

June 4, 1993, to September 1, 1994
4936 effective full-power hours - core edge
Rotated February 1,1994

Reactor:

Ford Nuclear Reactor
Phoenix Materials Laboratory
2301 Bonisteel Boulevard
Ann Arbor, Michigan 48109

Shipped to ORNL:

January 11, 1995

Capsule Contents:

Charpys, 1/2T, 1T, C(T), and CCA
See Figures D1 to D14
See Table D1

Irradiation Information:

Average temperatures, Table D2
Thermocouple locations, Page D-19
Capsule location, Figure C19, Page C-25
Fluence distributions, Table D3

Table D1.

Specimens	Number	Material	Row
Tenth Irradiation			
2T C(T)	2	Beltline	C
1T C(T)	8	Beltline	A and B
1T C(T)	22	Nozzle course	B and C
1/2T C(T)	6	Beltline	B
1/2T C(T)	10	Nozzle course	B
PCVN	25	Beltline	A and S3
Tensile	12	Beltline	C
Tensile	12	Nozzle course	C
Long tensile	12	Beltline	C
CCA (1-in. B)	10	Beltline	B and D
CCA (1.3-in. B)	5	Beltline	B and D
Annealing Program			
1T C(T)	10	72W	A
1T C(T)	4	73W	A
PCVN	5	64W	S3
CVN	36	Russian steel	S0
CVN	58	Russian steel	S2 and S3
Tensile	6	Russian steel	S0 and top
Tensile	4	Russian steel	S2

CAPSULE SIX LAYOUT

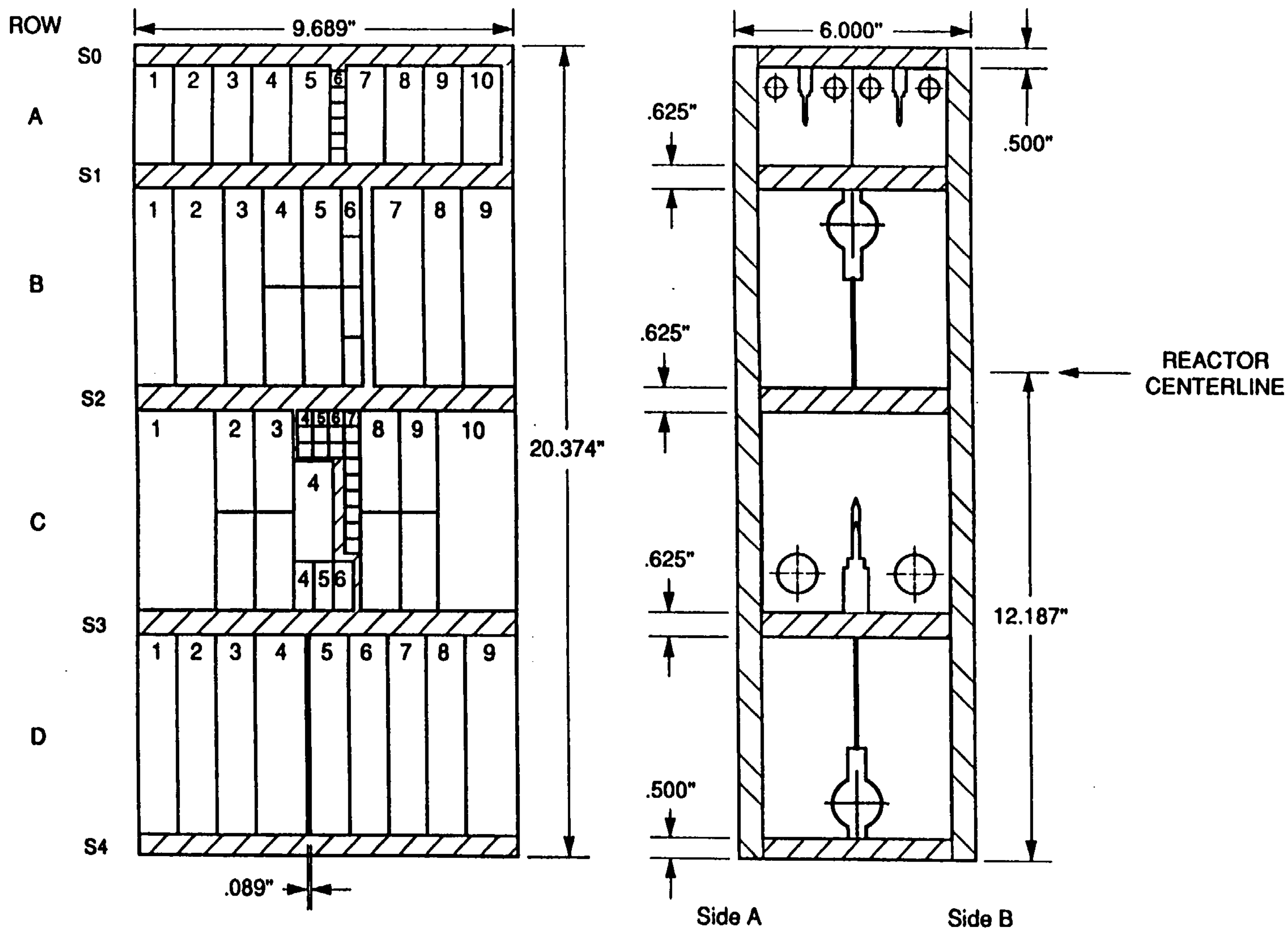

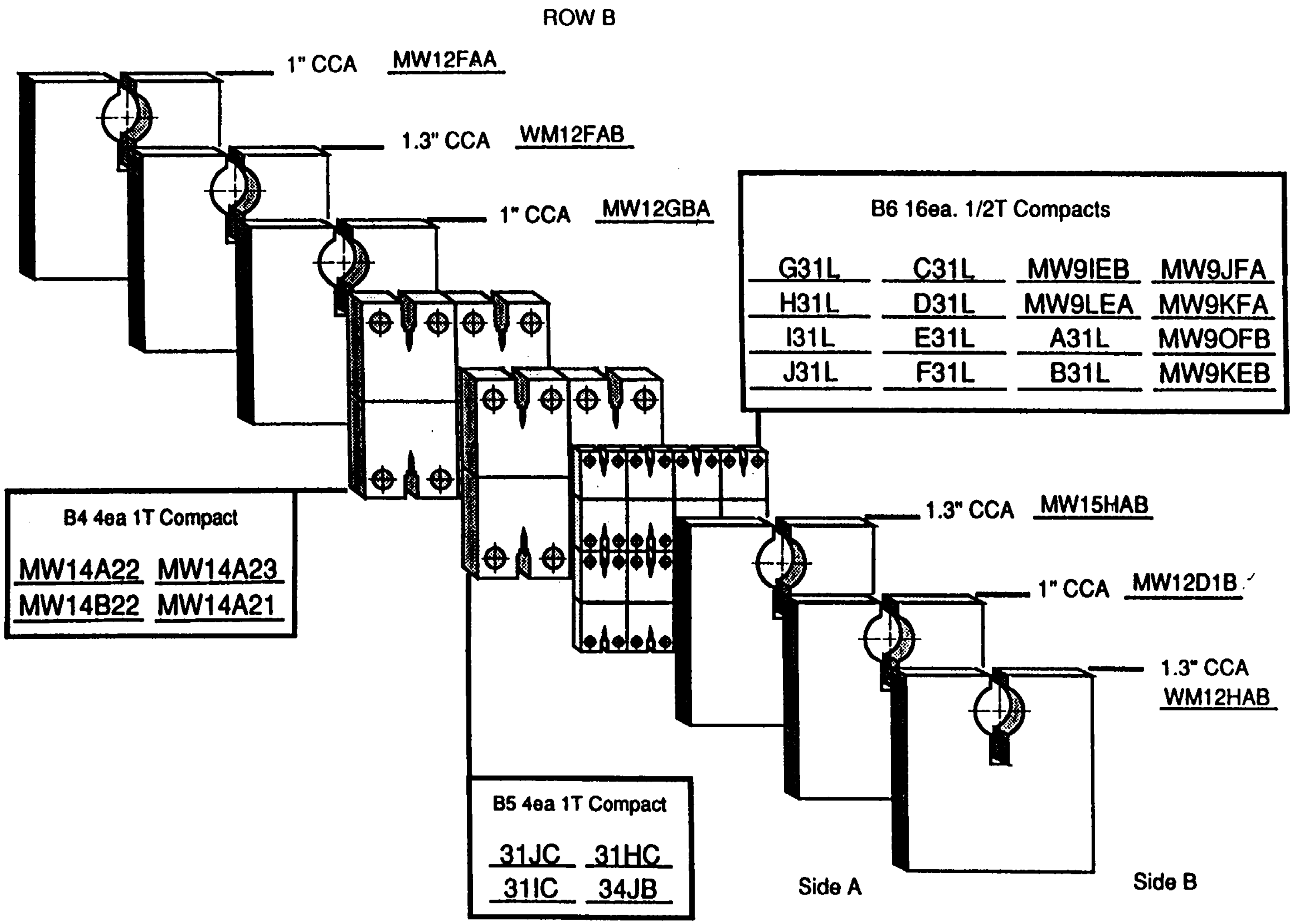
ROW B
1" CCA MW12FAA
1.3" CCA WM12FAB
1" CCA MW12GBA
B6 16ea. 1/2T Compacts
G31L C31L MW9IEB MW9JFA
H31L D31L MW9LEA MW9KFA
I31L E31L A31L MW9OFB
J31L F31L B31L MW9KEB
B4 4ea 1T Compact
MW14A22 MW14A23
MW14B22 MW14A21
1.3" CCA MW15HAB
1" CCA MW12D1B
1.3" CCA
WM12HAB
B5 4ea 1T Compact
31JC 31HC
31IC 34JB
Side A
Side B

DETAIL ROW C 1, 2, &3

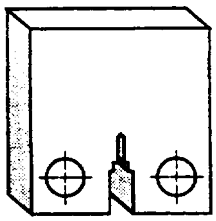

C-1 2T CT

MW10A1

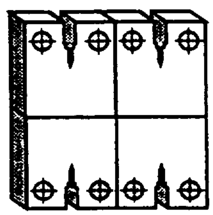

C-2 4ea 1T CT

34KD	34LE
31HE	31KC

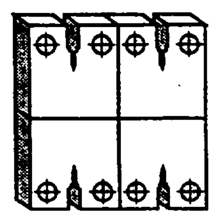

C-3 4ea 1T CT

34JD	31IE
31JC	34JA

Side A Side B

DETAIL ROW C 4,5,6,7

ROW C-4

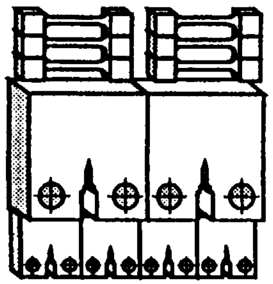

Tensile

Side A	Side B
2FE9	R405B
R1093	31P06
2GC7	R406E

1 TCT

31HD	31KE

1/2 TCT

72PH12 72PH02 72PH01 72PH06

ROW C-6

Tensile

Side A	Side B
R1074	13109B
31P12	MW11CE3
R10717	13110B

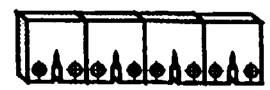

1/2 TCT

72PH11 72PH03 73QH13 73QH01

ROW C-5

Tensile

Side A	Side B
R1072	R405D
R1095	R405H
R10713	MW15AE2

1/2 TCT

73QH08 73QH07 73QH09 73QH06

ROW C-7

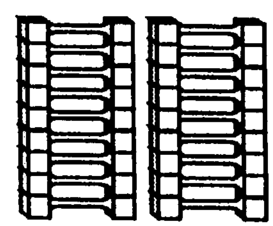

Tensile

Side A	Side B
R1078	MW11CE4
R1099	R406I
R10719	R406G
31P16	R406C
R10914	MW11DE2
R10916	13111B
2FC2	MW11EE2
R1096	64W22C
64W235C	13112B

DETAIL ROW C 8, 9, &10

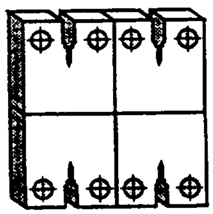

C-8 4ea 1T CT

34IB 34LB
34LA 34KB

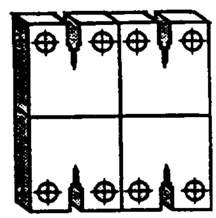

C-9 4ea 1T CT

31KB 31KA
31KA 34IA

Side A Side B

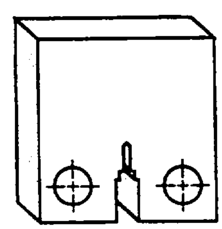

C-10 2T CT

MW10F1

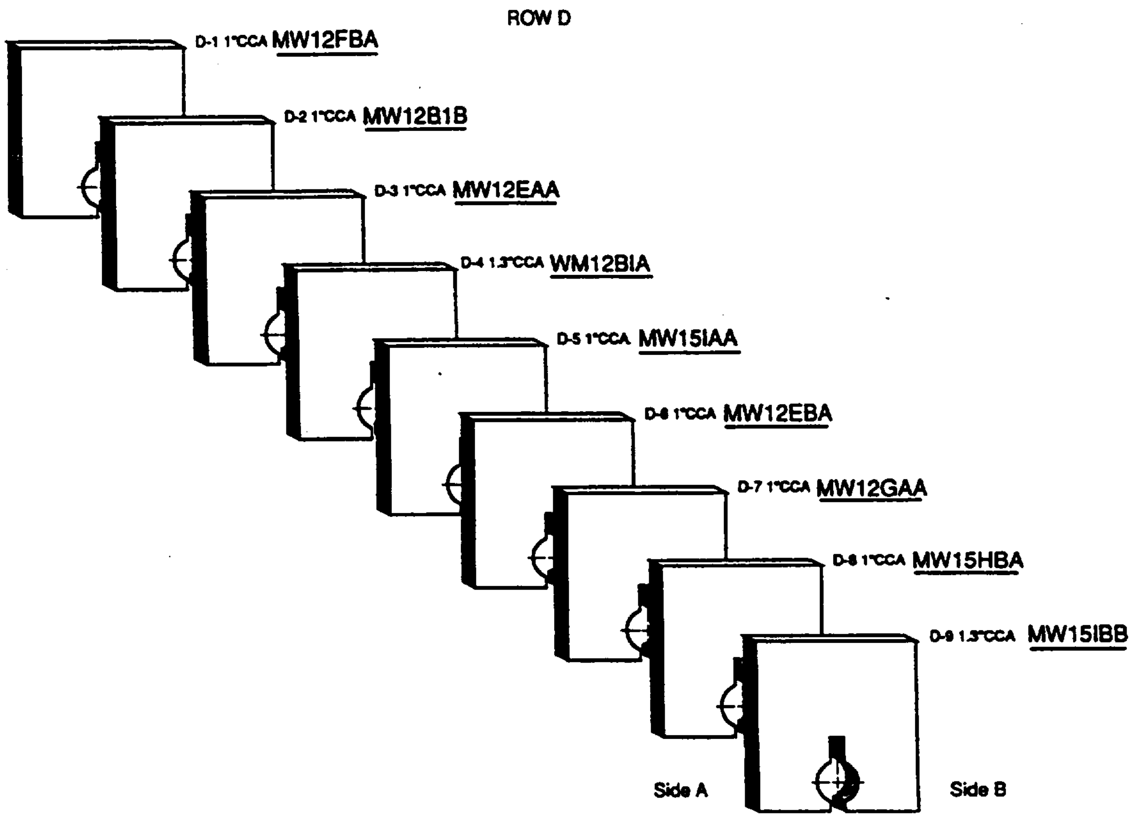
ROW D
D-1 1"CCA MW12FBA
D-2 1"CCA MW12B1B
D-3 1"CCA MW12EAA
D-4 1.3"CCA WM12BIA
D-5 1"CCA MW15IAA
D-6 1"CCA MW12EBA
D-7 1"CCA MW12GAA
D-8 1"CCA MW15HBA
D-9 1.3"CCA MW15IBB
Side A
Side B

SPACER SO

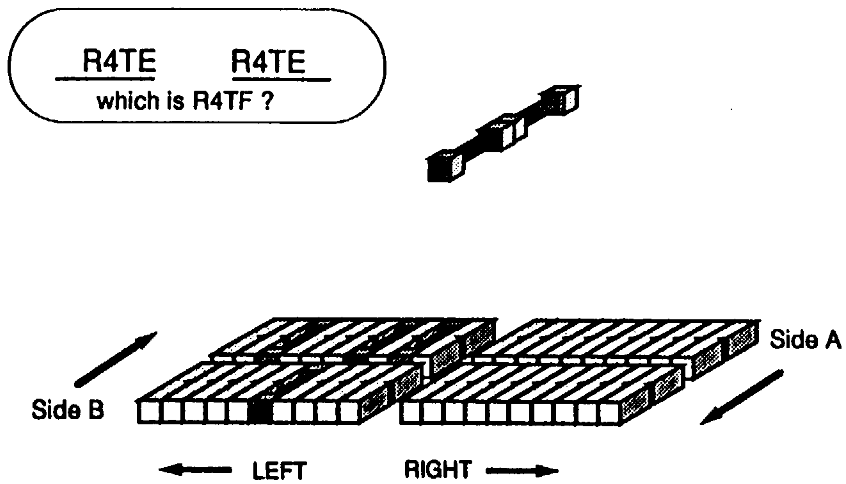

CHARPY SPECIMENS

Side A	Side B
R403J	R403E
R407A	R404D
R403H	R4TB
R404J	R404B
R403F	R404F
R4TD	R404E
R403D	R4TC
R403C	R404C
R403B	R4TA
R404I	R404G

↑ LEFT
RIGHT ↓

Side A	Side B
R401J	R402J
R401I	R402I
R401H	R402H
R401G	R402G
R401F	R402F
R401E	R402E
R401D	R402D
R401C	R402C
R401B	R402B
R401A	R404H

SPACER S1

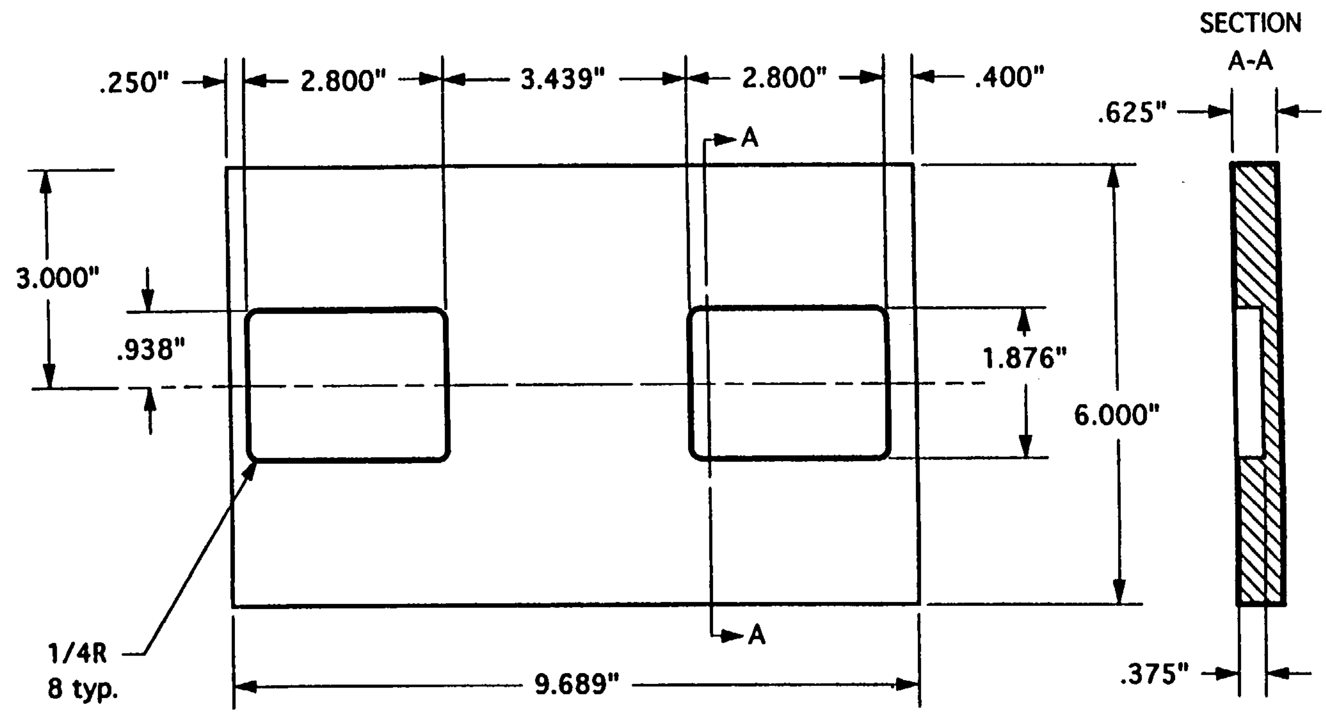

CAUTION
NUCLEAR EQUIPMENT

AVOID CONTACT AND/OR CONTAMINATION WITH MATERIALS CONTAINING: COPPER, SILVER, LEAD, (ALL SOLDERS), MERCURY, THORIUM, URANIUM, CHLORINE, FLUORINE, GRAPHITE, ___________.

ANY SUCH CONTAMINATION MUST BE REMOVED.

Material: C Steel

Tolerances

X.XXX = ±0.005
X.XX = ±0.01
All surfaces should be parallel and perpendicular as appropriate within 0.002". All dimensions in inches.
Surface finishes $\sqrt[64]{}$ or better.

SPACER S2 & S3

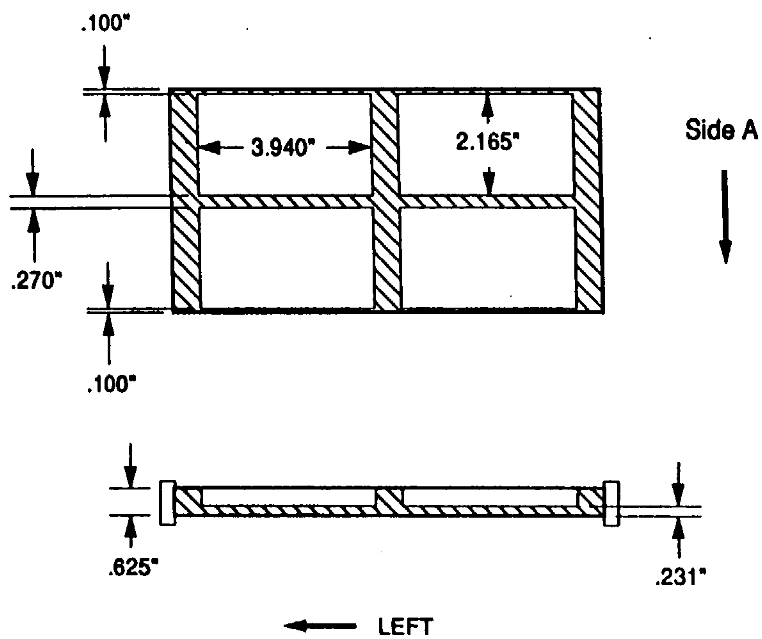

CAUTION
NUCLEAR EQUIPMENT

AVOID CONTACT AND/OR CONTAMINATION WITH MATERIALS CONTAINING: COPPER, SILVER, LEAD, (ALL SOLDERS), MERCURY, THORIUM, URANIUM, CHLORINE, FLUORINE, GRAPHITE, ___________

ANY SUCH CONTAMINATION MUST BE REMOVED.

Material: C Steel

Tolerances

X.XXX = ±0.005
X.XX = ±0.01

All surfaces should be parallel and perpendicular as appropriate within 0.002". All dimensions in inches. Surface finishes $\sqrt[64]{}$ or better.

SPACER S2

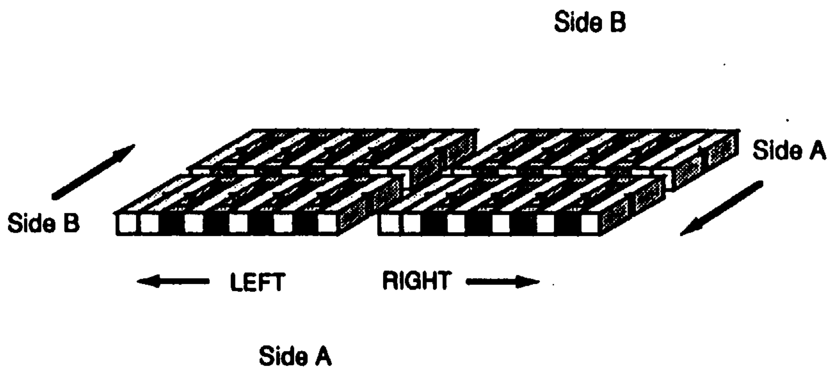

CHARPY SPECIMENS

Side A	Side B
R10911	R10715
R10910	2FE7
31P11	R1076
R1098	R11013
R11015	R10917
R1097	2GC3
31P10	R10915
R1094	2GC9
31P08	R10913
R1092	R10912

LEFT

RIGHT

Side A	Side B
R10710	R10918
R1079	31P15
31P07	R10718
R1077	31P14
R11014	R10716
R1075	R1091
31P05	R10714
R1073	31P13
31P04	R10712
R1071	R10711

[shaded box] = TENSILES

SPACER S3

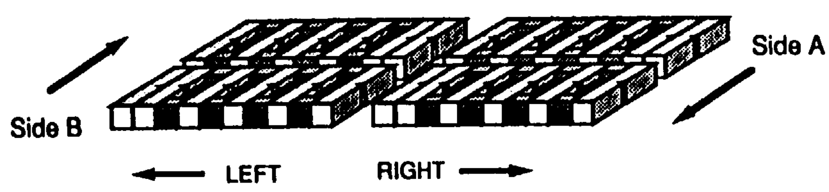

CHARPY SPECIMENS

Side A	Side B
MW11BE2	64W240C
MW11EE3	13I08B
13I01B	64W230C
MW11CE2	13I07B
2FE6	64W220C
MW15AE3	13I06B
2FE1	MW11EE4
MW15BE1	13I05B
2FC3	MW15AK3
R405F	MW11EE5

LEFT

RIGHT

Side A	Side B
R405J	R406J
R405I	13I02B
2EE2	R406H
R405G	13I03B
R11017	R406F
R405E	R11018
2EE3	R406D
R405C	13I04B
2EE7	R406B
R405A	R406A

[shaded] = TENSILES

SPACER S4

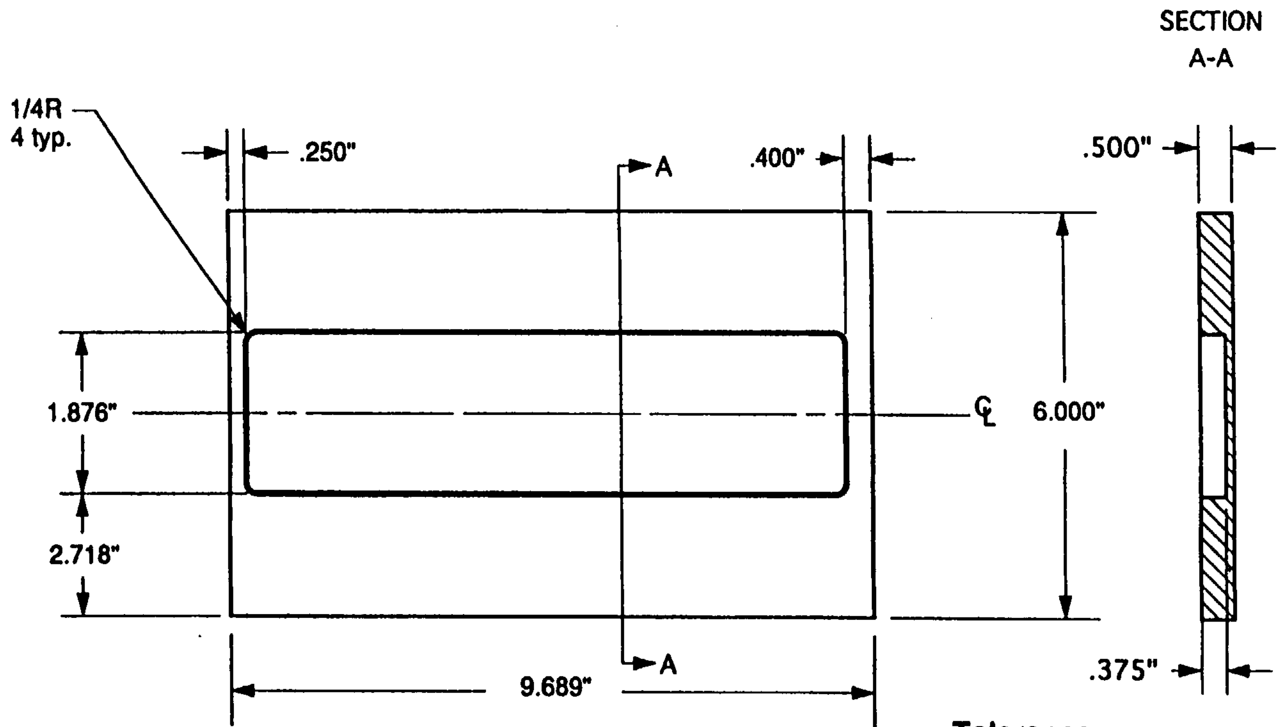

Tolerances
X.XXX = ±0.005
X.XX = ±0.01
All surfaces should be parallel and perpendicular as appropriate within 0.002". All dimensions in inches.
Surface finishes 64√ or better.

Material: C Steel

CAUTION
NUCLEAR EQUIPMENT

AVOID CONTACT AND/OR CONTAMINATION WITH MATERIALS CONTAINING: COPPER, SILVER, LEAD, (ALL SOLDERS), MERCURY, THORIUM, URANIUM, CHLORINE, FLUORINE, GRAPHITE, __________

ANY SUCH CONTAMINATION MUST BE REMOVED.

SPACER DETAILS

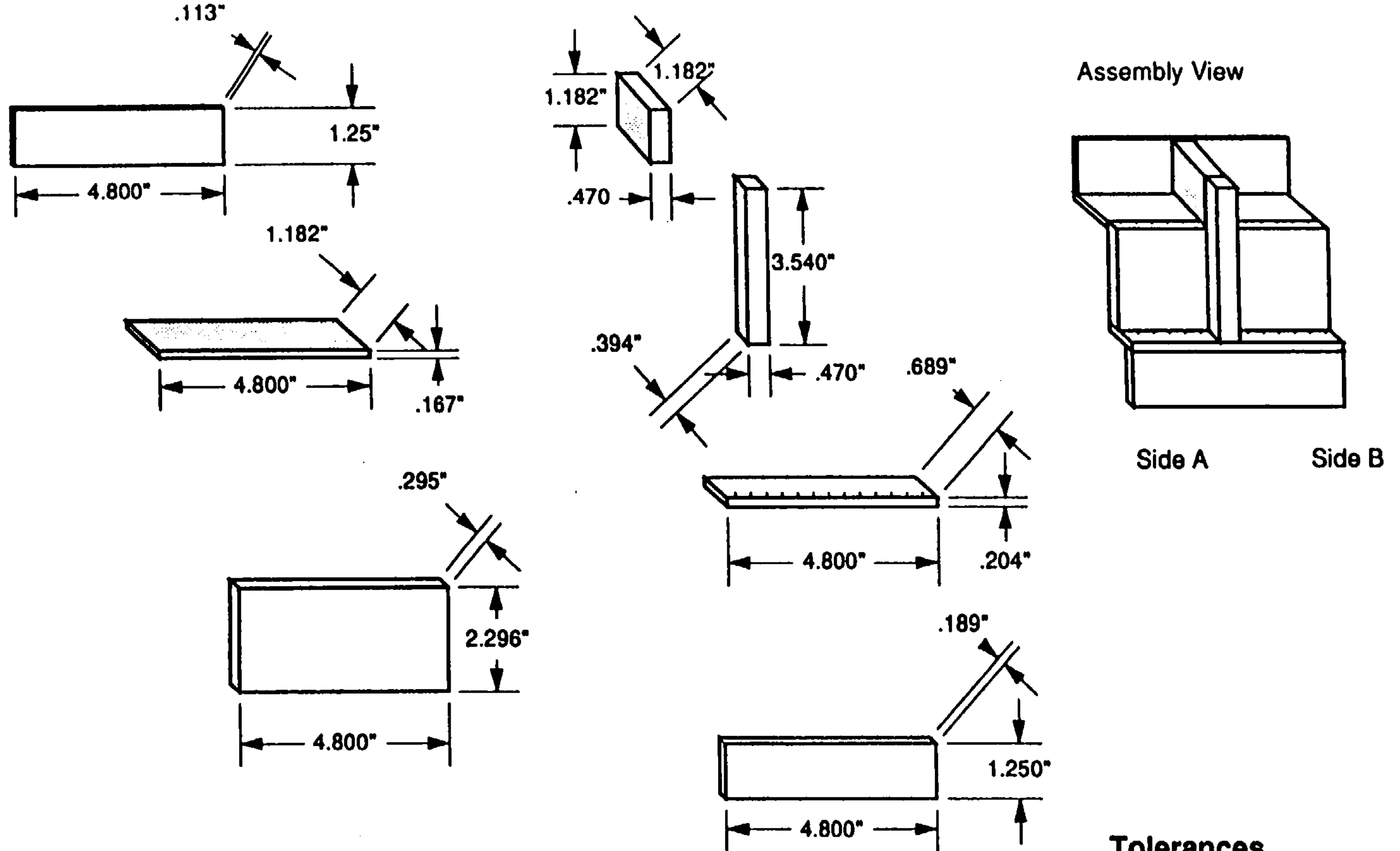

CAUTION
NUCLEAR EQUIPMENT

AVOID CONTACT AND/OR CONTAMINATION WITH MATERIALS CONTAINING: COPPER, SILVER, LEAD, (ALL SOLDERS), MERCURY, THORIUM, URANIUM, CHLORINE, FLUORINE, GRAPHITE, __________

ANY SUCH CONTAMINATION MUST BE REMOVED.

Material: C Steel

Tolerances

X.XXX = ±0.005
X.XX = ±0.01

All surfaces should be parallel and perpendicular as appropriate within 0.002". All dimensions in inches. Surface finishes $\sqrt[64]{}$ or better.

Table D2. Temperature control (thermocouple locations) for HSSI Capsule 10.06

Position	Temperature (°C)	Standard Deviation (°C)	Position	Temperature (°C)	Standard Deviation (°C)
1	290.9	1.56	24	284.5	1.85
2	288.2	0.91	25	279.9	2.13
3	288.0	0.42	26	283.1	1.22
4	289.0	2.50	27	279.9	1.25
5	289.4	1.07	28	286.3	0.94
6	288.1	1.49	29	280.2	0.82
7	288.4	0.81	30	286.2	3.30
8	288.7	1.10	31	292.2	2.04
9	288.4	1.05	32	290.0	1.08
10	275.3	0.95	33	293.5	1.62
11	284.7	1.08	34	289.8	1.69
12	280.1	0.90	35	282.3	1.78
13	273.0	0.88	36	291.9	0.90
14	277.6	0.74	37	291.2	1.04
15	279.2	0.64	38	284.6	1.61
16	278.6	1.31	39	289.1	2.30
17	278.1	3.44	40	289.3	3.81
18	271.9	1.64	41	288.0	3.52
19	274.3	0.99	42	288.9	1.20
20	278.0	0.84	43	283.9	0.99
21	277.2	1.00	44	281.7	1.01
22	286.1	1.00	45	289.8	1.86
23	273.5	2.55			

ORNL 98-6905/dgc

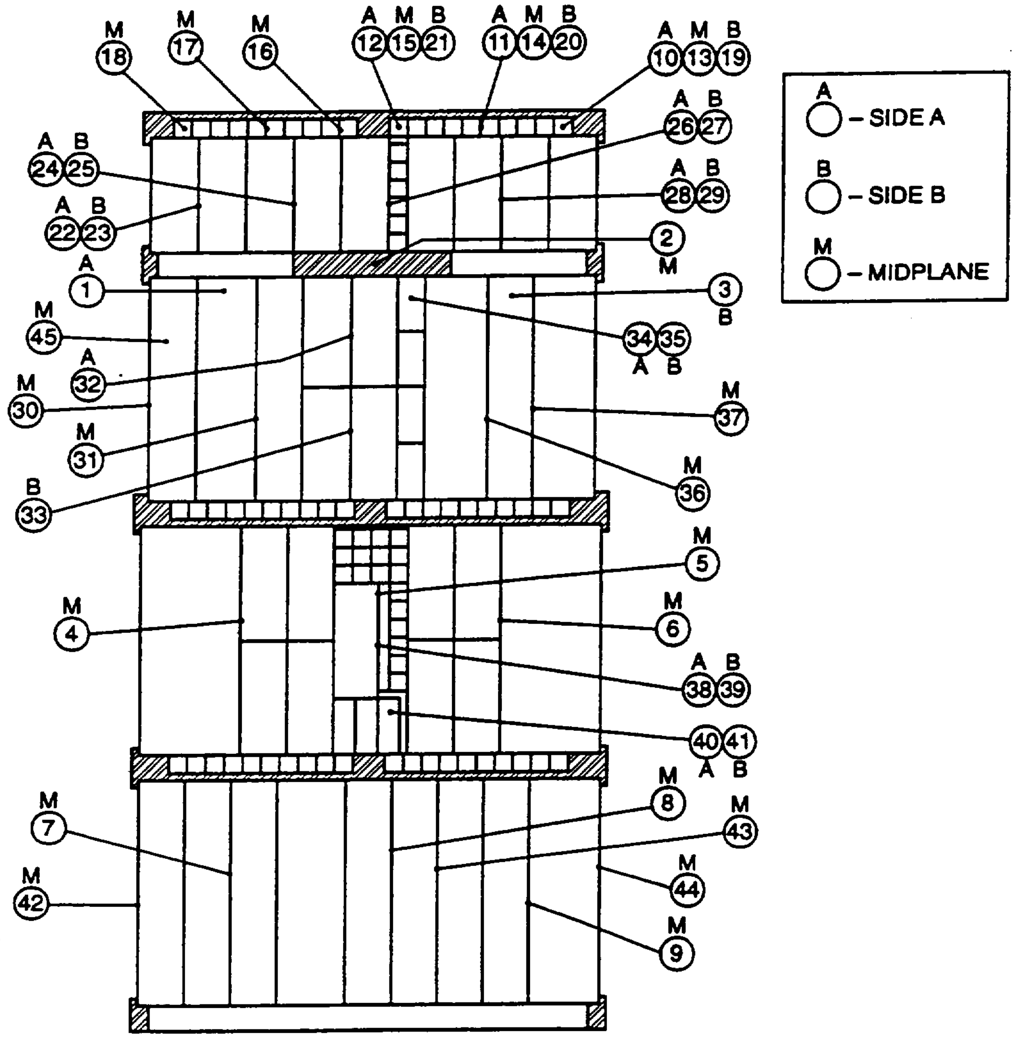

HSSI 10-6 Specimen Assembly

View of Side A

Table D3. Fluence (f) distribution for Capsule 10.06

Row	Distance[a] (cm)		$f/10^{19}$ n/cm^2 (>1 MeV)	Specimens
	Z	X		
S0	23.9	5.79	0.67	Charpy
	23.9	-5.79	0.67	Charpy
A	19.6	5.58	0.81	1T
	19.6	-1.27	0.87	Charpy
	19.6	-6.80	0.80	1T
B	9.46	6.48	1.02	CCA, 1 row 1T
	9.46	-1.20	1.12	1T, 1/2T
	9.46	-7.37	0.91	CCA
S2	2.56	5.54	1.11	Charpy, tensile
	2.56	-5.54	1.11	Charpy, tensile
C	-3.37	6.45	1.07	2T, 8 1T (C)T
	-4.25	0	1.08	1T, 1/2T, tensile
	-3.37	-6.45	1.07	1T, 2T
S3	-11.54	5.79	0.94	CVN, tensile
	-11.54	-5.29	0.93	CVN, tensile
	-18.73	8.38	0.61	CCA
	-18.73	0.19	0.68	CCA
	-18.73	-7.81	0.62	CCA

[a]Z = distance referenced from capsule midpoint (vertical);
X = distance referenced from capsule centerline.

NRC FORM 335 (2-89) NRCM 1102, 3201, 3202

U.S. NUCLEAR REGULATORY COMMISSION

BIBLIOGRAPHIC DATA SHEET

(See instructions on the reverse)

1. REPORT NUMBER (Assigned by NRC, Add Vol., Supp., Rev., and Addendum Numbers, if any.)

NUREG/CR-5736
ORNL/TM-13748

2. TITLE AND SUBTITLE

Evaluation of WF-70 Weld Metal from the Midland Unit 1 Reactor Vessel-

3. DATE REPORT PUBLISHED

MONTH	YEAR
November	2000

4. FIN OR GRANT NUMBER

5. AUTHOR(S)

D. E. McCabe, R. K. Nanstad, S. K. Iskander, D. W. Heatherly, and R. L. Swain

6. TYPE OF REPORT

W6953

7. PERIOD COVERED (Inclusive Dates)

Technical

8. PERFORMING ORGANIZATION – NAME AND ADDRESS (If NRC, provide Division, Office or Region, U.S. Nuclear Regulatory Commission, and mailing address; if contractor, provide name and mailing address.)

Oak Ridge National Laboratory
Oak Ridge, TN 37831-6285

9. SPONSORING ORGANIZATION – NAME AND ADDRESS (If NRC, type "Same as above"; if contractor, provide NRC Division, Office or Region, U.S. Nuclear Regulatory Commission, and mailing address.)

Division of Engineering Technology
Office of Nuclear Regulatory Research
U.S. Nuclear Regulatory Commission
Washington, DC 20555-0001

10. SUPPLEMENTARY NOTES

C. J. Fairbanks, NRC Project Manager

11. ABSTRACT (200 words or less)

The Heavy-Section Steel Irradiation Program has evaluated low upper-shelf (LUS) weld metal sampled from the Midland Unit 1 reactor vessel. The weld metal was designated to be WF-70 by Babcock and Wilcox Company code. The sampling was taken from both the nozzle course and beltline girth welds. The as-received materials characterization using Charpy curves, drop-weight nil-ductility transition, tensile tests, and chemical analysis surveys indicated that the materials from the two locations were essentially the same except for the copper content. The expected nominal copper contents were 0.40 and 0.26 wt % for the nozzle course and beltline welds, respectively. Because the experiment involved detailed evaluations of both unirradiated and irradiated (1×10^{19} n/cm^2) conditions, the two weld metals were evaluated separately.

Fracture mechanics data were obtained for both the unirradiated and irradiated conditions; two methods of evaluating the transition temperatures were (1) the American Society of Mechanical Engineers (ASME) *Boiler and Pressure Vessel Code*, augmented with the American Society for Testing and Materials (ASTM) Method E 185, and (2) the relatively new master curve method. The ASME method uses a reference temperature determination (RT_{NDT}) from nonfracture mechanics test practices; the master curve method uses a transition temperature, T_o, obtained from fracture mechanics-based data. The deficiencies of the ASME method as applied to LUS materials were evident. The master curve method, supplemented with fracture mechanics-based R-curve data, proved to have sufficient sensitivity to show differences between the nozzle course and beltline materials. The ASME-recommended methods failed to detect differences, thereby revealing the lower sensitivity of the empirical methods associated with RT_{NDT}.

12. KEY WORDS/DESCRIPTORS (List words or phrases that will assist researchers in locating the report.)

beltline weld
charpy curves
copper content
crack arrest
dropweight, nil-ductility transition
fracture toughness
irradiation
master curve
nozzle weld
reactor pressure vessel
R-curve
tensile tests
transition temperature

13. AVAILABILITY STATEMENT

Unlimited

14. SECURITY CLASSIFICATION

(This Page) Unclassified

(This Report) Unclassified

15. NUMBER OF PAGES

16. PRICE

NRC FORM 335 (2-89)

UNITED STATES
NUCLEAR REGULATORY COMMISSION
WASHINGTON, D.C. 20555-0001

1975 25 2000
years